marine drugs

MDPI

Review

Untapped Potential of Marine-Associated *Cladosporium* Species: An Overview on Secondary Metabolites, Biotechnological Relevance, and Biological Activities

Gamal A. Mohamed [1,*] and Sabrin R. M. Ibrahim [2,3]

[1] Department of Natural Products and Alternative Medicine, Faculty of Pharmacy, King Abdulaziz University, Jeddah 21589, Saudi Arabia
[2] Preparatory Year Program, Batterjee Medical College, Jeddah 21442, Saudi Arabia; sabrin.ibrahim@bmc.edu.sa
[3] Department of Pharmacognosy, Faculty of Pharmacy, Assiut University, Assiut 71526, Egypt
* Correspondence: gahussein@kau.edu.sa; Tel.: +966-597-636-182

Abstract: The marine environment is an underexplored treasure that hosts huge biodiversity of microorganisms. Marine-derived fungi are a rich source of novel metabolites with unique structural features, bioactivities, and biotechnological applications. Marine-associated *Cladosporium* species have attracted considerable interest because of their ability to produce a wide array of metabolites, including alkaloids, macrolides, diketopiperazines, pyrones, tetralones, sterols, phenolics, terpenes, lactones, and tetramic acid derivatives that possess versatile bioactivities. Moreover, they produce diverse enzymes with biotechnological and industrial relevance. This review gives an overview on the *Cladosporium* species derived from marine habitats, including their metabolites and bioactivities, as well as the industrial and biotechnological potential of these species. In the current review, 286 compounds have been listed based on the reported data from 1998 until July 2021. Moreover, more than 175 references have been cited.

Keywords: bioactivity; biotechnology; *Cladosporium*; Cladosporiaceae; marine fungi; metabolite

Citation: Mohamed, G.A.; Ibrahim, S.R.M. Untapped Potential of Marine-Associated *Cladosporium* Species: An Overview on Secondary Metabolites, Biotechnological Relevance, and Biological Activities. *Mar. Drugs* **2021**, *19*, 645. https://doi.org/10.3390/md19110645

Academic Editor: Ipek Kurtboke

Received: 21 October 2021
Accepted: 16 November 2021
Published: 18 November 2021

1. Introduction

The marine environment covers approximately 70% of the Earth's surface and represents an enormous pool of biodiversity resources [1–3]. Marine microorganisms possess the potential for several biotechnological and industrial applications and play an important ecological role [4,5]. The last decades have witnessed numerous studies in the natural metabolites derived from marine creatures or their associated microorganisms [6–8]. Marine-derived fungi consist of a wide range of parasites, saprotrophs, symbionts, epiphytes, and endophytes [9,10]. They can be obtained from various marine samples such as algae, seagrasses, corals, sponges, ascidians, crustaceans, bivalves, fishes, and inorganic matter [11,12]. Jones et al. reported 530 marine taxa in 321 genera, which included 12 Basidiomycota (nine genera), 94 asexual morphs (61 genera), and 424 Ascomycota (251 genera) [13]. In 2011, the number of marine fungi was estimated to be 10,000 to 12,500 species based on substrates and geographical locations [14]. Currently, 1901 species have been listed on the marine fungi website, in 769 genera, 88 orders, 226 families, 22 classes, and seven phyla [15]. They are acknowledged as a rich source of novel metabolites with unique structural features, bioactivities, and biotechnological applications that attracted the attention of many biologists and chemists [16]. *Cladosporium* (Cladosporiaceae) is one of the largest genera of dematiaceous hyphomycetes [17]. *Cladosporium* species are frequent airborne molds, which can be isolated from almost every environment and geographic location, because their small conidia are easily dispersed [18–21]. *C. herbarum*, *C. cladosporioides*, and *C. sphaerospermum* are its three major species [22]. It comprises many important plant pathogens causing stem rots and leaf spots such as *C. fulvum* is the causal agent of tomato leaf mold [23,24]. Some

species are also known as common contaminants in clinical laboratories and cause allergic lung diseases [25–28]. Some species have been reported as endophytes and possessed a positive influence, for example, *C. sphaerospermum* isolated from *Glycine max* roots which can promote its growth [29]. Several species were linked to allergic rhinitis and respiratory arrest in asthmatic patients, and some are described as a cause of opportunistic phaeohyphomycosis, including subcutaneous and deep infections in humans and animals [30,31]. Some species are fungicolous that possess a potential for biological control in agriculture and forestry [32,33]. Moreover, many *Cladosporium* species have the potential to be used in various industrial processes [34,35]. Marine-associated *Cladosporium* species have attracted considerable interest because of their ability to produce a wide array of metabolites, including macrolides, pyrones, phenolics, alkaloids, diketopiperazines, terpenes, sterols, quinones, lactones, and tetramic acid derivatives. These metabolites possess versatile bioactivities such as anticancer, antimicrobial, antiviral, insecticidal, antifouling, anti-malarial, anti-hyperlipidemic, and α-glucosidase and protein tyrosine phosphatase inhibiton [36–42]. It has been shown that these species have significant impacts on biotechnology, ecosystems, and food production. They are a wealthy source of enzymes such as pectinases, agarases, carrageenases, xylanases, laccases, peroxidases, tannases, invertases, cellulases, and reductases that have wide biotechnological influences in developing eco-friendly technologies in the pulp and paper industry, food and feed industries, biomasses and contaminants bioremediation and biodegradation, and generation chemicals and liquid fuels [11,12,43–50]. The main goal of this review is the focus on the reported research in *Cladosporium* species derived from a marine habitat, including the structures and bioactivities of the reported metabolites, as well as the industrial and biotechnological potential of these species (Tables 1 and 2). This work covers the studies that have appeared in literature from 1998 until July 2021. The structures and bioactivities of reported metabolites from *Cladosporium* species have been highlighted. Furthermore, the biotechnological and industrial potential of *Cladosporium* species has been summarized. We hope that this work can provide knowledge that can help for the dereplication and bioactivities evaluation of these marine-associated *Cladosporium* species. The present data were collected through the search on the various databases, including Web of Knowledge, ScienceDirect, SCOPUS, Taylor & Francis, Wiley Online Library, PubMed, JACS, Springer, and Google Scholar.

2. Importance of Marine Associated *Cladosporium* Species

Recently, cold-active microbial enzymes have attracted a great attention, and they are preferred to the thermophilic and mesophilic enzymes due to the reduction in the energy expenditure and costs of processing accompanied by industrial heating steps [51]. Many marine-associated *Cladosporium* species display noticeable enzyme production capacity. Many of these enzymes are exclusively produced at low temperature and high salt concentrations. Therefore, they play a substantial ecological role in lignin-cellulosic materials decomposition in the marine environment. Besides, these enzymes can be utilized in various biotechnological applications and allow the performance of industrial processes even in harsh conditions. In this review, the biotechnological and industrial relevance of *Cladosporium* species has been highlighted.

The polycyclic aromatic hydrocarbons (PAHs) are volatile pollutants that can cause various environmental pollutions such as oceanic and freshwater contamination, which can take place during storage, use, or transportation of crude oil and its products. PAHs inhalation or ingestion through contaminated food and airborne contaminants leads to serious health disorders such as endocrine disruption, cancer, and reproductive and birth problems [52]. Therefore, introducing marine-adapted microorganisms to increase the PAH-biodegradation rate is an important approach to reduce PAHs concentration in the contaminated regions. Investigation of the PAH biodegradation potential of various marine-derived fungi revealed that *Cladosporium* sp. CBMAI 1237 had a great potential for bioremediation and biodegradation of PAHs (e.g., anthracene, anthrone, anthraquinone, acenaphthene, phenanthrene, fluorene, pyrene fluoranthene, and nitropyrene) even in a non-marine environment [44].

Table 1. Secondary metabolites reported from marine associated *Cladosporium* species.

Compound Name	Mol. Wt.	Mol. Formula	Fungal Source	Host (Sample, Family)	Place	Ref.
1. Tetramic acid derivatives						
Cladosin A (**1**)	282	$C_{14}H_{22}N_2O_4$	*C. sphaerospermum* 2005-01-E3	Deep-sea sludge, Pacific Ocean	Qingdao, China	[42]
Cladosin B (**2**)	268	$C_{13}H_{20}N_2O_4$	*C. sphaerospermum* 2005-01-E3	Deep-sea sludge, Pacific Ocean	Qingdao, China	[42]
			C. sphaerospermum SW67	*Hydractinia echinata* (Marine hydroid, Hydractiniidae)	South Korea	[53]
Cladosin C (**3**)	250	$C_{13}H_{18}N_2O_3$	*C. sphaerospermum* 2005-01-E3	Deep-sea sludge, Pacific Ocean	Qingdao, China	[42]
			C. sphaerospermum SW67	*Hydractinia echinata* (Marine hydroid, Hydractiniidae)	South Korea	[53]
Cladosin D (**4**)	250	$C_{13}H_{18}N_2O_3$	*C. sphaerospermum* 2005-01-E3	Deep-sea sludge, Pacific Ocean	Qingdao, China	[42]
Cladosin F (**5**)	268	$C_{13}H_{20}N_2O_4$	*C. sphaerospermum* 2005-01-E3	Deep-sea sludge, Pacific Ocean	Qingdao, China	[54]
			C. sphaerospermum SW67	*Hydractinia echinata* (Marine hydroid, Hydractiniidae)	South Korea	[53]
Cladosin G (**6**)	282	$C_{14}H_{22}N_2O_4$	*C. sphaerospermum* 2005-01-E3	Deep-sea sludge, Pacific Ocean	Qingdao, China	[54]
Cladosin H (**7**)	358	$C_{20}H_{26}N_2O_4$	*C. sphaerospermum* L3P3	Marine sediment	Mariana Trench, South Pacific Ocean, China	[55]
Cladosin I (**8**)	358	$C_{20}H_{26}N_2O_4$	*C. sphaerospermum* L3P3	Marine sediment	Mariana Trench, South Pacific Ocean, China	[55]
Cladosin J (**9**)	419	$C_{25}H_{29}N_3O_3$	*C. sphaerospermum* L3P3	Marine sediment	Mariana Trench, South Pacific Ocean, China	[55]
Cladosin K (**10**)	419	$C_{25}H_{29}N_3O_3$	*C. sphaerospermum* L3P3	Marine sediment	Mariana Trench, South Pacific Ocean, China	[55]
Cladosin L (**11**)	270	$C_{13}H_{22}N_2O_4$	*C. sphaerospermum* SW67	*Hydractinia echinata* (Marine hydroid, Hydractiniidae)	South Korea	[53]
Cladosporicin A (**12**)	401	$C_{21}H_{27}N_3O_5$	*C. sphaerospermum* SW67	*Hydractinia echinata* (Marine hydroid, Hydractiniidae)	South Korea	[38]
Cladodionen (**13**)	233	$C_{13}H_{15}NO_3$	*Cladosporium* sp. OUCMDZ-1635	Unidentified sponge	Xisha Islands, China	[56]
			C. sphaerospermum EIODSF 008.	Deep sea sediment	East Indian Ocean, China	[57]
			C. sphaerospermum L3P3	Marine sediment	Mariana Trench, South Pacific Ocean, China	[55]
Cladosporiumin A (**14**)	349	$C_{19}H_{27}NO_5$	*Cladosporium* sp. SCSIO z0025	Deep sea sediment	Okinawa, Japan	[58]
Cladosporiumin B (**15**)	349	$C_{19}H_{27}NO_5$	*Cladosporium* sp. SCSIO z0025	Deep sea sediment	Okinawa, Japan	[58]
Cladosporiumin C (**16**)	349	$C_{19}H_{27}NO_5$	*Cladosporium* sp. SCSIO z0025	Deep sea sediment	Okinawa, Japan	[58]
Cladosporiumin D (**17**)	253	$C_{13}H_{19}NO_4$	*Cladosporium* sp. SCSIO z0025	Deep sea sediment	Okinawa, Japan	[58]
Cladosporiumin E (**18**)	251	$C_{13}H_{17}NO_4$	*Cladosporium* sp. SCSIO z0025	Deep sea sediment	Okinawa, Japan	[58]
Cladosporiumin F (**19**)	269	$C_{13}H_{19}NO_5$	*Cladosporium* sp. SCSIO z0025	Deep sea sediment	Okinawa, Japan	[58]
Cladosporiumin G (**20**)	253	$C_{13}H_{19}NO_4$	*Cladosporium* sp. SCSIO z0025	Deep sea sediment	Okinawa, Japan	[58]
Cladosporiumin H (**21**)	285	$C_{14}H_{23}NO_5$	*Cladosporium* sp. SCSIO z0025	Deep sea sediment	Okinawa, Japan	[58]
Cladosporiumin I (**22**)	235	$C_{13}H_{17}NO_3$	*C. sphaerospermum* EIODSF 008.	Deep sea sediment	East Indian Ocean, China	[57]
Cladosporiumin J (**23**)	251	$C_{13}H_{17}NO_4$	*C. sphaerospermum* EIODSF 008.	Deep sea sediment	East Indian Ocean, China	[57]
Cladosporiumin K (**24**)	251	$C_{13}H_{17}NO_4$	*C. sphaerospermum* EIODSF 008.	Deep sea sediment	East Indian Ocean. China	[57]
Cladosporiumin L (**25**)	887	$C_{41}H_{65}N_3O_{15}Mg_2$	*C. sphaerospermum* EIODSF 008.	Deep sea sediment	East Indian Ocean, China	[57]
Cladosporiumin M (**26**)	233	$C_{13}H_{15}NO_3$	*C. sphaerospermum* EIODSF 008.	Deep sea sediment	East Indian Ocean, China	[57]
Cladosporiumin N (**27**)	253	$C_{13}H_{19}NO_4$	*C. sphaerospermum* EIODSF 008.	Deep sea sediment	East Indian Ocean. China	[57]
Cladosporiumin O (**28**)	251	$C_{13}H_{17}NO_4$	*C. sphaerospermum* EIODSF 008.	Deep sea sediment	East Indian Ocean, China	[57]
Cladosporiumin I (**29**)	349	$C_{19}H_{27}NO_5$	*C. sphaerospermum SW67*	*Hydractinia echinata* (Marine hydroid, Hydractiniidae)	South Korea	[38]
Cladosporiumin J (**30**)	349	$C_{19}H_{27}NO_5$	*C. sphaerospermum SW67*	*Hydractinia echinata* (Marine hydroid, Hydractiniidae)	South Korea	[38]
2. Diketopiperazines						
Cyclo-(Pro, Trp) (**31**)	283	$C_{16}H_{17}N_3O_2$	*Cladosporium* sp. EF424419	*Porphyra yezoensis* (Red alga, Bangiaceae)	Lianyungang, Jiangsu, China	[59]

Table 1. *Cont.*

Compound Name	Mol. Wt.	Mol. Formula	Fungal Source	Host (Sample, Family)	Place	Ref.
Cyclo-(Val-Pro) (**32**)	196	$C_{10}H_{16}N_2O_2$	*Cladosporium* sp. EF424419	*Porphyra yezoensis* (Red alga, Bangiaceae)	Lianyungang, Jiangsu, China	[59]
Cyclo-(Phe-Pro) (**33**)	244	$C_{14}H_{16}N_2O_2$	*Cladosporium* sp. F14	Seawater from mangrove stand	Kei Ling Ha Lo Wai, Sai Kung, China	[60]
Cyclo-(Phe-Val) (**34**)	246	$C_{14}H_{18}N_2O_2$	*Cladosporium* sp. F14	Seawater from mangrove stand	Kei Ling Ha Lo Wai, Sai Kung, China	[60]
Cyclo-(Gly-Leu) (**35**)	170	$C_8H_{14}N_2O_2$	*Cladosporium* sp. SCSIO41007	*Callyspongia* sp. (Sponge, Callyspongiidae)	Xuwen, Guangdong, China	[61]
Cladosporin A (**36**)	460	$C_{22}H_{24}N_2O_5S_2$	*Cladosporium* sp.	Marine sediment	Yangshashan Bay, Ningbo, Zhejiang, China	[62]
Cladosporin B (**37**)	442	$C_{22}H_{22}N_2O_4S_2$	*Cladosporium* sp.	Marine sediment	Yangshashan Bay, Ningbo, Zhejiang, China	[62]
Haematocin (**38**)	502	$C_{24}H_{26}N_2O_6S_2$	*Cladosporium* sp.	Marine sediment	Yangshashan Bay, Ningbo, Zhejiang, China	[62]
3. Alkaloids						
3.1. Indole alkaloids						
3.1.1 Simple indole alkaloids						
N-Acetyltryptamine (**39**)	202	$C_{12}H_{14}N_2O$	*Cladosporium* sp. EF424419	*Porphyra yezoensis* (Red alga, Bangiaceae)	Lianyungang, Jiangsu, China	[59]
N-methyl-1*H*-indole-2-carboxamide (**40**)	174	$C_{10}H_{10}N_2O$	*C. cladosporioides*	*Cliona* sp. (Sponge, Clionaidae)	Los Molles, Chile	[63]
Indole-3-carboxylic acid (**41**)	161	$C_9H_7NO_2$	*Cladosporium* sp. SCSIO41007	*Callyspongia* sp. (Sponge, Callyspongiidae)	Xuwen, Guangdong, China	[61]
3.1.2 Glyantrypine derivatives						
Glyantrypine (**42**)	344	$C_{20}H_{16}N_4O_2$	*Cladosporium* sp. PJX-41	Soil around a mangrove	Guangzhou, China	[64]
3-Hydroxyglyantrypine (**43**)	360	$C_{20}H_{16}N_4O_3$	*Cladosporium* sp. PJX-41	Soil around a mangrove	Guangzhou, China	[64]
14*R*-Oxoglyantrypine (**44**)	358	$C_{20}H_{14}N_4O_3$	*Cladosporium* sp. PJX-41	Soil around a mangrove	Guangzhou, China	[64]
14*S*-Oxoglyantrypine (**45**)	358	$C_{20}H_{14}N_4O_3$	*Cladosporium* sp. PJX-41	Soil around a mangrove	Guangzhou, China	[64]
Prelapatin B (**46**)	344	$C_{20}H_{16}N_4O_2$	*Cladosporium* sp. PJX-41	Soil around a mangrove	Guangzhou, China	[64]
Cladoquinazoline (**47**)	418	$C_{23}H_{22}N_4O_4$	*Cladosporium* sp. PJX-41	Soil around a mangrove	Guangzhou, China	[64]
Epi-Cladoquinazoline (**48**)	418	$C_{23}H_{22}N_4O_4$	*Cladosporium* sp. PJX-41	Soil around a mangrove	Guangzhou, China	[64]
3.2. Quinazoline alkaloids						
Norquinadoline A (**49**)	471	$C_{26}H_{25}N_5O_4$	*Cladosporium* sp. PJX-41	Soil around a mangrove	Guangzhou, China	[64]
Quinadoline A (**50**)	485	$C_{27}H_{27}N_5O_5$	*Cladosporium* sp. PJX-41	Soil around a mangrove	Guangzhou, China	[64]
Deoxynortryptoquivaline (**51**)	516	$C_{28}H_{28}N_4O_6$	*Cladosporium* sp. PJX-41	Soil around a mangrove	Guangzhou, China	[64]
Deoxytryptoquivaline (**52**)	530	$C_{29}H_{30}N_4O_6$	*Cladosporium* sp. PJX-41	Soil around a mangrove	Guangzhou, China	[64]
Tryptoquivaline (**53**)	546	$C_{29}H_{30}N_4O_7$	*Cladosporium* sp. PJX-41	Soil around a mangrove	Guangzhou, China	[64]
CS-C (**54**)	546	$C_{29}H_{30}N_4O_7$	*Cladosporium* sp. PJX-41	Soil around a mangrove	Guangzhou, China	[64]
Quinadoline B (**55**)	439	$C_{25}H_{21}N_5O_3$	*Cladosporium* sp. PJX-41	Soil around a mangrove	Guangzhou, China	[64]
Circumdatin A (**56**)	391	$C_{22}H_{21}N_3O_4$	*Cladosporium* sp. MFC353-b	*Chondria crassicualis* (Red alga, Rhodomelaceae)	Yokji Island, Kyeongnam, Korea	[65]
3.3. Quinolone alkaloids						
Quinolactacin A1 (**57**)	270	$C_{16}H_{18}N_2O_2$	*C. oxysporum* BRS2A-AR2F	*Conocarpus erectus* (Mangrove plant, Combretaceae) *Laguncularia racemosa* (Mangrove plant, Combretaceae) *Rhizophora racemosa* (Mangrove plant, Rhizophoraceae)	Banks of the River Butre, Western Region of Ghana	[66]

Table 1. *Cont.*

Compound Name	Mol. Wt.	Mol. Formula	Fungal Source	Host (Sample, Family)	Place	Ref.
Quinolactacin A2 (**58**)	270	$C_{16}H_{18}N_2O_2$	*C. oxysporum* BRS2A-AR2F	*Conocarpus erectus* (Mangrove plant, Combretaceae) *Laguncularia racemosa* (Mangrove plant, Combretaceae) *Rhizophora racemosa* (Mangrove plant, Rhizophoraceae)	Banks of the River Butre, Western Region of Ghana	[66]
Quinolactacin B1 (**59**)	256	$C_{15}H_{16}N_2O_2$	*C. oxysporum* BRS2A-AR2F	*Conocarpus erectus* (Mangrove plant, Combretaceae) *Laguncularia racemosa* (Mangrove plant, Combretaceae) *Rhizophora racemosa* (Mangrove plant, Rhizophoraceae)	Banks of the River Butre, Western Region of Ghana	[66]
Quinolactacin B2 (**60**)	256	$C_{15}H_{16}N_2O_2$	*C. oxysporum* BRS2A-AR2F	*Conocarpus erectus* (Mangrove plant, Combretaceae) *Laguncularia racemosa* (Mangrove plant, Combretaceae) *Rhizophora racemosa* (Mangrove plant, Rhizophoraceae)	Banks of the River Butre, Western Region of Ghana	[66]
Quinolactacin C1 (**61**)	286	$C_{16}H_{18}N_2O_3$	*C. oxysporum* BRS2A-AR2F	*Conocarpus erectus* (Mangrove plant, Combretaceae) *Laguncularia racemosa* (Mangrove plant, Combretaceae) *Rhizophora racemosa* (Mangrove plant, Rhizophoraceae)	Banks of the River Butre, Western Region of Ghana	[66]
Quinolactacin C2 (**62**)	286	$C_{16}H_{18}N_2O_3$	*C. oxysporum* BRS2A-AR2F	*Conocarpus erectus* (Mangrove plant, Combretaceae) *Laguncularia racemosa* (Mangrove plant, Combretaceae) *Rhizophora racemosa* (Mangrove plant, Rhizophoraceae)	Banks of the River Butre, Western Region of Ghana	[66]
Quinolactacin D1 (**63**)	286	$C_{16}H_{18}N_2O_3$	*C. oxysporum* BRS2A-AR2F	*Conocarpus erectus* (Mangrove plant, Combretaceae) *Laguncularia racemosa* (Mangrove plant, Combretaceae) *Rhizophora racemosa* (Mangrove plant, Rhizophoraceae)	Banks of the River Butre, Western Region of Ghana	[66]
Quinolactacin D2 (**64**)	286	$C_{16}H_{18}N_2O_3$	*C. oxysporum* BRS2A-AR2F	*Conocarpus erectus* (Mangrove plant, Combretaceae) *Laguncularia racemosa* (Mangrove plant, Combretaceae) *Rhizophora racemosa* (Mangrove plant, Rhizophoraceae)	Banks of the River Butre, Western Region of Ghana	[66]
Quinocitrinine A (**65**)	272	$C_{16}H_{19}N_2O_2$	*C. oxysporum* BRS2A-AR2F	*Conocarpus erectus* (Mangrove plant, Combretaceae) *Laguncularia racemosa* (Mangrove plant, Combretaceae) *Rhizophora racemosa* (Mangrove plant, Rhizophoraceae)	Banks of the River Butre, Western Region of Ghana	[66]
Quinocitrinine B (**66**)	272	$C_{16}H_{19}N_2O_2$	*C. oxysporum* BRS2A-AR2F	*Conocarpus erectus* (Mangrove plant, Combretaceae) *Laguncularia racemosa* (Mangrove plant, Combretaceae) *Rhizophora racemosa* (Mangrove plant, Rhizophoraceae)	Banks of the River Butre, Western Region of Ghana	[66]

Table 1. *Cont.*

Compound Name	Mol. Wt.	Mol. Formula	Fungal Source	Host (Sample, Family)	Place	Ref.
Quinolactacide (**67**)	236	$C_{14}H_8N_2O_2$	*C. oxysporum* BRS2A-AR2F	*Conocarpus erectus* (Mangrove plant, Combretaceae) *Laguncularia racemosa* (Mangrove plant, Combretaceae) *Rhizophora racemosa* (Mangrove plant, Rhizophoraceae)	Banks of the River Butre, Western Region of Ghana	[66]
3.4. Citrinadin derivatives						
Citrinadin A (**68**)	624	$C_{35}H_{52}N_4O_6$	*C. oxysporum* BRS2A-AR2F	*Conocarpus erectus* (Mangrove plant, Combretaceae) *Laguncularia racemosa* (Mangrove plant, Combretaceae) *Rhizophora racemosa* (Mangrove plant, Rhizophoraceae)	Banks of the River Butre, Western Region of Ghana	[66]
Citrinadin B (**69**)	481	$C_{28}H_{39}N_3O_4$	*C. oxysporum* BRS2A-AR2F	*Conocarpus erectus* (Mangrove plant, Combretaceae) *Laguncularia racemosa* (Mangrove plant, Combretaceae) *Rhizophora racemosa* (Mangrove plant, Rhizophoraceae)	Banks of the River Butre, Western Region of Ghana	[66]
Butrecitrinadin (**70**)	682	$C_{38}H_{57}N_4O_7$	*C. oxysporum* BRS2A-AR2F	*Conocarpus erectus* (Mangrove plant, Combretaceae) *Laguncularia racemosa* (Mangrove plant, Combretaceae) *Rhizophora racemosa* (Mangrove plant, Rhizophoraceae)	Banks of the River Butre, Western Region of Ghana	[66]
PF1270 A (**71**)	566	$C_{32}H_{43}N_3O_6$	*C. oxysporum* BRS2A-AR2F	*Conocarpus erectus* (Mangrove plant, Combretaceae) *Laguncularia racemosa* (Mangrove plant, Combretaceae) *Rhizophora racemosa* (Mangrove plant, Rhizophoraceae)	Banks of the River Butre, Western Region of Ghana	[66]
PF1270 B (**72**)	552	$C_{31}H_{41}N_3O_6$	*C. oxysporum* BRS2A-AR2F	*Conocarpus erectus* (Mangrove plant, Combretaceae) *Laguncularia racemosa* (Mangrove plant, Combretaceae) *Rhizophora racemosa* (Mangrove plant, Rhizophoraceae)	Banks of the River Butre, Western Region of Ghana	[66]
PF1270 C (**73**)	538	$C_{30}H_{39}N_3O_6$	*C. oxysporum* BRS2A-AR2F	*Conocarpus erectus* (Mangrove plant, Combretaceae) *Laguncularia racemosa* (Mangrove plant, Combretaceae) *Rhizophora racemosa* (Mangrove plant, Rhizophoraceae)	Banks of the River Butre, Western Region of Ghana	[66]
3.5. Pyrrolidine derivatives						
Cladosporitin A (**74**)	505	$C_{32}H_{43}NO_4$	*Cladosporium* sp. HNWSW-1	*Ceriops tagal* (Mangrove plant, Rhizophoraceae)	Dong Zhai Gang, Hainan, China	[67]
Cladosporitin B (**75**)	505	$C_{32}H_{43}NO_4$	*Cladosporium* sp. HNWSW-1	*Ceriops tagal* (Mangrove plant, Rhizophoraceae)	Dong Zhai Gang, Hainan, China	[67]
Talaroconvolutin A (**76**)	487	$C_{32}H_{41}NO_3$	*Cladosporium* sp. HNWSW-1	*Ceriops tagal* (Mangrove plant, Rhizophoraceae)	Dong Zhai Gang, Hainan, China	[67]
Cladosporamide A (**77**)	273	$C_{14}H_{11}NO_5$	*Cladosporium* sp. TPU1507	Unidentified marine sponge	Manado, Indonesia	[68]

Table 1. *Cont.*

Compound Name	Mol. Wt.	Mol. Formula	Fungal Source	Host (Sample, Family)	Place	Ref.
3.6. Other class of alkaloids						
Cladosporilactam A (**78**)	181	$C_{10}H_{15}NO_2$	*Cladosporium* sp. RA07-1	*Anthogorgia ochracea* (Gorgonian, Acanthogorgiidae)	Weizhou coral reef, South China Sea	[69]
Cladospamide A (**79**)	268	$C_{13}H_{20}N_2O_4$	*Cladosporium* sp. SCNU-F0001	Mangrove plant	Zhuhai Mangrove Nature, Guangdong, China	[70]
Cladosporin A (**80**)	233	$C_{13}H_{15}NO_3$	*C. cladosporioides* SCSIO z015	Deep sea sediment	Okinawa, Japan	[36]
Cladosporin B (**81**)	233	$C_{13}H_{15}NO_3$	*C. cladosporioides* SCSIO z015	Deep sea sediment	Okinawa, Japan	[36]
2′-Deoxythymidine (**82**)	241	$C_{11}H_{15}NO_5$	*Cladosporium* sp. SCSIO41007	*Callyspongia* sp. (Sponge, Callyspongiidae)	Xuwen, Guangdong, China	[61]
Nicotinic acid (**83**)	123	$C_6H_5NO_2$	*Cladosporium* sp. EF424419	*Porphyra yezoensis* (Red alga, Bangiaceae)	Lianyungang, Jiangsu, China	[59]
2-Methylacetate-3,5,6-trimethylpyrazine (**84**)	194	$C_{10}H_{14}N_2O_2$	*Cladosporium* sp. JS1-2	*Ceriops tagal* (Mangrove plant, Rhizophoraceae)	Dongzhaigang, Hainan, China	[71]
Cytochalasin D (**85**)	507	$C_{30}H_{37}NO_6$	*Cladosporium* sp. JS1-2	*Ceriops tagal* (Mangrove plant, Rhizophoraceae)	Dongzhaigang, Hainan, China	[71]
Cladosin E (**86**)	251	$C_{13}H_{17}NO_4$	*C. sphaerospermum* 2005-01-E3	Deep-sea sludge, Pacific Ocean	Qingdao, China	[42]
N-Acetyltyramine (**87**)	179	$C_{10}H_{13}NO_2$	*Cladosporium* sp. EF424419	*Porphyra yezoensis* (Red alga, Bangiaceae)	Lianyungang, Jiangsu, China	[59]
4. Macrolides						
Cladospolide A (**88**)	228	$C_{12}H_{20}O_4$	*Cladosporium* sp. FT-0012	Sponge	Pohnpei island, Federated State of Micronesia	[72]
			Cladosporium sp. IFB3lp-2	*Rhizophora stylosa* (Mangrove plant, Rhizophoraceae)	Mangrove forest, Hainan, China	[73]
Cladospolide B (**89**)	228	$C_{12}H_{20}O_4$	*Cladosporium* sp. FT-0012	Sponge	Pohnpei island, Federated State of Micronesia	[72]
			C. herbarum (Pers.)	*Callyspongia aerizusa* (Sponge, Callyspongiidae)	Bali Bata National Park, Indonesia,	[74]
			Cladosporium sp. RA07-1	*Anthogorgia ochracea* (Gorgonian, Acanthogorgiidae)	Weizhou coral reef, South China Sea	[69]
			Cladosporium sp. SCNU-F0001	Mangrove plant	Zhuhai Mangrove Nature, Guangdong, China	[70]
Cladospolide C (**90**)	228	$C_{12}H_{20}O_4$	*C. cladosporioides* MCCC 3A00182	Marine sediment	Southwest Pacific Ocean	[75]
Cladospolide D (**91**)	226	$C_{12}H_{18}O_4$	*Cladosporium* sp. FT-0012	Sponge	Pohnpei island, Federated State of Micronesia	[72]
Cladospolide E (**92**)	188	$C_8H_{12}O_5$	*Cladosporium* sp. F14.	Seawater nearby mangrove stand	Kei Ling Ha Lo Wai, Sai Kung, Hong Kong, China	[76]
Pandangolide 1 (**93**)	244	$C_{12}H_{20}O_5$	*Cladosporium* sp.	*Niphates rowi* (Sponge, Niphatidae)	Gulf of Aqaba, Israel	[77]
			Cladosporium sp. F14	Seawater from mangrove stand	Kei Ling Ha Lo Wai, Sai Kung, China	[60]
			Cladosporium sp. IFB3lp-2	*Rhizophora stylosa* (Mangrove plant, Rhizophoraceae)	Mangrove forest, Hainan, China	[73]
			C. cladosporioides MA-299	*Bruguiera gymnorrhiza* (Mangrove plant, Rhizophoraceae)	Hainan Island, China	[40]
Pandangolide 1a (**94**)	244	$C_{12}H_{20}O_5$	*Cladosporium* sp.	*Niphates rowi* (Sponge, Niphatidae)	Gulf of Aqaba, Israel	[77]
			Cladosporium sp. IFB3lp-2	*Rhizophora stylosa* (Mangrove plant, Rhizophoraceae)	Mangrove forest, Hainan, China	[73]
Pandangolide 2 (**95**)	318	$C_{14}H_{22}O_6S$	*C. herbarum* (Pers.)	*Callyspongia aerizusa* (Sponge, Callyspongiidae)	Bali Bata National Park, Indonesia	[74]
			Cladosporium sp. IFB3lp-2	*Rhizophora stylosa* (Mangrove plant, Rhizophoraceae)	Mangrove forest, Hainan, China	[73]

Table 1. *Cont.*

Compound Name	Mol. Wt.	Mol. Formula	Fungal Source	Host (Sample, Family)	Place	Ref.
Pandangolide 3 (**96**)	362	$C_{16}H_{26}O_7S$	*C. herbarum* (Pers.)	*Callyspongia aerizusa* (Sponge, Callyspongiidae)	Bali Bata National Park, Indonesia,	[74]
			Cladosporium sp. IFB3lp-2	*Rhizophora stylosa* (Mangrove plant, Rhizophoraceae)	Mangrove forest, Hainan, China	[73]
			C. cladosporioides MA-299	*Bruguiera gymnorrhiza* (Mangrove plant, Rhizophoraceae)	Hainan Island, China	[39]
			C. oxysporum HDN13-314	*Avicennia marina* (Mangrove plant, Acanthaceae)	Hainan, China	[78]
Pandangolide 4 (**97**)	486	$C_{24}H_{38}O_8S$	*C. herbarum* (Pers.)	*Callyspongia aerizusa* (Sponge, Callyspongiidae)	Bali Bata National Park, Indonesia	[74]
5*R*-Hydroxyrecifeiolide (**98**)	212	$C_{12}H_{20}O_3$	*C. cladosporioides* MA-299	*Bruguiera gymnorrhiza* (Mangrove plant, Rhizophoraceae)	Hainan Island, China	[40]
5*S*-Hydroxyrecifeiolide (**99**)	212	$C_{12}H_{20}O_3$	*C. cladosporioides* MA-299	*Bruguiera gymnorrhiza* (Mangrove plant, Rhizophoraceae)	Hainan Island, China	[40]
Methyl 2-(((4R,6R,12R)-6-hydroxy-12-methyl-2,5-dioxooxacyclododecan-4-yl)thio)acetate (**100**)	332	$C_{15}H_{24}O_6S$	*Cladosporium* sp. IFB3lp-2	*Rhizophora stylosa* (Mangrove plant, Rhizophoraceae)	Mangrove forest, Hainan, China	[73]
Thiocladospolide A (**101**)	346	$C_{16}H_{26}O_6S$	*C. cladosporioides* MA-299	*Bruguiera gymnorrhiza* (Mangrove plant, Rhizophoraceae)	Hainan Island, China	[39]
			C. oxysporum HDN13-314	*Avicennia marina* (Mangrove plant, Acanthaceae)	Hainan, China	[78]
Thiocladospolide B (**102**)	360	$C_{16}H_{24}O_7S$	*C. cladosporioides* MA-299	*Bruguiera gymnorrhiza* (Mangrove plant, Rhizophoraceae)	Hainan Island, China	[39]
Thiocladospolide C (**103**)	330	$C_{15}H_{22}O_6S$	*C. cladosporioides* MA-299	*Bruguiera gymnorrhiza* (Mangrove plant, Rhizophoraceae)	Hainan Island, China	[39]
Thiocladospolide D (**104**)	364	$C_{16}H_{28}O_7S$	*C. cladosporioides* MA-299	*Bruguiera gymnorrhiza* (Mangrove plant, Rhizophoraceae)	Hainan Island, China	[39]
Thiocladospolide E (**105**)	306	$C_{14}H_{26}O_5S$	*Cladosporium* sp. SCNU-F0001	Mangrove plant	Zhuhai Mangrove Nature, Guangdong, China	[70]
Thiocladospolide F (**106**)	332	$C_{16}H_{28}O_5S$	*C. cladosporioides* MA-299	*Bruguiera gymnorrhiza* (Mangrove plant, Rhizophoraceae)	Hainan Island, China	[79]
Thiocladospolide F (**107**)	386	$C_{24}H_{38}O_8S$	*C. oxysporum* HDN13-314	*Avicennia marina* (Mangrove plant, Acanthaceae)	Hainan, China	[78]
Thiocladospolide G (**108**)	348	$C_{16}H_{28}O_6S$	*C. cladosporioides* MA-299	*Bruguiera gymnorrhiza* (Mangrove plant, Rhizophoraceae)	Hainan Island, China	[79]
Thiocladospolide G (**109**)	348	$C_{15}H_{24}O_7S$	*C. oxysporum* HDN13-314	*Avicennia marina* (Mangrove plant, Acanthaceae)	Hainan, China	[78]
Thiocladospolide H (**110**)	332	$C_{15}H_{24}O_6S$	*C. oxysporum* HDN13-314	*Avicennia marina* (Mangrove plant, Acanthaceae)	Hainan, China	[78]
Thiocladospolide I (**111**)	560	$C_{27}H_{44}O_{10}S$	*C. oxysporum* HDN13-314	*Avicennia marina* (Mangrove plant, Acanthaceae)	Hainan, China	[78]
Thiocladospolide J (**112**)	558	$C_{27}H_{42}O_{10}S$	*C. oxysporum* HDN13-314	*Avicennia marina* (Mangrove plant, Acanthaceae)	Hainan, China	[78]
Sporiolide A (**113**)	348	$C_{19}H_{24}O_6$	*Cladosporium* sp. L037	*Actinotrichia fragilis* (Red alga, Galaxauraceae)	Seragaki Beach, Okinawa Island, Japan	[80]
Sporiolide B (**114**)	258	$C_{13}H_{22}O_5$	*Cladosporium* sp. L037	*Actinotrichia fragilis* (Red alga, Galaxauraceae)	Seragaki Beach, Okinawa Island, Japan	[80]
(6*R*,12*S*)-6-Hydroxy-12-methyl-1-oxacyclododecane-2,5-dione (**115**)	228	$C_{12}H_{20}O_4$	*Cladosporium* sp. F14	Seawater from the mangrove stand	Kei Ling Ha Lo Wai, Sai Kung, China	[60]

Table 1. *Cont.*

Compound Name	Mol. Wt.	Mol. Formula	Fungal Source	Host (Sample, Family)	Place	Ref.
(3*R*,6*S*)-6-Hydroxy-12-methyl-2,5-dioxooxacyclododecan-3-yl (E)-4,11-dihydroxydodec-2-enoate (**116**)	456	$C_{24}H_{40}O_8$	*Cladosporium* sp. IFB3lp-2	*Rhizophora stylosa* (Mangrove plant, Rhizophoraceae)	Mangrove forest, Hainan, China	[73]
Dendrodolide A (**117**)	256	$C_{13}H_{20}O_5$	*Cladosporium* sp. RA07-1	*Anthogorgia ochracea* (Gorgonian, Acanthogorgiidae)	Weizhou coral reef, South China Sea	[69]
Dendrodolide C (**118**)	242	$C_{12}H_{18}O_5$	*Cladosporium* sp. RA07-1	*Anthogorgia ochracea* (Gorgonian, Acanthogorgiidae)	Weizhou coral reef, South China Sea	[69]
Dendrodolide L (**119**)	228	$C_{12}H_{20}O_4$	*Cladosporium* sp. RA07-1	*Anthogorgia ochracea* (Gorgonian, Acanthogorgiidae)	Weizhou coral reef, South China Sea	[69]
Dendrodolide M (**120**)	256	$C_{13}H_{20}O_5$	*Cladosporium* sp. RA07-1	*Anthogorgia ochracea* (Gorgonian, Acanthogorgiidae)	Weizhou coral reef, South China Sea	[69]
Cladocladosin A (**121**)	224	$C_{12}H_{16}O_4$	*C. cladosporioides* MA-299	*Bruguiera gymnorrhiza* (Mangrove plant, Rhizophoraceae)	Hainan Island, China	[79]
5. Butenolides and butanolides						
Cladospolide F (**122**)	230	$C_{12}H_{22}O_4$	*Cladosporium* sp. TZP29	Unidentified soft coral	Guangzhou, China	[41]
Ent-cladospolide F (**123**)	230	$C_{14}H_{24}O_5$	*C. cladosporioides* MA-299	*Bruguiera gymnorrhiza* (Mangrove plant, Rhizophoraceae)	Hainan Island, China	[40]
Cladospolide G (**124**)	272	$C_{14}H_{24}O_5$	*C. cladosporioides* MA-299	*Bruguiera gymnorrhiza* (Mangrove plant, Rhizophoraceae)	Hainan Island, China	[40]
11-Hydroxy-γ-dodecalactone (**125**)	214	$C_{12}H_{22}O_3$	*Cladosporium* sp. TZP29	Unidentified soft coral	Guangzhou, China	[41]
Iso-Cladospolide B (**126**)	228	$C_{12}H_{20}O_4$	*C. herbarum* (Pers.)	*Callyspongia aerizusa* (Sponge, Callyspongiidae)	Bali Bata National Park, Indonesia,	[74]
			Cladosporium sp.	*Niphates rowi* (Sponge, Niphatidae)	Gulf of Aqaba, Israel	[77]
			Cladosporium sp. F14	Seawater from the mangrove stand	Kei Ling Ha Lo Wai, Sai Kung, China	[60]
			Cladosporium sp. IFB3lp-2	*Rhizophora stylosa* (Mangrove plant, Rhizophoraceae)	Mangrove forest, Hainan, China	[73]
			Cladosporium sp. RA07-1	*Anthogorgia ochracea* (Gorgonian, Acanthogorgiidae)	Weizhou coral reef, South China Sea	[70]
			Cladosporium sp. TZP29	Unidentified soft coral	Guangzhou, China	[41]
			C. cladosporioides MA-299	*Bruguiera gymnorrhiza* (Mangrove plant, Rhizophoraceae)	Hainan Island, China	[40]
			C. oxysporum HDN13-314	*Avicennia marina* (Mangrove plant, Acanthaceae)	Hainan, China	[78]
Cladospolide H (**127**)	210	$C_{12}H_{18}O_3$	*C. cladosporioides* MA-299	*Bruguiera gymnorrhiza* (Mangrove plant, Rhizophoraceae)	Hainan Island, China	[40]
6. Seco-acids						
Cladospolide A II (**128**)			*Cladosporium* sp. IFB3lp-2	*Rhizophora stylosa* (Mangrove plant, Rhizophoraceae)	Mangrove forest, Hainan, China	[73]
Cladospolide E (**129**)	228	$C_{12}H_{20}O_4$	*Cladosporium* sp. TZP29	Unidentified soft coral	Guangzhou, China	[41]
Seco-Patulolide A (**130**)	228	$C_{12}H_{20}O_4$	*Cladosporium* sp. TZP29	Unidentified soft coral	Guangzhou, China	[41]
Seco-Patulolide C (**131**)	230	$C_{12}H_{22}O_4$	*Cladosporium* sp. F14	Seawater from the Mangrove stand	Kei Ling Ha Lo Wai, Sai Kung, China	[60]
			Cladosporium sp. TZP29	Unidentified soft coral	Guangzhou, China	[41]
			C. cladosporioides MA-299	*Bruguiera gymnorrhiza* (Mangrove plant, Rhizophoraceae)	Hainan Island, China	[39]
Seco-Secopatulolide C (**132**)	230	$C_{12}H_{22}O_4$	*C. oxysporum* HDN13-314	*Avicennia marina* (Mangrove plant, Acanthaceae)	Hainan, China	[78]
Cladosporester A (**133**)	244	$C_{13}H_{24}O_4$	*C. cladosporioides* OUCMDZ-187	*Rhizophora stylosa* (Mangrove plant, Rhizophoraceae)	Shankou, Guangxi, China	[81]

Table 1. *Cont.*

Compound Name	Mol. Wt.	Mol. Formula	Fungal Source	Host (Sample, Family)	Place	Ref.
Cladosporester B (**134**)	244	$C_{13}H_{24}O_4$	*C. cladosporioides* OUCMDZ-187	*Rhizophora stylosa* (Mangrove plant, Rhizophoraceae)	Shankou, Guangxi, China	[81]
Cladosporacid A (**135**)	230	$C_{12}H_{22}O_4$	*C. cladosporioides* OUCMDZ-187	*Rhizophora stylosa* (Mangrove plant, Rhizophoraceae)	Shankou, Guangxi, China	[81]
Cladosporacid B (**136**)	230	$C_{12}H_{22}O_4$	*C. cladosporioides* OUCMDZ-187	*Rhizophora stylosa* (Mangrove plant, Rhizophoraceae)	Shankou, Guangxi, China	[81]
Cladosporacid D (**137**)	228	$C_{12}H_{20}O_4$	*C. cladosporioides* OUCMDZ-187	*Rhizophora stylosa* (Mangrove plant, Rhizophoraceae)	Shankou, Guangxi, China	[81]
Cladosporester C (**138**)	288	$C_{14}H_{24}O_6$	*C. cladosporioides* OUCMDZ-187	*Rhizophora stylosa* (Mangrove plant, Rhizophoraceae)	Shankou, Guangxi, China	[81]
Cladosporacid C (**139**)	230	$C_{12}H_{22}O_4$	*C. cladosporioides* OUCMDZ-187	*Rhizophora stylosa* (Mangrove plant, Rhizophoraceae)	Shankou, Guangxi, China	[81]
Cladosporacid E (**140**)	200	$C_{10}H_{16}O_4$	*C. cladosporioides* OUCMDZ-187	*Rhizophora stylosa* (Mangrove plant, Rhizophoraceae)	Shankou, Guangxi, China	[81]
11-Hydroxy-4,5-dioxododecanoic acid (**141**)	244	$C_{10}H_{16}O_4$	*Cladosporium* sp. IFB3lp-2	*Rhizophora stylosa* (Mangrove plant, Rhizophoraceae)	Mangrove forest, Hainan, China	[73]
7. Tetralones (napthalenones)						
Cladosporol/Cladosporol A (**142**)	352	$C_{20}H_{16}O_6$	*Cladosporium* sp. KcFL6′	*Kandelia candel* (Mangrove plant, Rhizophoraceae)	Daya Bay, Shenzhen city, Guangdong, China	[82]
Cladosporol C (**143**)	338	$C_{20}H_{18}O_5$	*Cladosporium* sp. KcFL6′	*Kandelia candel* (Mangrove plant, Rhizophoraceae)	Daya Bay, Shenzhen city, Guangdong, China	[82]
			C. cladosporioides HDN14-342	Marine sediment	Indian Ocean, Qingdao, China	[83]
			C. cladosporioides EN-399	*Laurencia okamurai* (Red alga, Rhodomelaceae)	Qingdao, China	[84]
			Cladosporium sp. JS1-2	*Ceriops tagal* (Mangrove plant, Rhizophoraceae)	Dongzhaigang, Hainan, China	[71]
			C. cladosporioides MCCC 3A00182	Marine sediment	Southwest Pacific Ocean	[75]
Cladosporol D (**144**)	354	$C_{20}H_{18}O_6$	*Cladosporium* sp. KcFL6′	*Kandelia candel* (Mangrove plant, Rhizophoraceae)	Daya Bay, Shenzhen city, Guangdong, China	[82]
Cladosporol E (**145**)	370	$C_{20}H_{18}O_7$	*C. cladosporioides* HDN14-342	Marine sediment	Indian Ocean, Qingdao, China	[83]
			Cladosporium sp. JS1-2	*Ceriops tagal* (Mangrove plant, Rhizophoraceae)	Dongzhaigang, Hainan, China	[71]
Cladosporol F (**146**)	352	$C_{21}H_{20}O_5$	*C. cladosporioides* HDN14-342	Marine sediment	Indian Ocean, Qingdao, China	[83]
			C. cladosporioides EN-399	*Laurencia okamurai* (Red alga, Rhodomelaceae)	Qingdao, China	[84]
Cladosporol G (**147**)	388	$C_{20}H_{17}ClO_6$	*C. cladosporioides* HDN14-342	Marine sediment	Indian Ocean, Qingdao, China	[83]
Cladosporol G (**148**)	352	$C_{21}H_{20}O_5$	*C. cladosporioides* EN-399	*Laurencia okamurai* (Red alga, Rhodomelaceae)	Qingdao, China	[84]
Cladosporol H (**149**)	336	$C_{20}H_{16}O_5$	*C. cladosporioides* EN-399	*Laurencia okamurai* (Red alga, Rhodomelaceae)	Qingdao, China	[84]
Cladosporol I = Cladosperanol A (**150**)	338	$C_{20}H_{18}O_5$	*C. cladosporioides* EN-399	*Laurencia okamurai* (Rhodomelaceae)	Qingdao, China	[84]
			Cladosporium sp. KFD33	Blood cockle (Bivalve mollusk, Cardiidae)	Haikou Bay, China	[85]
	338	$C_{20}H_{18}O_5$	*C. perangustum* FS62	-	China	[86]
Cladosporol J (**151**)	338	$C_{20}H_{18}O_5$	*C. cladosporioides* EN-399	*Laurencia okamurai* (Red alga, Rhodomelaceae)	Qingdao, China	[84]
Cladosporone A (**152**)	352	$C_{20}H_{16}O_6$	*Cladosporium* sp. KcFL6′	*Kandelia candel* (Mangrove plant, Rhizophoraceae)	Daya Bay, Shenzhen city, Guangdong, China	[82]

Table 1. *Cont.*

Compound Name	Mol. Wt.	Mol. Formula	Fungal Source	Host (Sample, Family)	Place	Ref.
Altertoxin XII (**153**)	322	$C_{20}H_{18}O_4$	*Cladosporium* sp. KFD33	Blood cockle (Bivalve mollusk, Cardiidae)	Haikou Bay, China	[85]
Clindanone A (**154**)	394	$C_{22}H_{18}O_7$	*C. cladosporioides* HDN14-342	Marine sediment	Indian Ocean, Qingdao, China	[83]
Clindanone B (**155**)	394	$C_{22}H_{18}O_7$	*C. cladosporioides* HDN14-342	Marine sediment	Indian Ocean, Qingdao, China	[83]
	178	$C_{10}H_{10}O_3$	*C. perangustm* FS62	Marine sediment	South China Sea, china	[87]
Isosclerone = (-)-(4*R*)-Regiolone (**156**)	178	$C_{10}H_{10}O_3$	*C. cladosporioides* HDN14-342	Marine sediment	Indian Ocean, Qingdao, China	[83]
	178	$C_{10}H_{10}O_3$	*Cladosporium* sp. JJM22	*Ceriops tagal* (Mangrove plant, Rhizophoraceae)	South China Sea, Dongzhaigang, Hainan, China	[88]
(-)-*trans*-(3*R*,4*R*)-3,4,8-Trihydroxy-6,7-dimethyl-3,4- dihydronaphthalen-1(2*H*)-one (**157**)	222	$C_{12}H_{14}O_4$	*Cladosporium* sp. JJM22	*Ceriops tagal* (Mangrove plant, Rhizophoraceae)	South China Sea, Dongzhaigang, Hainan, China	[88]
(3*S*)-3,8-Dihydroxy-6,7-dimethyl-*α*-tetralone (**158**)	206	$C_{12}H_{14}O_3$	*Cladosporium* sp. JJM22	*Ceriops tagal* (Mangrove plant, Rhizophoraceae)	South China Sea, Dongzhaigang, Hainan, China	[88]
(3*R*,4*R*)-3,4-Dihydro-3,4,8-trihydroxy-1(2*H*)-napthalenone (**159**)	194	$C_{10}H_{10}O_4$	*Cladosporium* sp. JJM22	*Ceriops tagal* (Mangrove plant, Rhizophoraceae)	South China Sea, Dongzhaigang, Hainan, China	[88]
			Cladosporium sp. HDN17-58	Deep-sea sediment	Western Pacific Ocean, China	[89]
Aladothalen (**160**)	194	$C_{10}H_{10}O_4$	*Cladosporium* sp. HDN17-58	Deep-sea sediment	Western Pacific Ocean, China	[89]
8. Perylenequinones						
Altertoxin VIII (**161**)	304	$C_{20}H_{16}O_3$	*Cladosporium* sp. KFD33	Blood cockle (Bivalve mollusk, Cardiidae)	Haikou Bay, Hainan, China	[85]
Altertoxin IX (**162**)	290	$C_{20}H_{18}O_2$	*Cladosporium* sp. KFD33	Blood cockle (Bivalve mollusk, Cardiidae)	Haikou Bay, China	[85]
Altertoxin X (**163**)	290	$C_{20}H_{18}O_2$	*Cladosporium* sp. KFD33	Blood cockle (Bivalve mollusk, Cardiidae)	Haikou Bay, China	[85]
Altertoxin XI (**164**)	304	$C_{21}H_{20}O_2$	*Cladosporium* sp. KFD33	Blood cockle (Bivalve mollusk, Cardiidae)	Haikou Bay, China	[85]
9. Naphthalene derivatives						
8-Methoxynaphthalen-1-ol (**165**)	174	$C_{11}H_{10}O_2$	*Cladosporium* sp. JJM22	*Ceriops tagal* (Mangrove plant, Rhizophoraceae)	South China Sea, China	[90]
1,8-Dimethoxynaphthalene (**166**)	188	$C_{12}H_{12}O_2$	*Cladosporium* sp. JJM22	*Ceriops tagal* (Mangrove plant, Rhizophoraceae)	South China Sea, Dongzhaigang, Hainan, China	[88]
			Cladosporium sp. JJM22	*Ceriops tagal* (Mangrove plant, Rhizophoraceae)	South China Sea, China	[90]
			Cladosporium sp. JJM22	*Ceriops tagal* (Mangrove plant, Rhizophoraceae)	South China Sea, China	[91]
4-Methoxynaphthalene-1,5-diol (**167**)	190	$C_{11}H_{10}O_3$	*Cladosporium* sp. JJM22	*Ceriops tagal* (Mangrove plant, Rhizophoraceae)	South China Sea, China	[91]
8-Methoxynaphthalene-1,7-diol (**168**)	190	$C_{11}H_{10}O_3$	*Cladosporium* sp. JJM22	*Ceriops tagal* (Mangrove plant, Rhizophoraceae)	South China Sea, China	[91]
Cladonaphchrom A (**169**)	350	$C_{22}H_{22}O_4$	*Cladosporium* sp. JJM22	*Ceriops tagal* (Mangrove plant, Rhizophoraceae)	South China Sea, China	[90]
Cladonaphchrom B (**170**)	350	$C_{22}H_{22}O_4$	*Cladosporium* sp. JJM22	*Ceriops tagal* (Mangrove plant, Rhizophoraceae)	South China Sea, China	[90]

Table 1. *Cont.*

Compound Name	Mol. Wt.	Mol. Formula	Fungal Source	Host (Sample, Family)	Place	Ref.
10. Xanthones						
8-Hydroxy-6-methylxanthone-1-carboxylic acid (**171**)	270	$C_{15}H_{10}O_5$	*C. halotolerans* GXIMD 02502	*Porites lutea* (Stony coral, Poritidae)	Weizhou Islands coral reef, Guangxi Zhuang autonomous region, China	[92]
Methyl 8-hydroxy-6-methyl-9-oxo-9H-xanthene-1-carboxylate (**172**)	284	$C_{16}H_{12}O_5$	*C. halotolerans* GXIMD 02502	*Porites lutea* (Stony coral, Poritidae)	Weizhou Islands coral reef, Guangxi Zhuang autonomous region, China	[92]
Methyl 8-hydroxy-6- (hydroxymethyl)-9-oxo-9H-xanthene-1-carboxylate (**173**)	300	$C_{16}H_{12}O_6$	*C. halotolerans* GXIMD 02502	*Porites lutea* (Stony coral, Poritidae)	Weizhou Islands coral reef, Guangxi Zhuang autonomous region, China	[92]
Vertixanthone (**174**)	270	$C_{15}H_{10}O_5$	*C. halotolerans* GXIMD 02502	*Porites lutea* (Stony coral, Poritidae)	Weizhou Islands coral reef, Guangxi Zhuang autonomous region, China	[92]
8-(Methoxycarbonyl)-1-hydroxy-9-oxo-9H-xanthene-3-carboxylic acid (**175**)	314	$C_{16}H_{10}O_7$	*C. halotolerans* GXIMD 02502	*Porites lutea* (Stony coral, Poritidae)	Weizhou Islands coral reef, Guangxi Zhuang autonomous region, China	[92]
3,8-Dihydroxy-6-methyl-9-oxo-9H-xanthene-1-Carboxylate (**176**)	300	$C_{16}H_{12}O_6$	*C. halotolerans* GXIMD 02502	*Porites lutea* (Stony coral, Poritidae)	Weizhou Islands coral reef, Guangxi Zhuang autonomous region, China	[92]
Conioxanthone A (**177**)	316	$C_{16}H_{12}O_7$	*C. halotolerans* GXIMD 02502	*Porites lutea* (Stony coral, Poritidae)	Weizhou Islands coral reef, Guangxi Zhuang autonomous region, China	[92]
11. Tropolones						
Malettinin A (**178**)	288	$C_{16}H_{16}O_5$	*Cladosporium* sp. KF501	Water sample	German Wadden Sea	[93]
Malettinin B (**179**)	292	$C_{16}H_{20}O_5$	*Cladosporium* sp. KF501	Water sample	German Wadden Sea	[93]
Malettinin C (**180**)	292	$C_{16}H_{20}O_5$	*Cladosporium* sp. KF501	Water sample	German Wadden Sea	[93]
Malettinin E (**181**)	292	$C_{16}H_{20}O_5$	*Cladosporium* sp. KF501	Water samples	German Wadden Sea	[93]
12. Binaphthopyrones						
Cladosporinone (**182**)	650	$C_{33}H_{30}O_{14}$	C. *cladosporioides*	Sediment of a hypersaline lake El Hamra	Wadi el Natrun, Egypt	[94]
Viriditoxin (**183**)	662	$C_{34}H_{30}O_{14}$	C. *cladosporioides*	Sediment of a hypersaline lake El Hamra	Wadi el Natrun, Egypt	[94]
Viriditoxin derivative 1 (**184**)	646	$C_{34}H_{30}O_{13}$	C. *cladosporioides*	Sediment of a hypersaline lake El Hamra	Wadi el Natrun, Egypt	[94]
Viriditoxin derivative 2 (**185**)	646	$C_{34}H_{30}O_{13}$	C. *cladosporioides*	Sediment of a hypersaline lake El Hamra	Wadi el Natrun, Egypt	[94]
13. Benzopyranes, benzopyrones, and pyrones						
(2*S*)-5-Hydroxy-2-methyl-chroman-4-one (**186**)	178	$C_{10}H_{10}O_3$	*Cladosporium* sp. JJM22	*Ceriops tagal* (Mangrove plant, Rhizophoraceae)	South China Sea, Dongzhaigang, Hainan, China	[88]
(*R*)-5-Hydroxy-2-methylchroman-4-one (**187**)	178	$C_{10}H_{10}O_3$	*Cladosporium* sp. JJM22	*Ceriops tagal* (Mangrove plant, Rhizophoraceae)	South China Sea, China	[90]
(2*R*)-7-*O*-*α*-D-Ribofuranosyl-5-hydroxy-2-methyl chroman-4-one (**188**)	326	$C_{15}H_{18}O_8$	*Cladosporium* sp. OUCMDZ-302	*Excoecaria agallocha* (Mangrove plant, Euphorbiaceae)	Wenchang, Hainan, China	[95]
			Cladosporium sp. OUCMDZ-302	*Excoecaria agallocha* (Mangrove plant, Euphorbiaceae)	Wenchang, Hainan, China	[95]
			Cladosporium sp. JJM22	*Ceriops tagal* (Mangrove plant, Rhizophoraceae)	South China Sea, China	[91]

Table 1. *Cont.*

Compound Name	Mol. Wt.	Mol. Formula	Fungal Source	Host (Sample, Family)	Place	Ref.
(2*S*)-7-*O*-*α*-D-Ribofuranosyl-5-hydroxy-2-methylchroman-4-one (**189**)	326	$C_{15}H_{108}O_8$	*Cladosporium* sp. OUCMDZ-302	*Excoecaria agallocha* (Mangrove plant, Euphorbiaceae)	Wenchang, Hainan, China	[95]
(±)-5,7-Dihydroxy-2-methyl chroman-4-one (**190**)	194	$C_{10}H_{10}O_4$	*Cladosporium* sp. OUCMDZ-302	*Excoecaria agallocha* (Mangrove plant, Euphorbiaceae)	Wenchang, Hainan, China	[95]
5-Hydroxy-2-methyl-4*H*-chromen-4-one (**191**)	176	$C_{10}H_8O_3$	*Cladosporium* sp. JJM22	*Ceriops tagal* (Mangrove plant, Rhizophoraceae)	South China Sea, China	[90]
Clapone (**192**)	216	$C_{13}H_{12}O_3$	*Cladosporium* sp. HNWSW-1	*Ceriops tagal* (Mangrove plant, Rhizophoraceae)	Dong Zhai Gang Mangrove, Hainan, China	[67]
7-*O*-*α*-D-Ribosyl-5-hydroxy-2-propylchromone (**193**)	352	$C_{17}H_{20}O_8$	*Cladosporium* sp. OUCMDZ-302	*Excoecaria agallocha* (Mangrove plant, Euphorbiaceae)	Wenchang, Hainan, China	[95]
Coniochaetone A (**194**)	230	$C_{13}H_{10}O_4$	*C. halotolerans* GXIMD 02502	*Porites lutea* (Stony coral, Poritidae)	Weizhou Islands coral reef, Guangxi Zhuang autonomous region, China	[92]
Coniochaetone B (**195**)	232	$C_{13}H_{12}O_4$	*C. halotolerans* GXIMD 02502	*Porites lutea* (Stony coral, Poritidae)	Weizhou Islands coral reef, Guangxi Zhuang autonomous region, China	[92]
Coniochaetone K (**196**)	262	$C_{13}H_{10}O_6$	*C. halotolerans* GXIMD 02502	*Porites lutea* (Stony coral, Poritidae)	Weizhou Islands coral reef, Guangxi Zhuang autonomous region, China	[92]
α-Diversonolic ester (**197**)	320	$C_{16}H_{16}O_7$	*C. halotolerans* GXIMD 02502	*Porites lutea* (Poritidae)	Weizhou Islands coral reef, Guangxi Zhuang autonomous region, China	[92]
β-Diversonolic ester (**198**)	320	$C_{16}H_{16}O_7$	*C. halotolerans* GXIMD 02502	*Porites lutea* (Stony coral, Poritidae)	Weizhou Islands coral reef, Guangxi Zhuang autonomous region, China	[92]
Secalonic acid D (**199**)	638	$C_{32}H_{30}O_{14}$	*Cladosporium* sp. JS1-2	*Ceriops tagal* (Mangrove plant, Rhizophoraceae)	Dongzhaigang, Hainan, China	[71]
(2*S*,3*S*,4*R*)-2-Methylchroman-3,4,5-triol (**200**)	196	$C_{10}H_{12}O_4$	*Cladosporium* sp. OUCMDZ-302	*Excoecaria agallocha* (Mangrove plant, Euphorbiaceae)	Wenchang, Hainan, China	[95]
(2*S*,4*S*)-4-Methoxy-2-methylchroman-5-ol (**201**)	194	$C_{11}H_{14}O_3$	*Cladosporium* sp. OUCMDZ-302	*Excoecaria agallocha* (Mangrove plant, Euphorbiaceae)	Wenchang, Hainan, China	[95]
(2*R*,4*R*)-3,4-Dihydro-4-methoxy-2-methyl-2H-1-benzopyran-5-ol (**202**)	194	$C_{11}H_{14}O_3$	*Cladosporium* sp. JJM22	*Ceriops tagal* (Mangrove plant, Rhizophoraceae)	South China Sea, China	[91]
(2*S*,4*S*)-2-methylchroman-4,5-diol (**203**)	180	$C_{10}H_{12}O_3$	*Cladosporium* sp. OUCMDZ-302	*Excoecaria agallocha* (Mangrove plant, Euphorbiaceae)	Wenchang, Hainan, China	[95]
(2*R*,4*S*)-2,3-Dihydro-2-methyl-benzopyran-4,5-diol (**204**)	180	$C_{10}H_{12}O_3$	*Cladosporium* sp. JJM22	*Ceriops tagal* (Mangrove plant, Rhizophoraceae)	South China Sea, China	[91]
(2*R**,4*R**)-3,4-Dihydro-5-methoxy-2-methyl-1(2*H*)-benzopyran-4-ol (**205**)	164	$C_{10}H_{12}O_2$	*Cladosporium* sp. JJM22	*Ceriops tagal* (Mangrove plant, Rhizophoraceae)	South China Sea, Dongzhaigang, Hainan, China	[88]
Citrinin H1 (**206**)	428	$C_{24}H_{28}O_7$	*Cladosporium* sp. JS1-2	*Ceriops tagal* (Mangrove plant, Rhizophoraceae)	Dongzhaigang, Hainan, China	[71]
Cladosporin C (**207**)	248	$C_{14}H_{16}O_4$	*C. cladosporioides* SCSIO z015	Deep sea sediment	Okinawa, Japan	[36]
(*S*)-5-Hydroxy-4-methylchroman-2-one (**208**)	178	$C_{10}H_{10}O_3$	*Cladosporium* sp. JJM22	*Ceriops tagal* (Mangrove plant, Rhizophoraceae)	South China Sea, China	[91]

Table 1. *Cont.*

Compound Name	Mol. Wt.	Mol. Formula	Fungal Source	Host (Sample, Family)	Place	Ref.
(3*R*)-3-(2-Hydroxypropyl)-6,8-dihydroxy-3,4-dihydroiso-coumarin (**209**)	238	$C_{12}H_{14}O_5$	*Cladosporium* sp. CSIO41007	*Callyspongia* sp. (Sponge, Callyspongiidae)	Xuwen, Guangdong, China	[61]
Phomasatin (**210**)	208	$C_{10}H_8O_5$	*C. cladosporioides* MCCC 3A00182	Marine sediment	Southwest Pacific Ocean	[75]
14. Pyrone derivatives						
Herbarin A (**211**)	236	$C_{12}H_{12}O_5$	*C. herbarum* (Pers.)	*Aplysina aerophoba* (Sponge, Aplysinidae)	Bali Bata National Park, Indonesia	[96]
				Callyspongia aerizusa (Sponge, Callyspongiidae)	Bali Bata National Park, Indonesia	[96]
Herbarin B (**212**)	210	$C_{10}H_{10}O_5$	*C. herbarum* (Pers.)	*Aplysina aerophoba* (Sponge, Aplysinidae)	Bali Bata National Park, Indonesia	[96]
				Callyspongia aerizusa (Sponge, Callyspongiidae)	Bali Bata National Park, Indonesia	[96]
Citreoviridin A (**213**)	402	$C_{23}H_{30}O_6$	*C. herbarum* (Pers.)	*Aplysina aerophoba* (Sponge, Aplysinidae)	Bali Bata National Park, Indonesia	[96]
				Callyspongia aerizusa (Sponge, Callyspongiidae)	Bali Bata National Park, Indonesia	[96]
Vermistatin (**214**)	328	$C_{18}H_{16}O_6$	*Cladosporium* sp. JS1-2	*Ceriops tagal* (Mangrove plant, Rhizophoraceae)	Dongzhaigang, Hainan, China	[71]
15. Lactones, cyclohexene, and azaphilone derivatives						
(*R*)-Mevalonolactone (**215**)	130	$C_8H_{10}O_3$	*Cladosporium* sp. EF424419	*Porphyra yezoensis* (Red alga, Bangiaceae)	Lianyungang, Jiangsu, China	[59]
Cladosporactone A (**216**)	196	$C_{10}H_{12}O_4$	*C. cladosporioides* MCCC 3A00182	Marine Sediment	Southwest Pacific Ocean	[75]
Helicascolide A (**217**)	212	$C_{12}H_{20}O_3$	*Cladosporium* sp. JJM22	*Ceriops tagal* (Mangrove plant, Rhizophoraceae)	South China Sea, China	[91]
Cladoscyclitol A (**218**)	244	$C_{12}H_{20}O_5$	*Cladosporium* sp. JJM22	*Ceriops tagal* (Mangrove plant, Rhizophoraceae)	Dongzhaigang of Hainan Province, China	[97]
Cladoscyclitol B (**219**)	290	$C_{13}H_{22}O_7$	*Cladosporium* sp. JJM22	*Ceriops tagal* (Mangrove plant, Rhizophoraceae)	Dongzhaigang of Hainan Province, China	[97]
Cladoscyclitol C (**220**)	230	$C_{12}H_{22}O_4$	*Cladosporium* sp. JJM22	*Ceriops tagal* (Mangrove plant, Rhizophoraceae)	Dongzhaigang of Hainan Province, China	[97]
Cladoscyclitol D (**221**)	246	$C_{12}H_{22}O_5$	*Cladosporium* sp. JJM22	*Ceriops tagal* (Mangrove plant, Rhizophoraceae)	Dongzhaigang of Hainan Province, China	[97]
2-Butyryl-3,5-dihydroxycyclohex-2-enone (**222**)	198	$C_{10}H_{14}O_4$	*Cladosporium* sp. OUCMDZ-302	*Excoecaria agallocha* (Mangrove plant, Euphorbiaceae)	Wenchang, Hainan, China	[95]
Perangustol A (**223**)	210	$C_{11}H_{14}O_4$	*C. perangustm* FS62	Marine sediment	South China Sea, China	[87]
Perangustol B (**224**)	210	$C_{11}H_{14}O_4$	*C. perangustm* FS62	Marine sediment	South China Sea, China	[87]
Bicyclic diol (**225**)	210	$C_{11}H_{14}O_4$	*C. perangustm* FS62	Marine sediment	South China Sea, China	[87]
16. Phenolics and other aromatic compounds						
3-Phenyl-propionic acid (**226**)	210	$C_{11}H_{14}O_4$	*Cladosporium* sp. JJM22	*Ceriops tagal* (Rhizophoraceae)	South China Sea, China	[91]
P-Toluic acid (**227**)	136	$C_8H_8O_2$	*C. cladosporioides*	Marine sponge	Argentina	[98]
L-*β*-Phenyllactic acid (**228**)	166	$C_9H_{10}O_3$	*Cladosporium* sp. EF424419	*Porphyra yezoensis* (Red alga, Bangiaceae)	Lianyungang, Jiangsu, China	[59]
α-Resorcylic acid (**229**)	154	$C_7H_6O_4$	*Cladosporium* sp. EF424419	*Porphyra yezoensis* (Red alga, Bangiaceae)	Lianyungang, Jiangsu, China	[59]

Table 1. *Cont.*

Compound Name	Mol. Wt.	Mol. Formula	Fungal Source	Host (Sample, Family)	Place	Ref.
Phenylacetic acid (**230**)	136	$C_8H_8O_2$	*Cladosporium* sp. EF424419	*Porphyra yezoensis* (Red alga, Bangiaceae)	Lianyungang, Jiangsu, China	[59]
P-Hydroxyphenylacetic acid (**231**)	152	$C_8H_8O_3$	*Cladosporium* sp. EF424419	*Porphyra yezoensis* (Red alga, Bangiaceae)	Lianyungang, Jiangsu, China	[59]
Cinnamic acid (3-Phenyl-2-propenoic acid) (**232**)	148	$C_9H_8O_2$	*Cladosporium* sp. F14	Seawater from the mangrove stand	Kei Ling Ha Lo Wai, Sai Kung, China	[60]
3-(2,3-Dihydroxy phenoxy) butanoic acid (**233**)	212	$C_{10}H_{12}O_5$	*Cladosporium* sp. OUCMDZ-302	*Excoecaria agallocha* (Mangrove plant, Euphorbiaceae)	Wenchang, Hainan, China	[95]
P-Hydroxy benzoic acid methyl ester (**234**)	152	$C_8H_8O_3$	*Cladosporium* sp. EF424419	*Porphyra yezoensis* (Red alga, Bangiaceae)	Lianyungang, Jiangsu, China	[59]
Methyl (3*S*)-3-(2,3-dihydroxy phenyloxy)butanoate (**235**)	226	$C_{11}H_{14}O_5$	*Cladosporium* sp. OUCMDZ-302	*Excoecaria agallocha* (Mangrove plant, Euphorbiaceae)	Wenchang, Hainan, China	[95]
P-Hydroxyphenylethyl alcohol (**236**)	138	$C_8H_{10}O_2$	*Cladosporium* sp. EF424419	*Porphyra yezoensis* (Red alga, Bangiaceae)	Lianyungang, Jiangsu Province, China	[59]
P-Hydroxybenzyl alcohol (**237**)	142	$C_7H_8O_2$	*Cladosporium* sp. EF424419	*Porphyra yezoensis* (Red alga, Bangiaceae)	Lianyungang, Jiangsu Province, China	[59]
2-Phenylethanol (**238**)	122	$C_8H_{10}O$	*Cladosporium* sp. F14	Seawater from the mangrove stand	Kei Ling Ha Lo Wai, Sai Kung, China	[60]
4-*O*-*α*-*D*-Ribofuranose-3-hydroxymethyl-2-pentyl- phenol (**239**)	342	$C_{17}H_{26}O_7$	*Cladosporium* sp. JJM22	*Ceriops tagal* (Mangrove plant, Rhizophoraceae)	South China Sea, Dongzhaigang, Hainan, China	[88]
4-*O*-*α*-D-Ribofuranose-2-pentyl-3-phemethylol (**240**)	326	$C_{17}H_{26}O_6$	*Cladosporium* sp. JJM22	*Ceriops tagal* (Mangrove plant, Rhizophoraceae)	Dongzhaigang of Hainan Province, China	[97]
Clavatol (**241**)	180	$C_{10}H_{12}O_3$	*Cladosporium* sp.MFC353-b	*Chondria crassicualis* (Red alga, Rhodomelaceae)	Yokji Island, Kyeongnam, Korea	[65]
1-(3,5-Dihydroxy-4-methylphenyl)propan-2-one (**242**)	180	$C_{10}H_{12}O_3$	*C. perangustm* FS62	Marine sediment	South China Sea, china	[87]
α-Acetylorcinol (**243**)	166	$C_9H_{10}O_3$	*C. perangustm* FS62	Marine sediment	South China Sea, china	[87]
1-(2,6-Dihydroxyphenyl) ethanone (**244**)	152	$C_8H_8O_3$	*Cladosporium* sp. OUCMDZ-302	*Excoecaria agallocha* (Mangrove plant, Euphorbiaceae)	Wenchang, Hainan, China	[95]
1-(2,6-Hihydroxyphenyl)-1-butanone (**245**)	180	$C_{10}H_{12}O_3$	*Cladosporium* sp. OUCMDZ-302	*Excoecaria agallocha* (Mangrove plant, Euphorbiaceae)	Wenchang, Hainan, China	[95]
(*R*)-3-Methoxyl-1-(2,6-dihydroxyphenyl)-butan-1-one (**246**)	210	$C_{11}H_{14}O_4$	*Cladosporium* sp. JJM22	*Ceriops tagal* (Rhizophoraceae)	South China Sea, China	[91]
Cladosporin D (**247**)	224	$C_{12}H_{16}O_4$	*C. cladosporioides* SCSIO z015	Deep sea sediment	Okinawa, Japan	[36]
(2*S*)-7,4′-dihydroxy-5-methoxy-8-(*γ*,*γ*-dimethylallyl)-flavanone (**248**)	354	$C_{21}H_{22}O_5$	*Cladosporium* sp. TPU1507	Unidentified marine sponge	Manado, Indonesia	[68]
Bis(2-Ethylhexyl)phthalate (**249**)	390	$C_{24}H_{38}O_4$	*Cladosporium* sp. F14	Seawater from the mangrove stand	Kei Ling Ha Lo Wai, Sai Kung, China	[60]
Herbaric acid (**250**)	196	$C_9H_8O_5$	*C. herbarum* (Pers.)	*Callyspongia aerizusa* (Sponge, Callyspongiidae)	Bali Bata National Park, Indonesia	[96]
Cladosacid (**251**)	250	$C_{15}H_{22}O_3$	*Cladosporium* sp. OUCMDZ-1635	Unidentified sponge	Xisha Islands, China	[56]
1,1′-Dioxine-2,2′-dipropionic acid (**252**)	228	$C_{10}H_{12}O_6$	*Cladosporium* sp. JS1-2	*Ceriops tagal* (Mangrove, plant, Rhizophoraceae)	Dongzhaigang, Hainan, China	[71]
Sumiki's acid (**253**)	142	$C_6H_6O_4$	*C. herbarum* (Pers.)	*Callyspongia aerizusa* (Sponge, Callyspongiidae)	Bali Bata National Park, Indonesia	[73]

Table 1. *Cont.*

Compound Name	Mol. Wt.	Mol. Formula	Fungal Source	Host (Sample, Family)	Place	Ref.
Acetyl Sumiki's acid (**254**)	184	$C_8H_8O_5$	*C. herbarum* (Pers.)	*Callyspongia aerizusa* (Sponge, Callyspongiidae)	Bali Bata National Park, Indonesia	[74]
17. Sterols and terpenes						
5*α*,8*α*-Epidioxy-24(*R*)-methyl-cholesta-6,22-diene-3-*β*-ol (**255**)	428	$C_{28}H_{44}O_3$	*C. sphaerospermum* Penz	*Ceramium condi* (Red alga, Ceramiaceae)	Ussuriysk Bay, Japan	[99]
			C.cladosporioides MCCC 3A00182	Marine sediment	Southwest Pacific Ocean	[75]
5*α*,8*α*-Epidioxy-ergosta-6,22E-dien-3*β*-ol (**256**)	428	$C_{28}H_{44}O_3$	*Cladosporium* sp. WZ-2008-0042	*Dichotella gemmacea* (Gorgonian, Ellisellidae)	Weizhou Island coral reef, South China Sea	[100]
			C. cladosporioides MCCC 3A00182	Marine Sediment	Southwest Pacific Ocean	[75]
5*α*,8*α*-Epidioxy-24(*R*)-methyl-cholesta-6,9(11),22-triene-3-*β*-ol (**257**)	426	$C_{28}H_{42}O_3$	*C. sphaerospermum* Penz	*Ceramium condi* (Red alga, Ceramiaceae)	Ussuriysk Bay, Japan	[99]
5*α*,8*α*-Epidioxy-ergosta-6,9,22*E*-triene-3*β*-ol (**258**)	426	$C_{28}H_{42}O_3$	*Cladosporium* sp. WZ-2008-0042	*Dichotella gemmacea* (Gorgonian, Ellisellidae)	Weizhou Island coral reef, South China Sea	[100]
3*β*,5*α*,6*β*-Trihydroxyergosta-7,22-diene = Cerevisterol (**259**)	430	$C_{28}H_{46}O_3$	*Cladosporium* sp. SCSIO41007	*Callyspongia* sp. (Sponge, Callyspongiidae)	Xuwen, Guangdong, China	[61]
Ergosta-7,22*E*-diene-3*β*,5*α*,6*β*-triol (**260**)	430	$C_{28}H_{46}O_3$	*Cladosporium* sp. WZ-2008-0042	*Dichotella gemmacea* (Gorgonian, Ellisellidae)	Weizhou Island coral reef, South China Sea	[100]
3*β*,5*α*,6*α*-Trihydroxy-(22E,24R) -ergosta-7,22-diene (**261**)	430	$C_{28}H_{46}O_3$	*C. cladosporioides* MCCC 3A00182	Marine Sediment	Southwest Pacific Ocean	[75]
3*β*,5*α*-Dihydroxy-6*β*-methoxyergosta-7,22-diene (**262**)	444	$C_{29}H_{48}O_3$	*Cladosporium* sp. WZ-2008-0042	*Dichotella gemmacea* (Gorgonian, Ellisellidae)	Weizhou Island coral reef, South China Sea	[100]
Ergosterol (**263**)	396	$C_{28}H_{44}O$	*Cladosporium* sp. WZ-2008-0042	*Dichotella gemmacea* (Gorgonian, Ellisellidae)	Weizhou Island coral reef, South China Sea	[100]
Cladosporisteroid A (**264**)	460	$C_{28}H_{44}O_5$	*Cladosporium* sp. SCSIO41007	*Callyspongia* sp. (Sponge, Callyspongiidae)	Xuwen, Guangdong, China	[61]
3*β*,5*α*,9*α*-Trihydroxy-(22*E*,24*R*)-ergosta-7,22-diene-6-one (**265**)	444	$C_{28}H_{44}O_4$	*Cladosporium* sp. SCSIO41007	*Callyspongia* sp. (Sponge, Callyspongiidae)	Xuwen, Guangdong, China	[61]
			C. cladosporioides MCCC 3A00182	Marine Sediment	Southwest Pacific Ocean	[75]
3*β*,5*α*-Dihydroxy-(22*E*,24*R*)-ergosta-7,22-diene-6-one (**266**)	428	$C_{28}H_{44}O_3$	*C. cladosporioides* MCCC 3A00182	Marine Sediment	Southwest Pacific Ocean	[75]
Stigma-5-en-3-*O*-*β*-glucopyranoside (**267**)	576	$C_{35}H_{60}O_6$	*Cladosporium* sp. WZ-2008-0042	*Dichotella gemmacea* (Gorgonian, Ellisellidae)	Weizhou Island coral reef, South China Sea	[100]
3*α*-Hydroxy-pregna-7-ene-6,20-dione = Cladosporisteroid B (**268**)	330	$C_{21}H_{30}O_3$	*Cladosporium* sp. WZ-2008-0042	*Dichotella gemmacea* (Gorgonian, Ellisellidae)	Weizhou Island coral reef, South China Sea	[100]
			Cladosporium sp. SCSIO41007	*Callyspongia* sp. (Sponge, Callyspongiidae)	Xuwen, Guangdong, China	[61]
			C. cladosporioides MCCC 3A00182	Marine Sediment	Southwest Pacific Ocean	[75]
			C. sphaerospermum SW67	*Hydractinia echinata* (Hydroid, Hydractiniidae)	South Korea	[101]

Table 1. *Cont.*

Compound Name	Mol. Wt.	Mol. Formula	Fungal Source	Host (Sample, Family)	Place	Ref.
Cladosporisteroid C (**269**)	374	$C_{23}H_{34}O_4$	*Cladosporium* sp. SCSIO41007	*Callyspongia* sp. (Sponge, Callyspongiidae)	Xuwen, Guangdong, China	[61]
Pregn-7-dien-3,6,20-trione (**270**)	328	$C_{21}H_{28}O_3$	*Cladosporium* sp. SCSIO41007	*Callyspongia* sp. (Sponge, Callyspongiidae)	Xuwen, Guangdong, China	[61]
18. Alcohols and aldehydes				70.43 μg/mL (EC_{50})		
Compound (**271**)	434	$C_{30}H_{58}O$	*Cladosporium* sp.	Marine sediment	San Antonio Oeste, Río Negro, Argentina	[102]
Compound (**272**)	458	$C_{32}H_{58}O$	*Cladosporium* sp.	Marine sediment	San Antonio Oeste, Río Negro, Argentina	[102]
Compound (**273**)	458	$C_{32}H_{58}O$	*Cladosporium* sp.	Marine sediment	San Antonio Oeste, Río Negro, Argentina	[102]
Compound (**274**)	458	$C_{32}H_{58}O$	*Cladosporium* sp.	Marine sediment	San Antonio Oeste, Río Negro, Argentina	[102]
Compound (**275**)	460	$C_{32}H_{60}O$	*Cladosporium* sp.	Marine sediment	San Antonio Oeste, Río Negro, Argentina	[102]
Compound (**276**)	460	$C_{32}H_{60}O$	*Cladosporium* sp.	Marine sediment	San Antonio Oeste, Río Negro, Argentina	[102]
Compound (**277**)	462	$C_{32}H_{62}O$	*Cladosporium* sp.	Marine sediment	San Antonio Oeste, Río Negro, Argentina	[102]
Compound (**278**)	462	$C_{32}H_{62}O$	*Cladosporium* sp.	Marine sediment	San Antonio Oeste, Río Negro, Argentina	[102]
Compound (**279**)	482	$C_{34}H_{58}O$	*Cladosporium* sp.	Marine sediment	San Antonio Oeste, Río Negro, Argentina	[102]
Compound (**280**)	484	$C_{34}H_{60}O$	*Cladosporium* sp.	Marine sediment	San Antonio Oeste, Río Negro, Argentina	[102]
Compound (**281**)	484	$C_{34}H_{60}O$	*Cladosporium* sp.	Marine sediment	San Antonio Oeste, Río Negro, Argentina	[102]
Compound (**282**)	484	$C_{34}H_{60}O$	*Cladosporium* sp.	Marine sediment	San Antonio Oeste, Río Negro, Argentina	[102]
Compound (**283**)	484	$C_{34}H_{60}O$	*Cladosporium* sp.	Marine sediment	San Antonio Oeste, Río Negro, Argentina	[102]
Compound (**284**)	486	$C_{34}H_{62}O$	*Cladosporium* sp.	Marine sediment	San Antonio Oeste, Río Negro, Argentina	[102]
(2*S*,3*S*,4*E*)-Hepta-4,6-diene-2,3-diol (**285**)	128	$C_7H_{12}O_2$	*Cladosporium* sp. OUCMDZ-302	*Excoecaria agallocha* (Mangrove plant, Euphorbiaceae)	Wenchang, Hainan, China	[95]
(3*E*,8*E*,6*S*)-Undeca-3,8,10-trien-1,6-diol (**286**)	182	$C_{11}H_{18}O_2$	*Cladosporium* sp. OUCMDZ-302	*Excoecaria agallocha* (Mangrove plant, Euphorbiaceae)	Wenchang, Hainan, China	[95]

Table 2. Biological activity of secondary metabolites isolated from *Cladosporium* species.

Compound Name	Biological Activity	Assay, Organism, or Cell Line	Biological Results	Positive Control	Ref.
Cladosin C (**3**)	Antiviral	Neuraminidase inhibition assay/Influenza A H1N1 virus	276.0 μM (IC_{50})	Ribavirin 131.0 μM (IC_{50})	[42]
Cladosin I (**8**)	Cytotoxicity	MTT/K562	4.1 μM (IC_{50})	Doxorubicin 0.3 μM (IC_{50})	[55]
	Cytotoxicity	MTT/HL-60	2.8 μM (IC_{50})	Doxorubicin 0.2 μM (IC_{50})	[55]
	Cytotoxicity	SEB/HCT-116	11.0 μM (IC_{50})	Doxorubicin 0.2 μM (IC_{50})	[55]
	Cytotoxicity	SRB/PC-3	13.0 μM (IC_{50})	Doxorubicin 1.0 μM (IC_{50})	[55]
	Cytotoxicity	SRB/SH-SY5Y	12.0 μM (IC_{50})	Doxorubicin 0.1 μM (IC_{50})	[55]
	Cytotoxicity	SRB/MGC-803	19.0 μM (IC_{50})	Doxorubicin 0.2 μM (IC_{50})	[55]

Table 2. *Cont.*

Compound Name	Biological Activity	Assay, Organism, or Cell Line	Biological Results	Positive Control	Ref.
Cladosin K (**10**)	Cytotoxicity	MTT/K562	5.9 μM (IC_{50})	Doxorubicin 0.3 μM (IC_{50})	[55]
	Cytotoxicity	MTT/HL-60	7.5 μM (IC_{50})	Doxorubicin 0.2 μM (IC_{50})	[55]
	Cytotoxicity	SEB/HCT-116	14.0 μM (IC_{50})	Doxorubicin 0.2 μM (IC_{50})	[55]
	Cytotoxicity	SRB/PC-3	18.0 μM (IC_{50})	Doxorubicin 1.0 μM (IC_{50})	[55]
Cladosporicin A (**12**)	Cytotoxicity	SRB/Bt549	70.88 μM (IC_{50})	Etoposide 1.82 μM (IC_{50})	[38]
	Cytotoxicity	SRB/HCC70	74.48 μM (IC_{50})	Etoposide 1.76 μM (IC_{50})	[38]
	Cytotoxicity	SRB/MDA-MB-231	75.54 μM (IC_{50})	Etoposide 2.27 μM (IC_{50})	[38]
	Cytotoxicity	SRB/MDA-MB-468	79.36 μM (IC_{50})	Etoposide 2.08 μM (IC_{50})	[38]
Cladodionen (**13**)	Cytotoxicity	MTT/K562	4.5 μM (IC_{50})	Doxorubicin 0.3 μM (IC_{50})	[55]
	Cytotoxicity	MTT/HL-60	6.6 μM (IC_{50})	Doxorubicin 0.2 μM (IC_{50})	[55]
	Cytotoxicity	SRB/HCT-116	12.0 μM (IC_{50})	Doxorubicin 0.2 μM (IC_{50})	[55]
	Cytotoxicity	SRB/PC-3	11.0 μM (IC_{50})	Doxorubicin 1.0 μM (IC_{50})	[55]
	Cytotoxicity	SRB/SH-SY5Y	15.0 μM (IC_{50})	Doxorubicin 0.1 μM (IC_{50})	[55]
	Cytotoxicity	SRB/MGC-803	22.0 μM (IC_{50})	Doxorubicin 0.2 μM (IC_{50})	[55]
	Cytotoxicity	MTT/MCF-7	18.7 μM (IC_{50})	Adriamycin 0.67 μM (IC_{50})	[56]
	Cytotoxicity	MTT/HeLa	19.1 μM (IC_{50})	Adriamycin 0.32 μM (IC_{50})	[56]
	Cytotoxicity	CCK-8/HCT-116	17.9 μM (IC_{50})	Adriamycin 0.21 μM (IC_{50})	[56]
	Cytotoxicity	MTT/HL-60	9.0 μM (IC_{50})	Adriamycin 0.02 μM (IC_{50})	[56]
Cladosporiumin I (**29**)	Cytotoxicity	SRB/Bt549	76.18 μM (IC_{50})	Etoposide 1.82 μM (IC_{50})	[38]
	Cytotoxicity	SRB/HCC70	85.29 μM (IC_{50})	Etoposide 1.76 μM (IC_{50})	[38]
	Cytotoxicity	SRB/MDA-MB-231	82.37 μM (IC_{50})	Etoposide 2.27 μM (IC_{50})	[38]
	Cytotoxicity	SRB/MDA-MB-468	81.44 μM (IC_{50})	Etoposide 2.08 μM (IC_{50})	[38]
Cladosporiumin J (**30**)	Cytotoxicity	SRB/Bt549	78.96 μM (IC_{50})	Etoposide 1.82 μM (IC_{50})	[38]
	Cytotoxicity	SRB/HCC70	76.41 μM (IC_{50})	Etoposide 1.76 μM (IC_{50})	[38]
	Cytotoxicity	SRB/MDA-MB-231	79.27 μM (IC_{50})	Etoposide 2.27 μM (IC_{50})	[38]
	Cytotoxicity	SRB/MDA-MB-468	74.64 μM (IC_{50})	Etoposide 2.08 μM (IC_{50})	[38]
Cyclo-(Val-Pro) (**32**)	Insecticidal	Inhibitinon 50%/*B. amphitrite*	37.82 μg/mL (EC_{50})	FSW with DMSO	[60]
		Lethality 50%/*B. amphitrite*	>200 μg/mL (LC_{50})	FSW with DMSO	[60]
		Inhibitinon 50%/*B. neritina*	>200 μg/mL (EC_{50})	FSW with DMSO	[60]
		Lethality 50%/*B. neritina*	>200 μg/mL (LC_{50})	FSW with DMSO	[60]

Table 2. *Cont.*

Compound Name	Biological Activity	Assay, Organism, or Cell Line	Biological Results	Positive Control	Ref.
Cyclo-(Val-Pro) (**32**)	Antimicrobial	Serial dilution/*L. hongkongensis*	80 μg/mL (MIC)	Streptomycin 250 μg/mL (MIC) Penicillin 0.25 μg/mL (MIC)	[60]
Cyclo-(Phe-Pro) (**33**)	Insecticidal	Inhibitinon 50%/*B. amphitrite*	68.57 μg/mL (EC_{50})	FSW with DMSO	[60]
		Lethality 50%/*B. amphitrite*	115.04 μg/mL (LC_{50})	FSW with DMSO	[60]
		Inhibitinon 50%/*B. neritina*	70.43 μg/mL (EC_{50})	FSW with DMSO	[60]
		Lethality 50%/*B. neritina*	>200 μg/mL (LC_{50})	FSW with DMSO	[60]
Cyclo-(Phe-Pro) (**33**)	Antimicrobial	Serial dilution/*L. hongkongensis*	200 μg/mL (MIC)	Streptomycin 1.0 250 μg/mL (MIC)	[60]
		Serial dilution/*M. luteus*	200 μg/mL (MIC)	Streptomycin 250 μg/mL (MIC) Penicillin 0.5 μg/mL (MIC)	[60]
		Serial dilution/*Ruegeria* sp.	100 μg/mL (MIC)	Streptomycin 500 μg/mL (MIC) Penicillin 0.25 μg/mL (MIC)	[60]
Glyantrypine (**42**)	Antiviral	CPE inhibition assay/Influenza A H1N1 virus	150 μM (IC_{50})	Ribavirin 87.0 μM (IC_{50})	[64]
3-Hydroxyglyantrypine (**43**)	Antiviral	CPE inhibition assay/Influenza A H1N1 virus	110 μM (IC_{50})	Ribavirin 87.0 μM (IC_{50})	[64]
14R-Oxoglyantrypine (**44**)	Antiviral	CPE inhibition assay/Influenza A H1N1 virus	130 μM (IC_{50})	Ribavirin 87.0 μM (IC_{50})	[64]
14S-Oxoglyantrypine (**45**)	Antiviral	CPE inhibition assay/Influenza A H1N1 virus	85 μM (IC_{50})	Ribavirin 87.0 μM (IC_{50})	[64]
Cladoquinazoline (**47**)	Antiviral	CPE inhibition assay/Influenza A H1N1 virus	150 μM (IC_{50})	Ribavirin 87.0 μM (IC_{50})	[64]
Epi-Cladoquinazoline (**48**)	Antiviral	CPE inhibition assay/Influenza A H1N1 virus	140 μM (IC50)	Ribavirin 87.0 μM (IC_{50})	[64]
Norquinadoline A (**49**)	Antiviral	CPE inhibition assay/Influenza A H1N1 virus	82 μM (IC_{50})	Ribavirin 87.0 μM (IC_{50})	[64]
Quinadoline A (**50**)	Antiviral	CPE inhibition assay/Influenza A H1N1 virus	130 μM (IC_{50})	Ribavirin 87.0 μM (IC_{50})	[64]
Deoxynortryptoquivaline (**51**)	Antiviral	CPE inhibition assay/Influenza A H1N1 virus	87 μM (IC_{50})	Ribavirin 87.0 μM (IC_{50})	[64]
Deoxytryptoquivaline (**52**)	Antiviral	CPE inhibition assay/Influenza A H1N1 virus	85 μM (IC_{50})	Ribavirin 87.0 μM (IC_{50})	[64]
Tryptoquivaline (**53**)	Antiviral	CPE inhibition assay/Influenza A H1N1 virus	89 μM (IC_{50})	Ribavirin 87.0 μM (IC_{50})	[64]
CS-C (**54**)	Antiviral	CPE inhibition assay/Influenza A H1N1 virus	140 μM (IC_{50})	Ribavirin 87.0 μM (IC_{50})	[64]
Quinadoline B (**55**)	Antiviral	CPE inhibition assay/Influenza A H1N1 virus	82 μM (IC_{50})	Ribavirin 87.0 μM (IC_{50})	[64]
Quinolactacin A2 (**58**)	Cytotoxicity	MTT/HepG-2	96.54 μM (IC_{50})	Curcumin 61.38 μM (IC_{50})	[66]
		MTT/HL-60	54.47 μM (IC_{50})	Curcumin 13.78 μM (IC_{50})	[66]
		MTT/MCF-7	94.49 μM (IC_{50})	Curcumin 20.68 μM (IC_{50})	[66]
		MTT/LNCap	45.71 μM (IC_{50})	Curcumin 6.15 μM (IC_{50})	[66]
	Anti-malarial	Flow cytometry/SYBR Green I fluorescence/*P. falciparum* chloroquine sensitive (3D7)	24.8 μM (EC_{50})	Artesunate 0.074 μM (EC_{50})	[66]
Citrinadin A (**68**)	Cytotoxicity	MTT/HepG-2	82.15 μM (IC_{50})	Curcumin 61.38 μM (IC_{50})	[66]
		MTT/HL-60	57.23 μM (IC_{50})	Curcumin 13.78 μM (IC_{50})	[66]
		MTT/MCF-7	66.07 μM (IC_{50})	Curcumin 20.68 μM (IC_{50})	[66]

Table 2. *Cont.*

Compound Name	Biological Activity	Assay, Organism, or Cell Line	Biological Results	Positive Control	Ref.
		MTT/LNCap	41.42 μM (IC_{50})	Curcumin 6.15 μM (IC_{50})	[66]
	Anti-malarial	Flow cytometry/SYBR Green I fluorescence/*P. falciparum* chloroquine sensitive (3D7)	>25.0 μM (EC_{50})	Artesunate 0.074 μM (EC_{50})	[66]
Butrecitrinadin (**70**)	Cytotoxicity	MTT/HepG-2	78.57 μM (IC_{50})	Curcumin 61.38 μM (IC_{50})	[66]
		MTT/HL-60	60.31 μM (IC_{50})	Curcumin 13.78 μM (IC_{50})	[66]
		MTT/MCF-7	51.32 μM (IC_{50})	Curcumin 20.68 μM (IC_{50})	[66]
		MTT/LNCap	32.94 μM (IC_{50})	Curcumin 6.15 μM (IC_{50})	[66]
	Anti-malarial	Flow cytometry/SYBR Green I fluorescence/*P. falciparum* chloroquine sensitive (3D7)	>25.0 μM (EC_{50})	Artesunate 0.074 μM (EC_{50})	[66]
Cladosporitin B (**74**)	Cytotoxicity	MTT/BEL-7042	29.4 μM (IC_{50})	Adriamycin 11.9 μM (IC_{50})	[67]
	Cytotoxicity	MTT/K562	25.6 μM (IC_{50})	Adriamycin 14.2 μM (IC_{50})	[67]
	Cytotoxicity	MTT/SGC-7901	41.7 μM (IC_{50})	Adriamycin 6.66 μM (IC_{50})	[67]
Talaroconvolutin A (**76**)	Cytotoxicity	MTT/HeLa	14.9 μM (IC_{50})	Adriamycin 11.5 μM (IC_{50})	[67]
	Cytotoxicity	MTT/BEL-7042	26.7 μM (IC_{50})	Adriamycin 11.9 μM (IC_{50})	[67]
Talaroconvolutin A (**76**)	α-Glucosidase inhibitory	Glucose oxidase method	78.2 μM (IC_{50})	Acarbose 275.7 μM (IC_{50})	[67]
Cladosporamide A (**77**)	Protein tyrosine phosphatase 1B inhibitory	PTP1B/Spectrophotometry	48.0 μM (IC_{50})	Oleanolic acid 0.9 μM (IC_{50})	[68]
		TCPTP/Spectrophotometry	54.0 μM (IC_{50})	Oleanolic acid 0.8 μM (IC_{50})	[68]
Cladosporilactam A (**78**)	Cytotoxicity	MTT/HeLa	0.76 μM (IC_{50})	Adriamycin	[69]
		MTT/HT-29	2.48 μM (IC_{50})	Adriamycin	[69]
		SRB/P388	1.35 μM (IC_{50})	Adriamycin	[69]
		SRB/A549	3.11 μM (IC_{50})	Adriamycin	[69]
2-Methylacetate-3,5,6-trimethylpyrazine (**84**)	Insecticidal	CM/Helicoverpa armigera Hubner larvae	100.0 μg/mL (IC_{50})	Azadirachtin 25.0 μg/mL (IC_{50})	[71]
	Antimicrobial	Microplate assay/*S. aureus*	12.5 μg/mL (MIC)	Ciprofloxacin 0.39 μg/mL (MIC)	[71]
Cytochalasin D (**85**)	Antimicrobial	Microplate assay/*S. aureus*	25.0 μg/mL (MIC)	Ciprofloxacin 0.39 μg/mL (MIC)	[71]
Pandangolide 3 (**96**)	Antimicrobial	Microplate assay/*C. glecosporioides*	2.0 μg/mL (MIC)	Amphotericin B 0.5 μg/mL (MIC)	[39]
		Microplate assay/*B. sorokiniana*	8.0 μg/mL (MIC)	Amphotericin B 0.5 μg/mL (MIC)	[39]
Thiocladospolide A (**101**)	Antimicrobial	Microplate assay/*E. tarda*	1.0 μg/mL (MIC)	Chloramphenicol 0.5 μg/mL (MIC)	[39]
		Microplate assay/*E. ictarda*	8.0 μg/mL (MIC)	Chloramphenicol 0.5 μg/mL (MIC)	[39]
		Microplate assay/*C. glecosporioides*	2.0 μg/mL (MIC)	Amphotericin B 0.5 μg/mL (MIC)	[39]

Table 2. *Cont.*

Compound Name	Biological Activity	Assay, Organism, or Cell Line	Biological Results	Positive Control	Ref.
Thiocladospolide B (**102**)	Antimicrobial	Microplate assay/*C. glecosporioides*	2.0 μg/mL (MIC)	Amphotericin B 0.5 μg/mL (MIC)	[39]
		Microplate assay/*P. piricola* Nose	32.0 μg/mL (MIC)	Amphotericin B 2.0 μg/mL (MIC)	[39]
		Microplate assay/*F. oxysporum* f. sp. *cucumerinum*	1.0 μg/mL (MIC)	Amphotericin B 0.5 μg/mL (MIC)	[39]
Thiocladospolide C (**103**)	Antimicrobial	Microplate assay/*C. glecosporioides*	1.0 μg/mL (MIC)	Amphotericin B 0.5 μg/mL (MIC)	[39]
		Microplate assay/*P. piricola* Nose	32.0 μg/mL (MIC)	Amphotericin B 2.0 μg/mL (MIC)	[39]
		Microplate assay/*F. oxysporum* f. sp. *cucumerinum*	32.0 μg/mL (MIC)	Amphotericin B 0.5 μg/mL (MIC)	[39]
Thiocladospolide D (**104**)	Antimicrobial	Microplate assay/*E. ictarda*	1.0 μg/mL (MIC)	Chloramphenicol 0.5 μg/mL (MIC)	[39]
		Microplate assay/*C. glecosporioides*	1.0 μg/mL (MIC)	Amphotericin B 0.5 μg/mL (MIC)	[39]
		Microplate assay/*P. piricola* Nose	32.0 μg/mL (MIC)	Amphotericin B 2.0 μg/mL (MIC)	[39]
		Microplate assay/*F. oxysporum* f. sp. *cucumerinum*	1.0 μg/mL (MIC)	Amphotericin B 0.5 μg/mL (MIC)	[39]
Thiocladospolide F (**106**)	Antimicrobial	Microplate assay/*E. tarda*	2.0 μg/mL (MIC)	Chloramphenicol 0.5 μg/mL (MIC)	[79]
	Antimicrobial	Microplate assay/*H. maydis*	4.0 μg/mL (MIC)	Amphotericin B 0.5 μg/mL (MIC)	[79]
Thiocladospolide G (**108**)	Antimicrobial	Microplate assay/*E. tarda*	2.0 μg/mL (MIC)	Chloramphenicol 0.5 μg/mL (MIC)	[79]
Thiocladospolide G (**109**)	Antimicrobial	Microplate assay/*E. tarda*	4.0 μg/mL (MIC)	Chloramphenicol 1.0 μg/mL (MIC)	[78]
Thiocladospolide H (**110**)	Antimicrobial	Microplate assay/*E. ictarda*	8.0 μg/mL (MIC)	Chloramphenicol 1.0 μg/mL (MIC)	[78]
Sporiolide A (**113**)	Cytotoxicity	MTT/L1210	0.13 μM (IC_{50})	-	[80]
Sporiolide B (**114**)	Cytotoxicity	MTT/L1210	0.81 μM (IC_{50})	-	[80]
Dendrodolide A (**117**)	Antimicrobial	Broth dilution assay/*B. cereus*	12.5 μM (MIC)	Ciprofloxacin 1.56 μM (MIC)	[69]
		Broth dilution assay/*T. halophilus*	3.13 μM (MIC)	Ciprofloxacin 1.56 μM (MIC)	[69]
		Broth dilution assay/*S. epidermidis*	6.25 μM (MIC)	Ciprofloxacin 0.78 μM (MIC)	[69]
		Broth dilution assay/*S. aureus*	6.25 μM (MIC)	Ciprofloxacin 0.39 μM (MIC)	[69]
		Broth dilution assay/*E. coli*	12.5 μM (MIC)	Ciprofloxacin 1.56 μM (MIC)	[69]
		Broth dilution assay/*P. putida*	12.5 μM (MIC)	Ciprofloxacin 0.39 μM (MIC)	[69]
		Broth dilution assay/*N. brasiliensis*	6.25 μM (MIC)	Ciprofloxacin 0.78 μM (MIC)	[69]
		Broth dilution assay/*V. parahaemolyticus*	12.5 μM (MIC)	Ciprofloxacin 1.56 μM (MIC)	[69]
Dendrodolide C (**118**)	Antimicrobial	Broth dilution assay/*B. cereus*	25.0 μM (MIC)	Ciprofloxacin 1.56 μM (MIC)	[69]
		Broth dilution assay/*T. halophilus*	3.13 μM (MIC)	Ciprofloxacin 1.56 μM (MIC)	[69]
		Broth dilution assay/*S. epidermidis*	25.0 μM (MIC)	Ciprofloxacin 0.78 μM (MIC)	[69]
		Broth dilution assay/*S. aureus*	25.0 μM (MIC)	Ciprofloxacin 0.39 μM (MIC)	[69]
		Broth dilution assay/*E. coli*	12.5 μM (MIC)	Ciprofloxacin 1.56 μM (MIC)	[69]
		Broth dilution assay/*P. putida*	25.0 μM (MIC)	Ciprofloxacin 0.39 μM (MIC)	[69]
		Broth dilution assay/*N. brasiliensis*	12.5 μM (MIC)	Ciprofloxacin 0.78 μM (MIC)	[69]

Table 2. *Cont.*

Compound Name	Biological Activity	Assay, Organism, or Cell Line	Biological Results	Positive Control	Ref.
		Broth dilution assay/*V. parahaemolyticus*	25.0 μM (MIC)	Ciprofloxacin 1.56 μM (MIC)	[69]
Dendrodolide M (**120**)	Antimicrobial	Broth dilution assay/*B. cereus*	6.25 μM (MIC)	Ciprofloxacin 1.56 μM (MIC)	[69]
		Broth dilution assay/*T. halophilus*	25.0 μM (MIC)	Ciprofloxacin 1.56 μM (MIC)	[69]
		Broth dilution assay/*S. epidermidis*	25.0 μM (MIC)	Ciprofloxacin 0.78 μM (MIC)	[69]
		Broth dilution assay/*S. aureus*	12.5 μM (MIC)	Ciprofloxacin 0.39 μM (MIC)	[69]
Dendrodolide C (**118**)	Antimicrobial	Broth dilution assay/*B. cereus*	25.0 μM (MIC)	Ciprofloxacin 1.56 μM (MIC)	[69]
		Broth dilution assay/*E. coli*	25.0 μM (MIC)	Ciprofloxacin 1.56 μM (MIC)	[69]
		Broth dilution assay/*P. putida*	6.25 μM (MIC)	Ciprofloxacin 0.39 μM (MIC)	[69]
		Broth dilution assay/*N. brasiliensis*	25.0 μM (MIC)	Ciprofloxacin 0.78 μM (MIC)	[69]
		Broth dilution assay/*V. parahaemolyticus*	25.0 μM (MIC)	Ciprofloxacin 1.56 μM (MIC)	[69]
Cladocladosin A (**121**)	Antimicrobial	Microplate assay/*E. tarda*	1.0 μg/mL (MIC)	Chloramphenicol 0.5 μg/mL (MIC)	[79]
	Antimicrobial	Microplate assay/*P. aeruginosa*	4.0 μg/mL (MIC)	Chloramphenicol 2.0 μg/mL (MIC)	[79]
Ent-cladospolide F (**123**)	AchE inhibitory	Modified Ellman's enzyme/Immunosorbent assay	40.26 μM (IC_{50})	Tacrine 0.5 μM (IC_{50})	[40]
Iso-cladospolide B (**126**)	Antimicrobial	Broth dilution assay/*B. cereus*	6.25 μM (MIC)	Ciprofloxacin 1.56 μM (MIC)	[69]
		Broth dilution assay/*T. halophilus*	6.25 μM (MIC)	Ciprofloxacin 1.56 μM (MIC)	[69]
		Broth dilution assay/*S. epidermidis*	25.0 μM (MIC)	Ciprofloxacin 0.78 μM (MIC)	[69]
		Broth dilution assay/*S. aureus*	25.0 μM (MIC)	Ciprofloxacin 0.39 μM (MIC)	[69]
		Broth dilution assay/*E. coli*	25.0 μM (MIC)	Ciprofloxacin 1.56 μM (MIC)	[69]
		Broth dilution assay/*P. putida*	6.25 μM (MIC)	Ciprofloxacin 0.39 μM (MIC)	[69]
		Broth dilution assay/*N. brasiliensis*	12.5 μM (MIC)	Ciprofloxacin 0.78 μM (MIC)	[69]
		Broth dilution assay/*V. parahaemolyticus*	25.0 μM (MIC)	Ciprofloxacin 1.56 μM (MIC)	[69]
		Microplate assay/*C. mandshurica* Miura	8.0 μg/mL (MIC)	Nystatin 1.0 μg/mL (MIC)	[78]
Cladosporol C (**143**)	Cytotoxicity	Trypan blue-cell viability assay/K562	>30.0 μM (IC_{50})	Trichostatin A 0.24 μM (IC_{50})	[82]
		Trypan blue-cell viability assay/A549	33.9 μM (IC_{50})	Trichostatin A 0.05 μM (IC_{50})	[82]
		Trypan blue-cell viability assay/Huh-7	>30.0 μM (IC_{50})	Trichostatin A 0.08 μM (IC_{50})	[82]
		Trypan blue-cell viability assay/H1975	45.6 μM (IC_{50})	Trichostatin A 0.09 μM (IC_{50})	[82]
		Trypan blue-cell viability assay/MCF-7	>30.0 μM (IC_{50})	Trichostatin A 0.78 μM (IC_{50})	[82]
		Trypan blue-cell viability assay/U937	>30.0 μM (IC_{50})	Trichostatin A 0.06 μM (IC_{50})	[82]
		Trypan blue-cell viability assay/BGC823	>30.0 μM (IC_{50})	Trichostatin A 0.09 μM (IC_{50})	[82]
		Trypan blue-cell viability assay/HL-60	72.5 μM (IC_{50})	Trichostatin A 0.09 μM (IC_{50})	[82]
		Trypan blue-cell viability assay/A549	>30.0 μM (IC_{50})	Trichostatin A 0.11 μM (IC_{50})	[82]

Table 2. *Cont.*

Compound Name	Biological Activity	Assay, Organism, or Cell Line	Biological Results	Positive Control	Ref.
		Trypan blue-cell viability assay/MOLT-4	14.4 μM (IC_{50})	Trichostatin A 0.03 μM (IC_{50})	[82]
		MTT/A549	14.0 μM (IC_{50})	Cisplatin 1.3 μM (IC_{50})	[84]
		MTT/HeLa	4.0 μM (IC_{50})	Paclitaxel 4.9 μM (IC_{50})	[84]
	Antimicrobial	Microplate assay/*E. coli*	8.0 μg/mL (MIC)	Chloramphenicol 0.025 μg/mL (MIC)	[84]
		Microplate assay/*M. luteus*	32.0 μg/mL (MIC)	Chloramphenicol 0.5 μg/mL (MIC)	[84]
		Microplate assay/*V. harveyi*	16.0 μg/mL (MIC)	Chloramphenicol 2.0 μg/mL (MIC)	[84]
		Microplate assay/*S. aureus*	6.25 μg/mL (MIC)	Ciprofloxacin 0.39 μg/mL (MIC)	[71]
		Microplate assay/*M. luteus*	12.5 μg/mL (MIC)	Ciprofloxacin 0.39 μg/mL (MIC)	[71]
Cladosporol D (**144**)	Anti-inflammatory	Spectrophotometry/Anti-COX-2/$PGF_{2\alpha}$ inhibition	60.2 μM (IC_{50})	Indomethacin 18.3 μM (IC_{50}) NS-398 1.0 μM (IC_{50})	[82]
Cladosporol E (**145**)	Insecticidal	Measuring the corrected mortality (CM)	150.0 μg/mL (IC_{50})	Azadirachtin 25.0 μg/mL (IC_{50})	[71]
	Antimicrobial	Microplate assay/*S. aureus*	1.56 μg/mL (MIC)	Ciprofloxacin 0.39 μg/mL (MIC)	[71]
		Microplate assay/*M. luteus*	12.5 μg/mL (MIC)	Ciprofloxacin 0.39 μg/mL (MIC)	[71]
Cladosporol F (**146**)	Cytotoxicity	MTT/K562	23.0 μM (IC_{50})	Doxorubicin 0.6 μM (IC_{50})	[83]
		SRB/HeLa	13.8 μM (IC_{50})	Doxorubicin 0.5 μM (IC_{50})	[83]
		SRB/HCT-116	23.0 μM (IC_{50})	Doxorubicin 0.2 μM (IC_{50})	[83]
		MTT/A549	15.0 μM (IC_{50})	Cisplatin 1.3 μM (IC_{50})	[84]
		MTT/HeLa	10.0 μM (IC_{50})	Paclitaxel 4.9 μM (IC_{50})	[84]
	Antimicrobial	Microplate assay/*E. coli*	32.0 μg/mL (MIC)	Chloramphenicol 0.025 μg/mL (MIC)	[84]
		Microplate assay/*M. luteus*	64.0 μg/mL (MIC)	chloramphenicol 0.5 μg/mL (MIC)	[84]
		Microplate assay/*V. harveyi*	32.0 μg/mL (MIC)	Chloramphenicol 2.0 μg/mL (MIC)	[84]
Cladosporol G (**147**)	Cytotoxicity	MTT/K562	8.8 μM (IC_{50})	Doxorubicin 0.6 μM (IC_{50})	[83]
		SRB/HeLa	3.9 μM (IC_{50})	Doxorubicin 0.5 μM (IC50)	[83]
		SRB/HCT-116	19.4 μM (IC_{50})	Doxorubicin 0.2 μM (IC_{50})	[83]
Cladosporol G (**148**)	Cytotoxicity	MTT/A549	13.0 μM (IC_{50})	Cisplatin 1.3 μM (IC_{50})	[84]
		MTT/H446	11.0 μM (IC_{50})	Adriamycin 4.0 μM (IC_{50})	[84]
		MTT/Huh7	10.0 μM (IC_{50})	Fluorouracil 6.2 μM (IC_{50})	[84]
		MTT/L02	11.0 μM (IC_{50})	Cisplatin 13.0 μM (IC_{50})	[84]
		MTT/LM3	14.0 μM (IC_{50})	Cisplatin 9.1 μM (IC_{50})	[84]
		MTT/SW1990	15.0 μM (IC_{50})	Gemcitabine 2.2 μM (IC_{50})	[84]
	Antimicrobial	Microplate assay/*E. coli*	64.0 μg/mL (MIC)	Chloramphenicol 0.025 μg/mL (MIC)	[84]
		Microplate assay/*M. luteus*	128.0 μg/mL (MIC)	Chloramphenicol 0.5 μg/mL (MIC)	[84]

Table 2. *Cont.*

Compound Name	Biological Activity	Assay, Organism, or Cell Line	Biological Results	Positive Control	Ref.
		Microplate assay/*V. harveyi*	64.0 μg/mL (MIC)	Chloramphenicol 2.0 μg/mL (MIC)	[84]
Cladosporol H (**149**)	Cytotoxicity	MTT/A549	5.0 μM (IC_{50})	Cisplatin 1.3 μM (IC_{50})	[84]
		MTT/H446	10.0 μM (IC_{50})	Adriamycin 4.0 μM (IC_{50})	[84]
		MTT/Huh7	1.0 μM (IC_{50})	Fluorouracil 6.2 μM (IC_{50})	[84]
		MTT/LM3	4.1 μM (IC_{50})	Cisplatin 9.1 μM (IC_{50})	[84]
		MTT/MCF-7	10.0 μM (IC_{50})	Paclitaxel 1.8 μM (IC_{50})	[84]
		MTT/SW1990	15.0 μM (IC_{50})	Gemcitabine 2.2 μM (IC_{50})	[84]
	Antimicrobial	Microplate assay/*E. coli*	32.0 μg/mL (MIC)	Chloramphenicol 0.025 μg/mL (MIC)	[84]
		Microplate assay/*M. luteus*	64.0 μg/mL (MIC)	Chloramphenicol 0.5 μg/mL (MIC)	[84]
		Microplate assay/*V. harveyi*	4.0 μg/mL (MIC)	Chloramphenicol 2.0 μg/mL (MIC)	[84]
Cladosporol I (**150**)	Cytotoxicity	MTT/HeLa	10.8 μM (IC_{50})	Paclitaxel 4.9 μM (IC_{50})	[84]
	Antimicrobial	Microplate assay/*E. coli*	64.0 μg/mL (MIC)	Chloramphenicol 0.025 μg/mL (MIC)	[84]
		Microplate assay/*M. luteus*	64.0 μg/mL (MIC)	Chloramphenicol 0.5 μg/mL (MIC)	[84]
		Microplate assay/*V. harveyi*	16.0 μg/mL (MIC)	Chloramphenicol 2.0 μg/mL (MIC)	[84]
Cladosporol J (**151**)		MTT/A549	15.0 μM (IC_{50})	Cisplatin 1.3 μM (IC_{50})	[84]
		MTT/H446	11.0 μM (IC_{50})	Adriamycin 4.0 μM (IC_{50})	[84]
		MTT/HeLa	15.0 μM (IC_{50})	Paclitaxel 4.9 μM (IC_{50})	[84]
		MTT/Huh7	20.0 μM (IC_{50})	Fluorouracil 6.2 μM (IC_{50})	[84]
		MTT/MCF-7	12.0 μM (IC_{50})	Paclitaxel 1.8 μM (IC_{50})	[84]
	Antimicrobial	Microplate assay/*E. coli*	16.0 μg/mL (MIC)	Chloramphenicol 0.025 μg/mL (MIC)	[84]
		Microplate assay/*M. luteus*	64.0 μg/mL (MIC)	Chloramphenicol 0.5 μg/mL (MIC)	[84]
		Microplate assay/*V. harveyi*	32.0 μg/mL (MIC)	Chloramphenicol 2.0 μg/mL (MIC)	[84]
Cladosporone A (**152**)	Cytotoxicity	Trypan blue-cell viability assay/K562	14.3 μM (IC_{50})	Trichostatin A 0.24 μM (IC_{50})	[82]
		Trypan blue-cell viability assay/A549	15.7 μM (IC_{50})	Trichostatin A 0.05 μM (IC_{50})	[82]
		Trypan blue-cell viability assay/Huh-7	29.9 μM (IC_{50})	Trichostatin A 0.08 μM (IC_{50})	[82]
		Trypan blue-cell viability assay/H1975	40.6 μM (IC_{50})	Trichostatin A 0.09 μM (IC_{50})	[82]
		Trypan blue-cell viability assay/MCF-7	21.3 μM (IC_{50})	Trichostatin A 0.78 μM (IC_{50})	[82]
		Trypan blue-cell viability assay/U937	10.5 μM (IC_{50})	Trichostatin A 0.06 μM (IC_{50})	[82]
		Trypan blue-cell viability assay/BGC823	17.0 μM (IC_{50})	Trichostatin A 0.09 μM (IC_{50})	[82]
		Trypan blue-cell viability assay/HL-60	10.1 μM (IC_{50})	Trichostatin A 0.09 μM (IC_{50})	[82]
		Trypan blue-cell viability assay/A549	53.7 μM (IC_{50})	Trichostatin A 0.11 μM (IC_{50})	[82]
		Trypan blue-cell viability assay/MOLT-4	14.6 μM (IC_{50})	Trichostatin A 0.03 μM (IC_{50})	[82]

Table 2. *Cont.*

Compound Name	Biological Activity	Assay, Organism, or Cell Line	Biological Results	Positive Control	Ref.
	Anti-inflammatory	Spectrophotometry/Anti-COX-2/$PGF_{2\alpha}$ inhibition	49.1 μM (IC_{50})	Indomethacin 18.3 μM (IC_{50}) NS-398 1.0 μM (IC_{50})	[82]
Aladothalen (**160**)	Antimicrobial	Agar dilution method/*B. cereus*	50.0 μM (MIC)	Ciprofloxacin < 0.4 μM (MIC)	[89]
		Agar dilution method/*M. phlei*	25.0 μM (MIC)	Ciprofloxacin < 0.4 μM (MIC)	[89]
		Agar dilution method/MRCNS	25.0 μM (MIC)	Ciprofloxacin 25.0 μM (MIC)	[89]
Cladonaphchrom A (**169**)	Antimicrobial	Microplate assay/*S. albus*	1.25 μg/mL (MIC)	Ciprofloxacin 0.6 μg/mL (MIC)	[90]
		Microplate assay/*E. coli*	2.5 μg/mL (MIC)	Ciprofloxacin 0.3 μg/mL (MIC)	[90]
		Microplate assay/*B. subtilis*	10.0 μg/mL (MIC)	Ciprofloxacin 0.6 μg/mL (MIC)	[90]
		Microplate assay/*M. tetragenus*	5.0 μg/mL (MIC)	Ciprofloxacin 0.3μg/mL (MIC)	[90]
		Microplate assay/*M. luteus*	10.0 μg/mL (MIC)	Ciprofloxacin 0.3 μg/mL (MIC)	[90]
		Microplate assay/*A. brassicicola*	50.0 μg/mL (MIC)	Prochloraz 12.5 μg/mL (MIC)	[90]
		Microplate assay/*P. parasitica* var. *nicotianae*	50.0 μg/mL (MIC)	Prochloraz 50.0 μg/mL (MIC)	[90]
		Microplate assay/*C. capsici*	25.0 μg/mL (MIC)	Prochloraz 12.5 μg/mL (MIC)	[90]
		Microplate assay/*B. oryzae*	100.0 μg/mL (MIC)	Prochloraz 50.0 μg/mL (MIC)	[90]
		Microplate assay/*D. medusaea*	50.0 μg/mL (MIC)	Prochloraz 50.0 μg/mL (MIC)	[90]
		Microplate assay/*C. paradoxa*	50.0 μg/mL (MIC)	Prochloraz 25.0 μg/mL (MIC)	[90]
Cladonaphchrom B (**170**)	Antimicrobial	Microplate assay/*S. albus*	2.5 μg/mL (MIC)	Ciprofloxacin 0.6 μg/mL (MIC)	[90]
		Microplate assay/*E. coli*	2.5 μg/mL (MIC)	Ciprofloxacin 0.3 μg/mL (MIC)	[90]
		Microplate assay/*B. subtilis*	5.0 μg/mL (MIC)	Ciprofloxacin 0.6 μg/mL (MIC)	[90]
		Microplate assay/*M. tetragenus*	5.0 μg/mL (MIC)	Ciprofloxacin 0.3μg/mL (MIC)	[90]
		Microplate assay/*M. luteus*	10.0 μg/mL (MIC)	Ciprofloxacin 0.3 μg/mL (MIC)	[90]
		Microplate assay/*A. brassicicola*	25.0 μg/mL (MIC)	Prochloraz 12.5 μg/mL (MIC)	[90]
		Microplate assay/*P. parasitica* var. *nicotianae*	50.0 μg/mL (MIC)	Prochloraz 50.0 μg/mL (MIC)	[90]
		Microplate assay/*C. capsici*	25.0 μg/mL (MIC)	Prochloraz 12.5 μg/mL (MIC)	[90]
		Microplate assay/*D. medusaea*	100.0 μg/mL (MIC)	Prochloraz 50.0 μg/mL (MIC)	[90]
		Microplate assay/*C. paradoxa*	50.0 μg/mL (MIC)	Prochloraz 25.0 μg/mL (MIC)	[90]
Malettinin A (**178**)	Antimicrobial	Microplate assay/*T. rubrum*	33.1 μM (IC_{50})	Clotrimazole 0.2 μM (IC_{50})	[93]
Malettinin B (**179**)		Microplate assay/*X. campestris*	28.3 μM ((IC_{50})	Chloramphenicol 2.1 μM (IC_{50})	[93]
		Microplate assay/*T. rubrum*	60.6 μM (IC_{50})	Clotrimazole 0.2 μM (IC_{50})	[93]
Malettinin C (**180**)	Antimicrobial	Microplate assay/*T. rubrum*	37.9 μM (IC_{50})	Clotrimazole 0.2 μM (IC_{50})	[93]
		Microplate assay/*X. campestris*	83.2 μM (IC_{50})	Chloramphenicol 2.1 μM (IC_{50})	[93]
Malettinin E (**181**)	Antimicrobial	Microplate assay/*T. rubrum*	28.7 μM (IC_{50})	Clotrimazole 0.2 μM (IC_{50})	[93]

Table 2. *Cont.*

Compound Name	Biological Activity	Assay, Organism, or Cell Line	Biological Results	Positive Control	Ref.
		Microplate assay/*X. campestris*	30.7 μM (IC_{50})	Chloramphenicol 2.1 μM ((IC_{50})	[93]
Cladosporinone (**182**)		Broth dilution assay/*S. aureus*	64.0 μg/mL(MIC)	-	[94]
Viriditoxin (**183**)		Broth dilution assay/*S. aureus*	0.015 μg/mL (MIC) 0.023 μM (MIC)	-	[94]
Viriditoxin derivative 1 (**184**)		Broth dilution assay/*S. aureus*	2.0 μg/mL (MIC)	-	[94]
Viriditoxin derivative 2 (**185**)		Broth dilution assay/*S. aureus*	16.0 μg/mL (MIC)	-	[94]
(2S,4S)-4-Methoxy-2-methylchroman-5-ol (**201**)	Antioxidant	DPPH assay	5.66 μM (IC_{50})	Ascorbic acid 3.29 μM (IC_{50})	[95]
(2S,4S)-2-Methylchroman-4,5-diol (**203**)	Antioxidant	DPPH assay	6.67 μM (IC_{50})	Ascorbic acid 3.29 μM (IC_{50})	[95]
Citrinin H1 (**206**)	Insecticidal	Measuring the corrected mortality (CM)	100.0 μg/mL (IC_{50})	Azadirachtin 25.0 μg/mL (IC_{50})	[71]
	Antimicrobial	Microplate assay/*S. aureus*	6.25 μg/mL (MIC)	Ciprofloxacin 0.39 μg/mL (MIC)	[71]
		Microplate assay/*E. coli*	12.5 μg/mL (MIC)	Ciprofloxacin 0.19 μg/mL (MIC)	[71]
		Microplate assay/*B. cereus*	12.5 μg/mL (MIC)	Ciprofloxacin 0.19 μg/mL (MIC)	[71]
Vermistatin (**214**)	Insecticidal	CM/Helicoverpa armigera Hubner larvae	150.0 μg/mL (IC_{50})	Azadirachtin 25.0 μg/mL (IC_{50})	[71]
	Antimicrobial	Microplate assay/*S. aureus*	25.0 μg/mL (MIC)	Ciprofloxacin 0.39 μg/mL (MIC)	[71]
		Microplate assay/*B. cereus*	25.0 μg/mL (MIC)	Ciprofloxacin 0.39 μg/mL (MIC)	[71]
Cladoscyclitol B (**219**)	α-Glucosidase inhibitory	Colorimetric assay	2.95 μM (IC_{50})	Acarbose 2.35 μM (IC_{50})	[97]
3-Phenyl-2-propenoic acid (**232**)	Insecticidal	Inhibitinon 50%/*B. amphitrite*	84.28 μg/mL (EC_{50})	FSW with DMSO	[60]
Cladosporinone (**182**)		Broth dilution assay/*S. aureus*	64.0 μg/mL(MIC)	-	[94]
		Lethality 50%/*B. amphitrite*	>200 μg/mL (LC_{50})	FSW with DMSO	[60]
		Inhibitinon 50%/*B. neritina*	11.15 μg/mL (EC_{50})	FSW with DMSO	[60]
		Lethality 50%/*B. neritina*	>200 μg/mL (LC_{50})	FSW with DMSO	[60]
	Antimicrobial	Serial dilution/*L. hongkongensis*	80 μg/mL (MIC)	Streptomycin 250 μg/mL (MIC) Penicillin 0.25 μg/mL (MIC)	[60]
3-(2,3-Dihydroxy phenoxy) butanoic acid (**233**)	Antioxidant	DPPH assay	0.24 μM (IC_{50})	Ascorbic acid 3.29 μM (IC_{50})	[95]
Methyl (3S)-3-(2,3-dihydroxy phenyloxy)butanoate (**235**)	Antioxidant	DPPH assay	2.65 μM (IC_{50})	Ascorbic acid 3.29 μM (IC_{50})	[95]
2-Phenylethanol (**238**)	Insecticidal	Inhibitinon 50%/*B. amphitrite*	53.65 μg/mL (EC_{50})	FSW with DMSO	[60]
		Lethality 50%/*B. amphitrite*	>200 μg/mL (LC_{50})	FSW with DMSO	[60]
		Inhibitinon 50%/*B. neritina*	102.23 μg/mL (EC_{50})	FSW with DMSO	[60]
		Lethality 50%/*B. neritina*	>200 μg/mL (LC_{50})	FSW with DMSO	[60]

Table 2. *Cont.*

Compound Name	Biological Activity	Assay, Organism, or Cell Line	Biological Results	Positive Control	Ref.
4-*O*-α-*D*-Ribofuranose-2-pentyl-3-phemethylol (**240**)	α-Glucosidase inhibitory	Colorimetric assay	2.05 μM (IC_{50})	Acarbose 2.35 μM (IC_{50})	[97]
Cladosporin D (247)	Antioxidant	DPPH assay	16.4 μM (IC_{50})	Ascorbic acid 4.9 μM (IC_{50})	[36]
(2S)-7,4′-dihydroxy-5-methoxy-8-(γ,γ-dimethylallyl)-flavanone (**248**)	Protein tyrosine phosphatase 1B inhibitory	PTP1B/Spectrophotometry	11.0 μM (IC_{50})	Oleanolic acid 0.9 μM (IC_{50})	[68]
		TCPTP/Spectrophotometry	27.0 μM (IC_{50})	Oleanolic acid 0.8 μM (IC_{50})	[68]
Bis(2-ethylhexyl)phthalate (**249**)	Insecticidal	Inhibitinon 50%/*B. amphitrite*	9.18 μg/mL (EC_{50})	FSW with DMSO	[60]
		Lethality 50%/*B. amphitrite*	>200 μg/mL (LC_{50})	FSW with DMSO	[60]
		Inhibitinon 50%/*B. neritina*	77.85 μg/mL (EC_{50})	FSW with DMSO	[60]
		Lethality 50%/*B. neritina*	>200 μg/mL (LC_{50})	FSW with DMSO	[60]
1,1′-Dioxine-2,2′-dipropionic acid (**252**)	Insecticidal	Measuring the corrected mortality (CM)/Helicoverpa armigera Hubner larvae	150.0 μg/mL (IC_{50})	Azadirachtin 25.0 μg/mL (IC_{50})	[70,71]
	Antimicrobial	Microplate assay/*S. aureus*	25.0 μg/mL (MIC)	Ciprofloxacin 0.39 μg/mL (MIC)	[71]
		Microplate assay/*E. coli*	25.0 μg/mL (MIC)	Ciprofloxacin 0.19 μg/mL (MIC)	[71]
		Microplate assay/*B. cereus*	12.5 μg/mL (MIC)	Ciprofloxacin 0.39 μg/mL (MIC)	[71]
5α,8α-Epidioxy-ergosta-6,22E-dien-3β-ol (**256**)	Antiviral	Neuraminidase inhibition assay/RSV	0.11 μM (IC_{50})	Ribavirin 0.08 μM (IC_{50})	[100]
3β,5α-Dihydroxy-6β-methoxyergosta-7,22-diene (**262**)	Antiviral	Neuraminidase inhibition assay/RSV	0.11 μM (IC_{50})	Ribavirin 0.08 μM (IC_{50})	[100]
5α,8α-Epidioxy-ergosta-6,9,22E-triene-3β-ol (**258**)	Antiviral	Neuraminidase inhibition assay/RSV	0.17 μM (IC_{50})	Ribavirin 0.08 μM (IC_{50})	[100]
3α-Hydroxy-pregna-7-ene-6,20-dione = Cladosporisteroid B (**268**)	Antiviral	Neuraminidase inhibition assay/RSV	0.12 μM (IC_{50})	Ribavirin 0.08 μM (IC_{50})	[100]
		CPE inhibition assay/ Influenza A H3N3 virus	16.2 μM (IC_{50})	Oseltamivir 34.0 nM (IC_{50})	[61]
(3E,8E,6S)-Undeca-3,8,10-trien-1,6-diol (**286**)	Cytotoxicity	SRB/H1975	10.0 μM (IC_{50})	Adriamycin 0.38 μM (IC_{50})	[95]

Pectinases are hydrolytic enzymes that are accountable for the hydrolysis of pectins. They are commonly found in fungi, bacteria, and plants. They have remarkable importance in the food industry such as vegetables and fruits processing, wine production, and olive oil extraction, as well as coffee, cocoa, and tea fermentation. They are utilized in the beverage industry to produce high yields due to improving clarification and pressing of concentrated fruit juices [103]. Bastos et al. purified pectinase enzymes PG and PME from *C. cladosporioides* using the Buescher and Furmanski procedure after 10-day incubation and precipitation with $(NH_4)_2SO_4$ and benzoate buffer at pH 4.0 [49].

Agarases and carrageenases can decompose algal biomass, producing carrageenans and agars that are the major components of the red algae cell wall. Furthermore, agarases hydrolyze agar, resulting in oligosaccharides that are employed as food additives with beneficial influences on human health [104,105]. Additionally, carrageenases are used to obtain carrageenans that have varied industrial applications as emulsifying, thickening, and gelling agents in the preparation of food, as well as bioactivities such as anti-tumor, antiviral, antithrombotic, immunomodulatory, anticoagulant, and antioxidant [106]. *Cladosporium* sp. isolated from the Antarctic macroalgae *Ascoseira mirabilis* and *Georgiella confuens* produced agarase that may have industrial importance in the extraction of agar or its byproducts such as bioactive galactose and oligosaccharides exist in the algal biomass to be utilized as substrates of 3rd generation bioethanol [11].

Xylan, the main component of hemicelluloses in the plant cell walls, represents about one-third of all renewable organic carbon on earth. Xylanases hydrolyze xylan to oligosaccharides that are further degraded to xylose. The latter is utilized for xylitol and bioethanol production. Xylanases have remarkable biotechnological influence in developing eco-friendly technologies in the pulp and paper industry and in food and feed industries, and for generating chemicals and liquid fuels from lignocellulose [107–109]. The cold-active xylanases have notable applications in bioremediation and food and textile and industries [110]. *Cladosporium* sp. isolated from Antarctic marine sponge had high xylanase potential when grown on wheat bran and pure xylans at lower temperatures that is a feature of cold-active enzymes [48]. Therefore, cold-active xylanases preparations from *Cladosporium* sp. could be convenient for many biotechnological processes, utilizing moderate- to low-temperature processes, especially those in food industries [48]. Gil-Durán et al. purified and characterized XynA, a cold-active endo-xylanase from *Cladosporium* sp. derived from Antarctic sponge. XynA is highly active on xylans with high arabinose content. Moreover, it is the most thermolabile endo-xylanase reported from filamentous fungus. Therefore, it could be a good alternative in some biotechnological operations to avoid heating, thereby reducing the costs [45].

The three main lignin-hydrolyzing enzymes that have great potential for industrial applications are LiP (lignin peroxidase), MnP (manganese-dependent peroxidase), and Lac (laccase) [111]. LiP is a high oxidant heme protein that oxidizes non-phenolic and phenolic substrates. MnP is a H_2O_2-dependent glycoprotein that needs Mn^{2+} for oxidizing aromatic dyes and mono-aromatic phenols [112]. Laccase is multi-copper oxidase, which oxidizes aromatic amines and catalyzes the O_2 reduction to H_2O [111]. *C. cladosporioides* CBMAI 857 isolated from the Brazilian cnidarian *Palythoa variabilis* produced ligninolytic enzymes (LiP, MnP, and Lac) with particular response to the various conditions of salinity and carbon sources. It possessed high values of MnP and laccase activities under salinity (12.5% and 23% *w*/*v*, respectively), indicating the potential use of this fungus for industrial applications and bioremediation of high-salt contaminated sites [50].

RBBR (Remazol Brilliant Blue R) and polymeric dyes decolorization has been assigned as an effective screening method for the fungi ability to degrade recalcitrant pollutants, including aromatic compounds such as PAHs. It was demonstrated that marine-derived fungi are often more effective than terrestrial fungi in treating various colored effluents because they are better adapted to perform under extreme conditions such as high salinity [113]. *C. cladosporioides* CBMAI-857 associated with the coral *Palythoa caribaeorum* was

tested for its RBBR decolorizing potential. It had efficient dye decolorization potential (93%) after 12 days in both liquid and solid media [114]. Further, *Cladosporium* sp. associated with the seagrass *Posidonia oceanica* produced tannases and ligninolytic enzymes at high salt concentrations. Its laccase and peroxidase activity was evident by the degradation of RBBR and Amaranth Red dyes [12,115].

Invertase is a β-fructo-furanosidase that catalyzes sucrose conversion into fructose and glucose, giving invert syrup. This invert syrup is utilized in the beverage and food industries as a humectant in non-crystallizing creams, candies, artificial honey, and jam preparation [116]. Molasses is a sugar solution that is obtained as a co-product of sugar production. Due to its high sucrose content and low cost, it is utilized as an invertase production substrate to produce industrially valuable substances [117]. However, it contains melanoidins, which are dark brown pigments. Its discharge in the soil prohibits seed germination and decreases manganese availability and soil alkalinity. Furthermore, it blocks photosynthesis and sunlight penetration in the aquatic system [118]. Therefore, its removal from molasses-based wastewater is potentially important for environmental safety. Taskin et al. reported that *C. herbarum* ER-25 possessed a high invertase potential and removed melanoidins from molasses through bio-adsorption and biodegradation mechanisms by Lac and MnP in the non-sterilized medium than in sterilized one at 5.5 pH and 20 °C. Therefore, this cold-adapted fungus can be used for molasses de-colorization [46].

Cellulose is a main component of the plant material that is abundantly utilized for the production of alternative liquid fuels such as bioethanol. *C. sphaerospermum* obtained from deteriorated seaweed *Ulva* through SSF (solid-state fermentation) produced cellulase that had saccharification potential of seaweed biomass using green seaweed *Ulva fasciata*. Therefore, this cellulase can be utilized for saccharification of cellulosic feedstock for bioethanol production from marine macro-algal feedstock [47].

Biocatalysis is an eco-friendly process for renewable raw materials and clean energy production and for the remediation of environmental contaminants [119]. Recently, the synthesis of industrial and chemically interesting complex molecules using biocatalysts, including enzymes and whole-cell systems is a grown-research field. Reductases have been utilized for various substrates reduction such as aldehydes, carboxylic acid derivatives, ketones, nitro compounds, and nitriles [119,120]. Furthermore, it has been reported that microorganisms' whole cells are a potential source for new enzymes used in carbonylated compounds reduction [121]. Knoevenagel condensation is a very useful synthetic tool for functionalization, as well as for increasing the carbon chains that is applied for the synthesis of intermediates polymers and various bioactive organic compounds [122]. Birolli et al. reported that the bio-reduction of Knoevenagel adducts between cyanoacetamide and aromatic aldehydes was achieved in considerable yields with whole-cells of *Cladosporium* sp. CBMAI 1237 isolated from *Dragmacidon reticulatum*, revealing the existence of ene-reductases [43]. Additionally, *C. cladosporioides* CBMAI-857 isolated from the Brazilian cnidarian *Palythoa caribaeorum* catalyzed the asymmetric bio-reduction of 1-(4-methoxyphenyl)ethanone to 1-(4-methoxyphenyl)ethanol [123]. Moreover, the sponge-associated *C. cladosporioides* CBMAI-857 catalyzed the enantio-selective bio-reduction of different aromatic ketones at pH 7.0 and 32 °C [124].

3. Secondary Metabolites and Bioactivities of Marine-Associated *Cladosporium* Species

Marine-associated *Cladosporium* species are rich with diverse types of metabolites with varied structural features such as macrolides, fatty acids, pyrones, phenolics, alkaloids, diketopiperazines, terpenes, sterols, quinones, lactones, and tetramic acid derivatives. Their classification was carried out here according to the chemical nature. During our search, it was found that some of the reported metabolites had the same structures and molecular formulae with different nomenclature. On the other hand, some metabolites had the same names with different structures. Moreover, some metabolites did not have names, thus they are named here using the AUPAC system for nomenclature. Herein, the reported

secondary metabolites from *Cladosporium* species, as well as their bioactivities have been discussed (Tables 1 and 2).

3.1. Tetramic Acid Derivatives

Tetramic acids are five-membered heterocycles with a pyrrolidine-2,4-dione core that are formed by the fusion of polyketide units and amino acid [125]. The tertarmic acid moiety is commonly present as 3-acyl or 4-*O*-alkyl ether derivatives [126]. These structures can be characterized as simple heterocycles or more complex systems possibly containing long chains or fused polycyclic skeletons [127]. They are found in varied natural metabolites and isolated from various terrestrial and marine species, such as bacteria, sponges, and fungi [127,128]. They exhibited a wide range of bioactivities: cytotoxic, antimicrobial, antiulcer, and antiviral [125]. Note that 30 tetramic acid derivatives have been reported from marine-derived *Cladosporium* species, 28 (93.3%) of them are from *C. sphaerospermum*.

The tetramic acid derivatives, cladosins A, B, D, and E (**1**, **2**, **4**, and **5**) biosynthesized by *C. sphaerospermum* 2005-01-E3 obtained from deep-sea sludge had no activity towards influenza A H1N1 virus (Figure 1). While **3** exhibited anti-H1N1 activity (IC_{50} 276.0 μM) in comparison to ribavirin (IC_{50} 131.0 μM) [42]. Moreover, they showed no NF-κB inhibitory and no cytotoxic effect towards BGC-823, HL-60, HCT-8, A2780, A549, and Bel-7402 cell lines, as well as no activity towards *Mycobacterium tuberculosis* in the disk diffusion method [42]. Moreover, cladosins B (**2**), C (**3**), F (**5**), and L (**11**) separated from *C. sphaerospermum* SW67 associated with *Hydractinia echinat* hydroid polyp were assessed for protection towards cisplatin-caused cell damage in LLC-PK1 cells [53]. The co-treatment with compounds **2** and **5** alleviated the LLC-PK1 cells damage induced by cisplatin (Conc. 25 μM). Compound **2** (Conc. 100 μM) recovered cell viability with 90.68% that was more than NAC (*N*-acetylcysteine, 88.23%, Conc. 500 μM), whereas **5** (Conc. 50 and 100 μM) increased cell viability by 77.65 and 85.60%, respectively. Thus, **2** may be a candidate for treating cisplatin-produced unwanted effects and/or to prohibited nephrotoxicity induced by anticancer drugs. It was proposed that the existence of the C-8 hydroxy group may be essential for the reno-protective effect towards cisplatin-produced toxicity in LLC-PK1 cells [53].

In 2015, by OSMAC (one strain many compounds) technique, Yu et al. separated compounds **5** and **6** from *C. sphaerospermum* 2005-01-E3 that did not have anti-influenza A H1N1, anticancer, and anti-tubercular, as well as no NF-κB inhibitory activities [54]. Note that a tetramic acid derivative named cladosin L with a different structure was separated in 2020 by Pan et al. from the plant-associated *C. sphaerospermum* WBS017 isolated from *Fritillaria unibracteata* var. *wabuensis* [14]. Cladosins H-K (**7**–**10**) and cladodionen (**13**) were isolated from sediment-derived *C. sphaerospermum* L3P3 and evaluated for cytotoxic capacity towards PC-3, MGC-803, SH-SY5Y, and HCT-116 cell lines using SRB method and against K562 and HL-60 using MTT method (Figure 2). Compounds **8**–**10** and **13** had a cytotoxic effect against HL-60 and K562 cell lines with IC_{50} ranging from 2.8 to 7.8 μM, while **7** (IC_{50} > 10 μM) was inactive. The results revealed that the C-8 absolute configuration and aniline moiety were essential for activity [55] (Table 2).

C. sphaerospermum SW67 associated with marine invertebrate *Hydractinia echinata* yielded three new spirocyclic tetramic acid-related metabolites **12**, **29**, and **30** (Figure 3). Compound **12** has a tetramic acid moiety conjugated with an unprecedented 2,7-diazaspiro[4.5]decane-1,4-dione core one, while **29** and **30** are tetramic acid stereoisomers with a C-3 quaternary center, bearing a six-membered lactone ring and a *trans*-hexylenic alcohol side chain. These metabolites had weak inhibitory effects versus HCC70, Bt549, MDA-MB-468, and MDA-MB-231 in the SRB bioassay (IC_{50} ranged from 70 to 85 μM), compared to etoposide (IC_{50} ranged from 1.76 to 2.27 μM) [38].

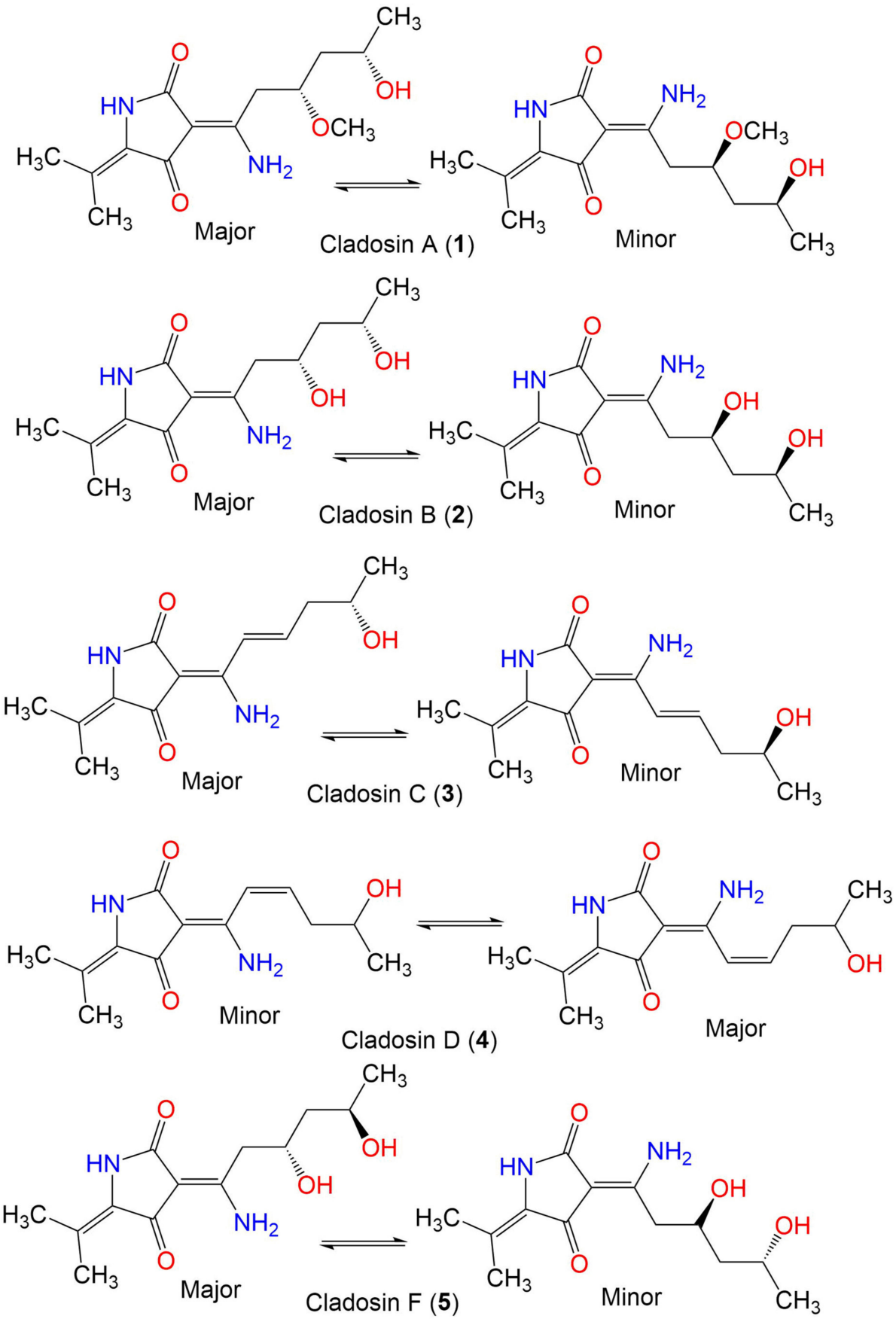

Figure 1. Tetramic acid derivatives **1**–**5**.

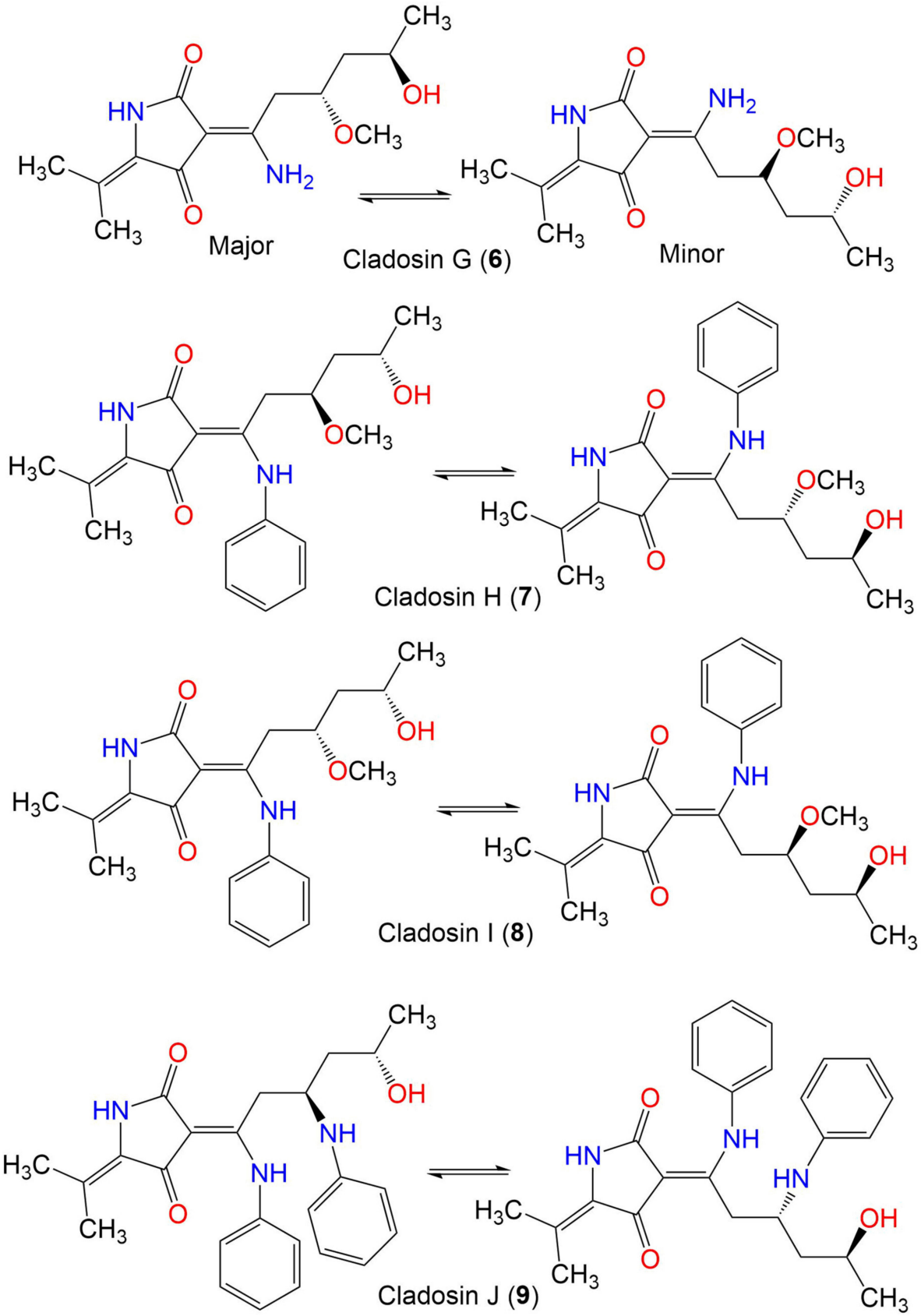

Figure 2. Tetramic acid derivatives **6**–**9**.

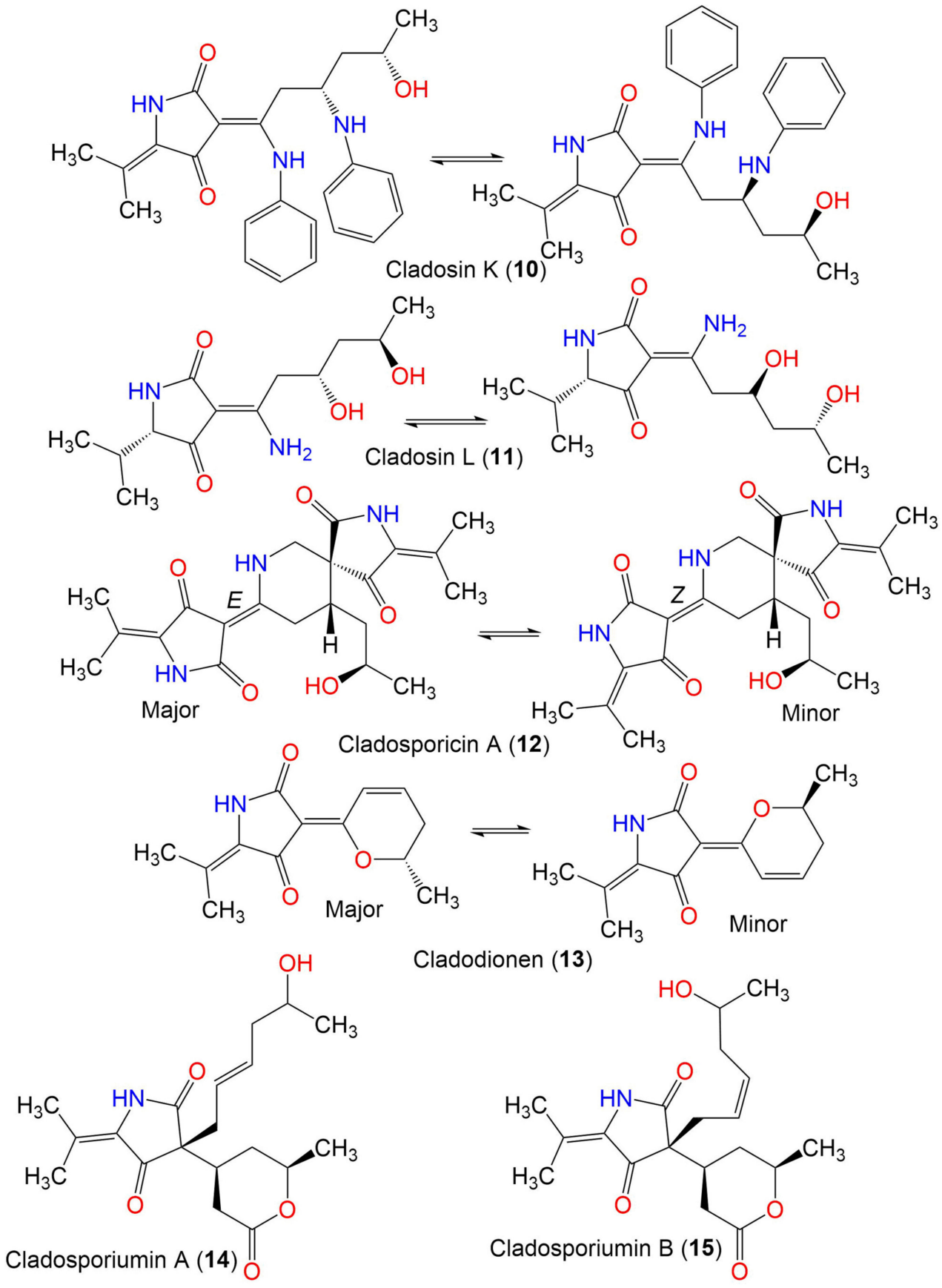

Figure 3. Tetramic acid derivatives **10**–**15**.

C. sphaerospermum EIODSF 008 isolated from the deep-sea sediment collected from the East Indian Ocean yielded tetramic acid derivatives **13** and **22**–**28** (Figures 4 and 5). They were assessed for cytotoxicity towards HL-60, HepG2, and MCF-7. Only **13** had cytotoxicity (IC_{50} 28.6 μM) towards the HL-60 cell line [57]. Additionally, they showed no antibacterial potential towards *E. coli*, *M. luteus*, and *B subtilis* [57]. Additionally, **13** showed cytotoxic capacity towards HL-60, HeLa, HCT-116, and MCF-7 cell lines (IC_{50} ranged from 9.1 to 19.1 μM), compared to ADR (adriamycin) (IC_{50} ranged from 0.02 to 0.67 μM). However, it did not have antibacterial activities (conc. 100 μg/mL) against *B. subtilis*, *P. aeruginosa*, *C. perfringens*, *S. aureus*, *E. coli*, and *C. albicans* [56]. Compounds **14**–**21**, new tetramic acid derivatives, were purified from the sea-sediment derived *Cladosporium* sp. acetone extract by Huang et al. in 2018. Compounds **14**–**16** are unusual 3-acyltetramic acids, having at C-3 of the pyrrolidine-2,4-dione core, a six-membered lactone ring, and hexyl-enic alcohol chain. They showed no obvious AchEI activity in the modified Ellman's enzyme assay [58]. Moreover, they displayed no anti-biofilm effect against *C. albicans* and *S. aureus* in the broth micro-dilution method and no cytotoxic effect towards HL60, HepG-2, and MCF-7 cell lines in the CCK8 assay [58].

3.2. Diketopiperazines

Diketopiperazines (DKPs) are cyclic dipeptides, consisting of two amino acids with or without extra structural modifications in the DKPs nucleus [108]. Their main skeleton comprises a six-membered piperazine nucleus produced from the double condensations among two amino acids [129,130]. The formation of peptide bonds in DKPs are catalyzed mainly by cyclodipeptide synthases (CDPSs) and non-ribosomal peptide synthetases (NRPSs) [131]. They possessed interesting bioactivities such as anti-Alzheimer, antimicrobial, antiviral, microtubule polymerization inhibitory, antitumor, anti-quorum-sensing, and haemosuppressor [129,130,132].

Cyclo-(Val-Pro) (**32**) and cyclo-(Phe-Pro) (**33**) were separated from the EtOAc extract of *Cladosporium* sp. F14 isolated from seawater and investigated for their anti-larval activity at conc. 50 μg/mL towards *Bugula neritina* and *Balanus amphitrite* larvae in the settlement inhibition assays [60] (Figure 6). They inhibited *B. neritina* settlement (EC_{50} 70.43 and >200 μg/mL, respectively) and *B. amphitrite* settlement (EC_{50} 68.57 and 37.82 μg/mL, respectively). Furthermore, **32** and **33** obviously prohibited *L. hongkongensis* growth (IZDs 8 mm and MICs 200 and 200 μg/mL, respectively), compared to streptomycin (MIC 250 μg/mL). The MICs of **33** towards *Ruegeria* sp. and *M. luteus* were 200 and 100 μg/mL, respectively, compared to streptomycin (MIC 500 and 250 μg/mL, respectively) [60]. On the other hand, thio-diketopiperazine derivatives, cladosporins A (**36**) and B (**37**), and haematocin (**38**) purified from the sediment-derived *Cladosporium* sp. were moderately cytotoxic towards HepG2 cell line (IC_{50} 48, 21, and 42 μg/mL, respectively) [62].

3.3. Alkaloids

Fungal alkaloids are nitrogen-containing metabolites that are derived from amino acid metabolism and the mevalonate pathway [133]. Many studies reported the detection of various classeses of alkaloids from marine-derived fungi such as pyrrolidine, indole, pyrrolizidine, quinazoline, quinoline, and purine classes [134–136]. These metabolites have shown broad biological activities: cytotoxic, anti-inflammatory, antioxidant, antibacterial, antifungal, antiviral, protease inhibitory. Therefore, they could have a potential for the development of innovative therapies [134–136]. In the current work, 49 alkaloids, belonging to different classes have been reported. Among them, 27 alkaloids were reported from unidentified *Cladosporium* species.

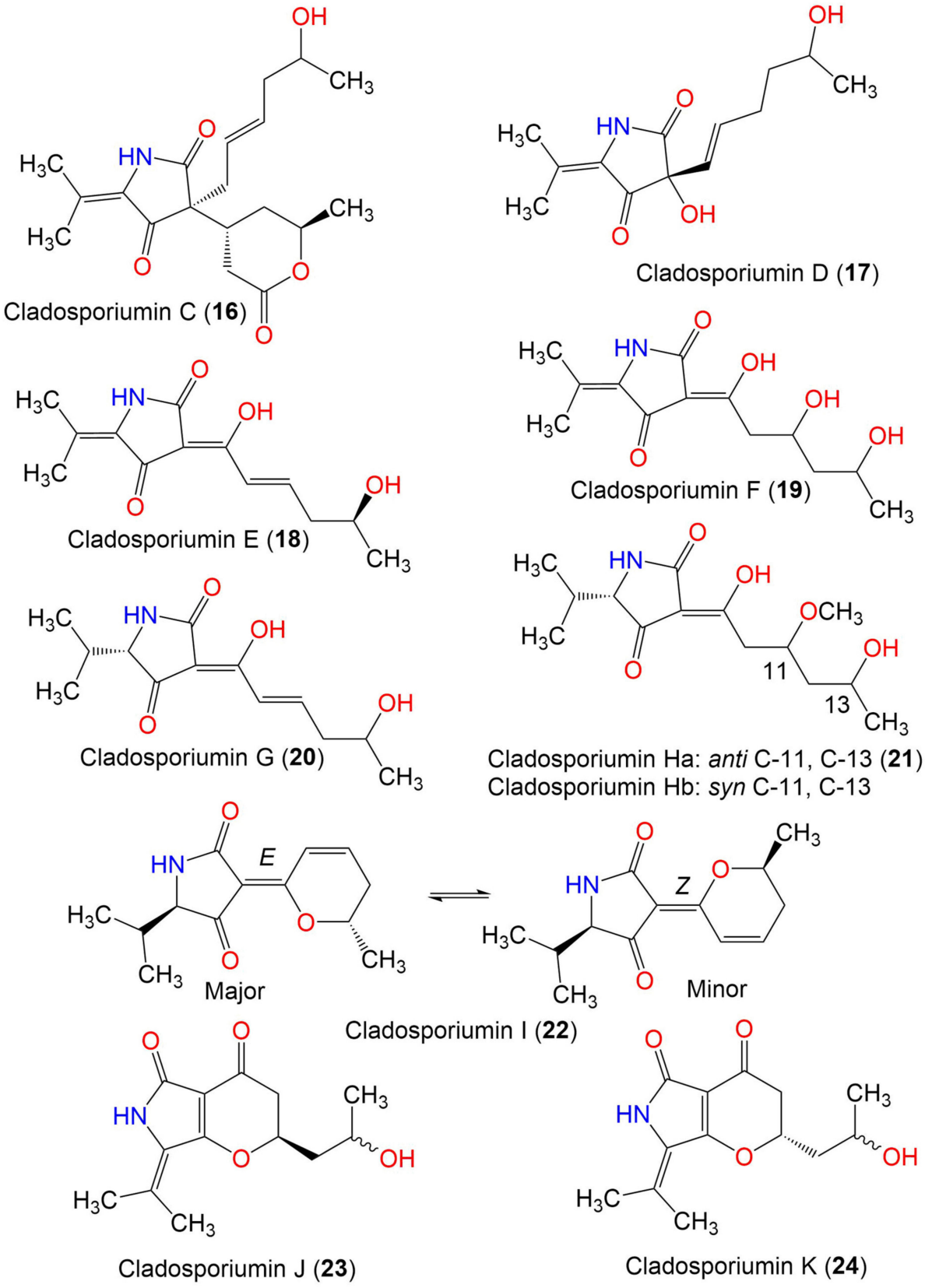

Figure 4. Tetramic acid derivatives **16**–**24**.

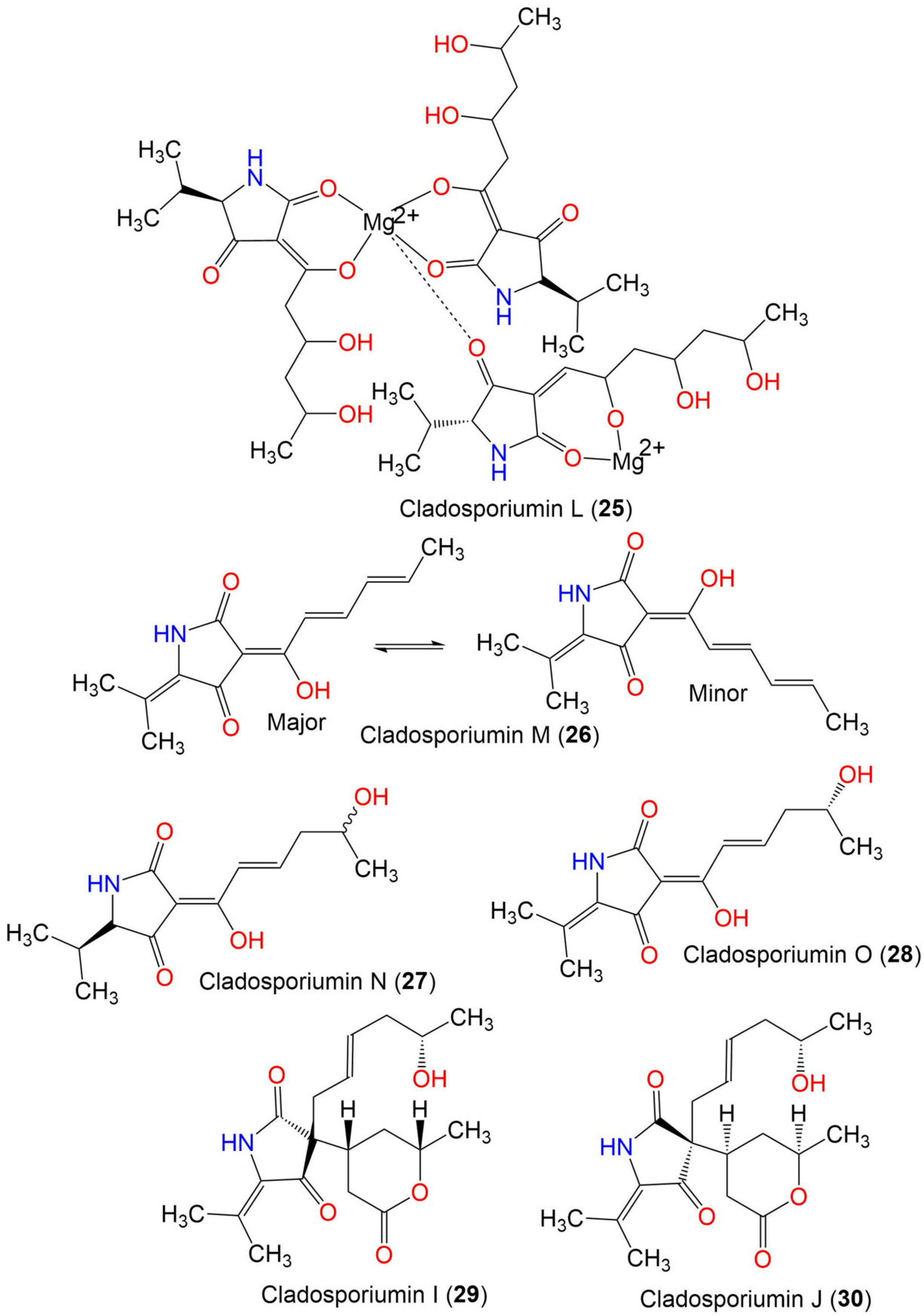

Figure 5. Tetramic acid derivatives **25**–**30**.

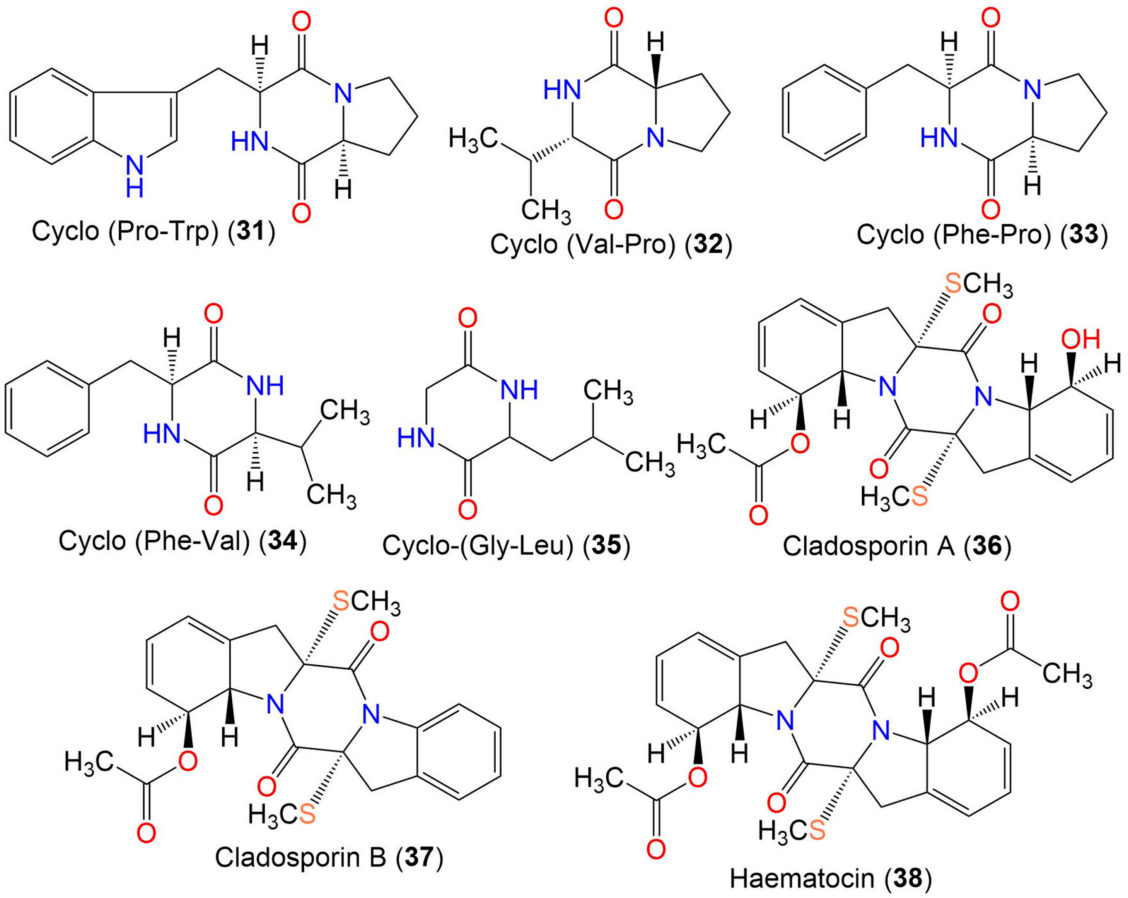

Figure 6. Diketopiperazine derivatives **31**–**38**.

The glyantrypine-type alkaloids, **42**–**55**, were separated from *Cladosporium* sp. PJX-41 isolated from mangrove and assessed for anti-H1N1 activity using CPE (cytopathic effect) inhibition assay (Figures 7 and 8). Compounds **45**, **49**, **51**–**53**, and **55** displayed remarkable anti-H1N1 activities (IC_{50} values ranged from 82 to 89 μM), compared to ribavirin (IC_{50} 87 μM), while **42**–**44**, **46**–**48**, **50**, and **54** (IC_{50} 100–150 μM) had weak activity [64]. The mycelium extract of the marine-derived *Cladosporium* sp. associated with *Chondria crassicualis* red alga afforded **56** that exhibited antioxidant potential (ED_{50} 82.0 μM) more than oxybenzone (sunscreen agent, ED_{50} 350 μM) as evident by their UV-A protecting potential [65]. Furthermore, it had a moderate antibacterial effect towards multidrug-resistant and methicillin-resistant *S. aureus* and *S. aureus* with MICs 31.0, 62.5, and 62.5, μg/mL, respectively [65]. The quinolactacins and citrinadins alkaloids **58**, **68**, and **70** separated from C. oxysporum were assessed for anti-plasmodial potential towards chloroquine-sensitive *Plasmodium falciparum* 3D7 [66] (Figure 9). Only **58** (conc. 3.13 μg to 25.0 μg) had an anti-plasmodial effect (EC_{50} 24.8 μM), while **68** and **70** displayed no activity (EC_{50} > 25.0 μM), compared to artesunate (EC_{50} 0.074 μM) in the SYBR Green I assay. Further, **58** (conc. ranged from 6.25 μM to 50.0 μM for 24 h) was investigated for apoptotic effect on 3D7-plasmodia strain by measuring the parasite ΔΨm (mitochondrial membrane potential). It induced loss of ΔΨm, leading to the release of cytochrome C from mitochondria to the cytosol resulted in parasite apoptosis. Therefore, it may provide a scaffold to apoptotic death in the stages of *P. falciparum* development [66]. Moreover, **58**, **68**, and **70** had no anti-buruli ulcer activity against *Mycobacterium ulcerans* (IC_{50} > 10 μM), compared to rifampicin (IC_{50} < 1 μM) in the Resazurin microtiter assay [66].

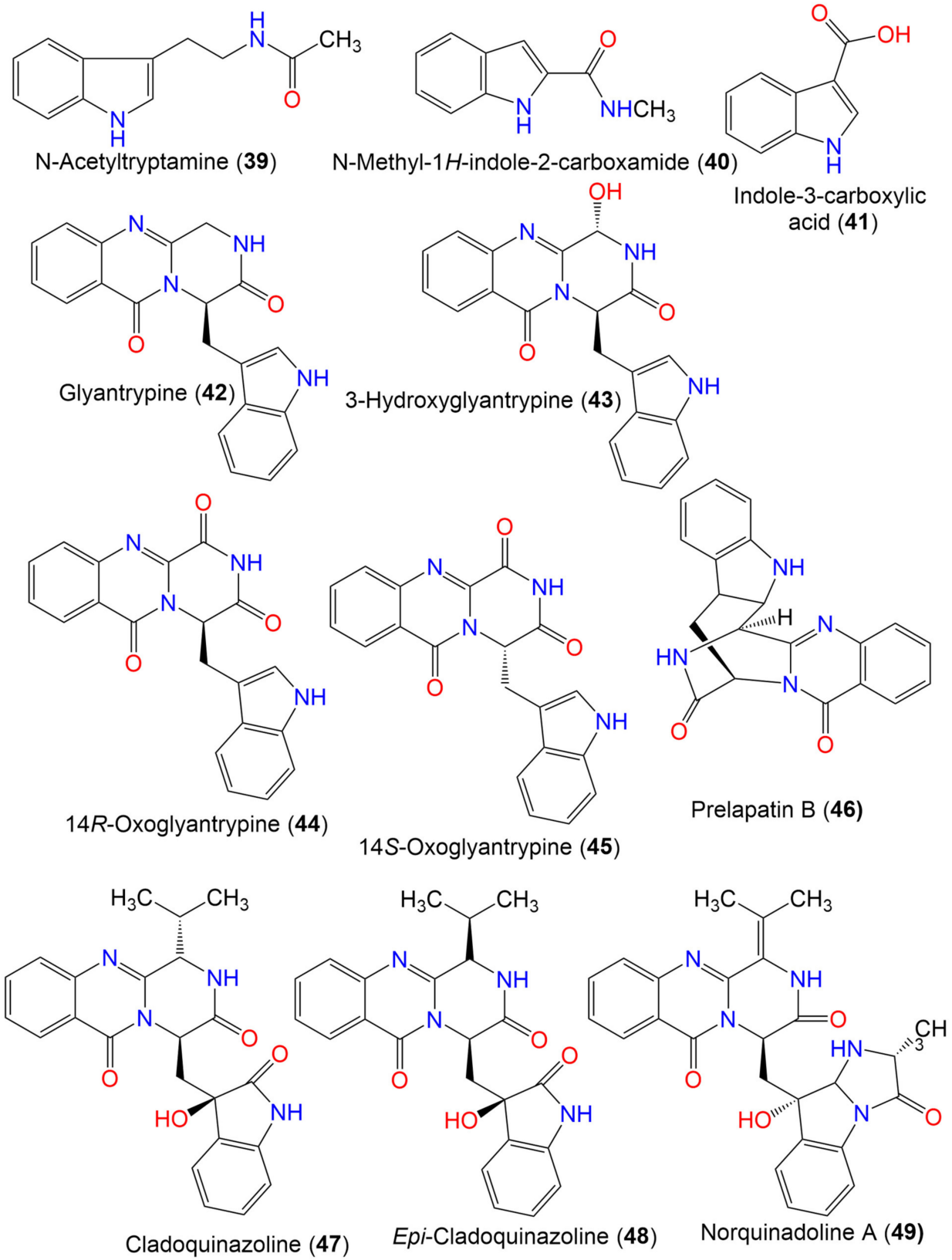

Figure 7. Alkaloids **39**–**49**.

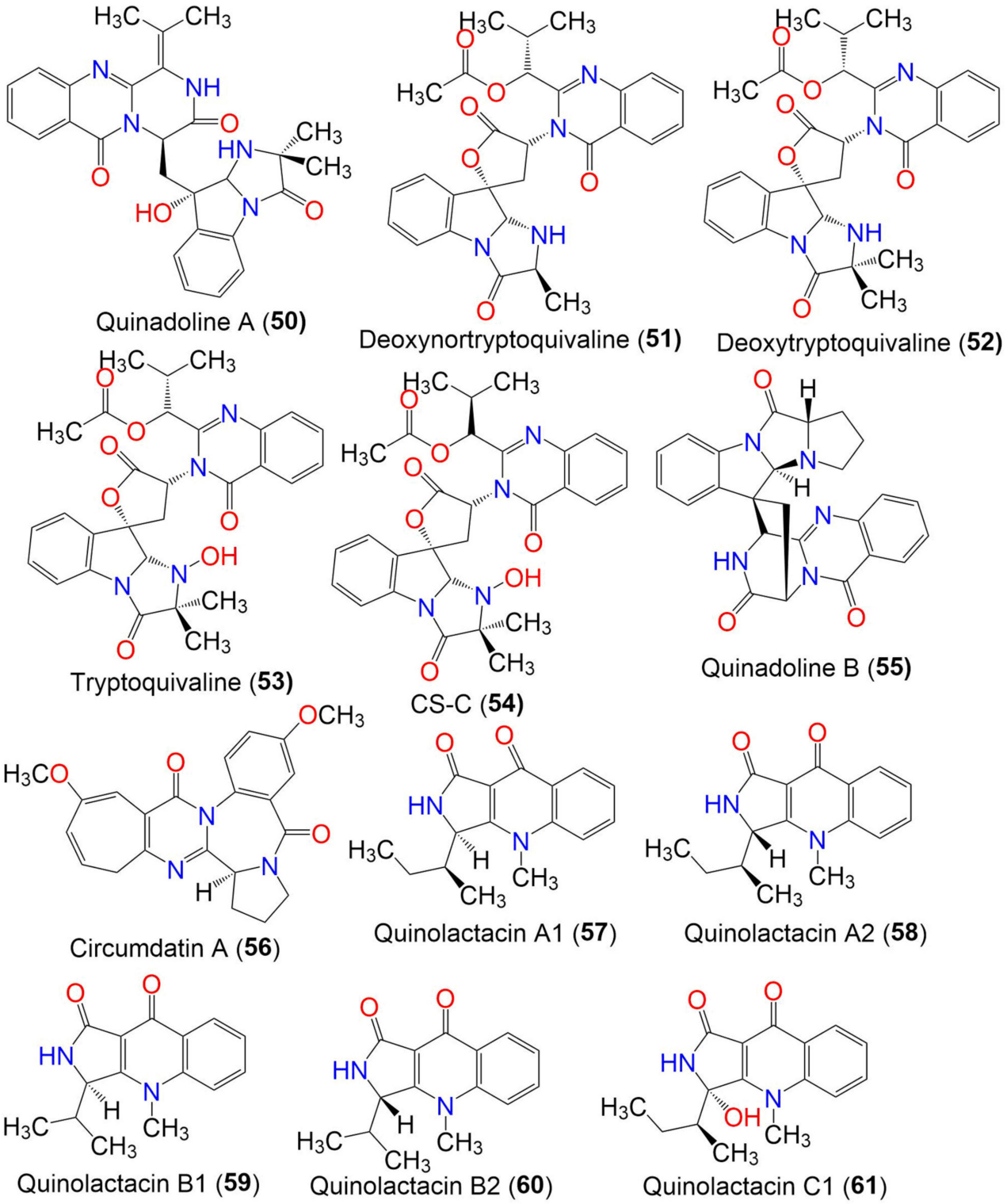

Figure 8. Alkaloids **50**–**61**.

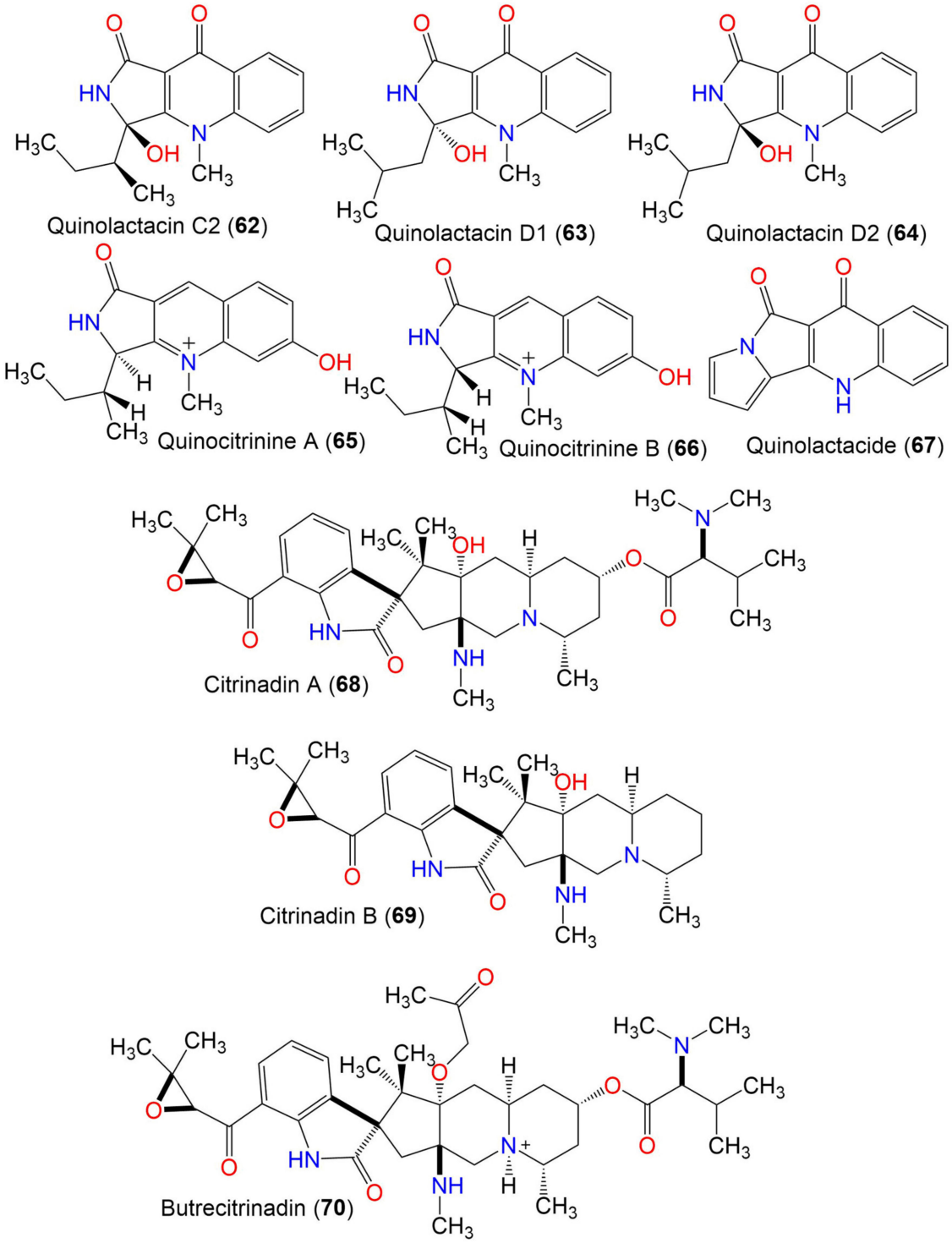

Figure 9. Alkaloids **62**–**70**.

They had significant activity towards HepG-2 and MCF-7 (IC_{50} ranging from 78.57 to 96.54 μM and from 51.32 to 94.49 μM, respectively), compared to curcumin (IC_{50} 61.38 and 20.68 μM, respectively). However, they showed moderate activity versus LNCap and LNCap (IC_{50} ranging from 32.94 to 45.71 μM and from 54.47 to 60.31 μM, respectively), in comparison to curcumin (IC_{50} 6.15 and 13.78 μM, respectively) in the MTT assay [66]. *Cladosporium* sp. HNWSW-1 associated with the mangrove plant *Ceriops tagal* biosynthesized compounds **74**–**76** that were assessed for their cytotoxic and α-glycosidase inhibitory effects (Figure 10). Compound **75** had cytotoxicity versus SGC-7901, K562, and BEL-7042

cell lines (IC_{50} 41.7, 25.6, and 29.4 μM, respectively), whereas **76** revealed cytotoxic potential towards BEL-7042 and Hela cell lines (IC_{50} 26.7 and 14.9 μM μM, respectively) in the MTT assay.

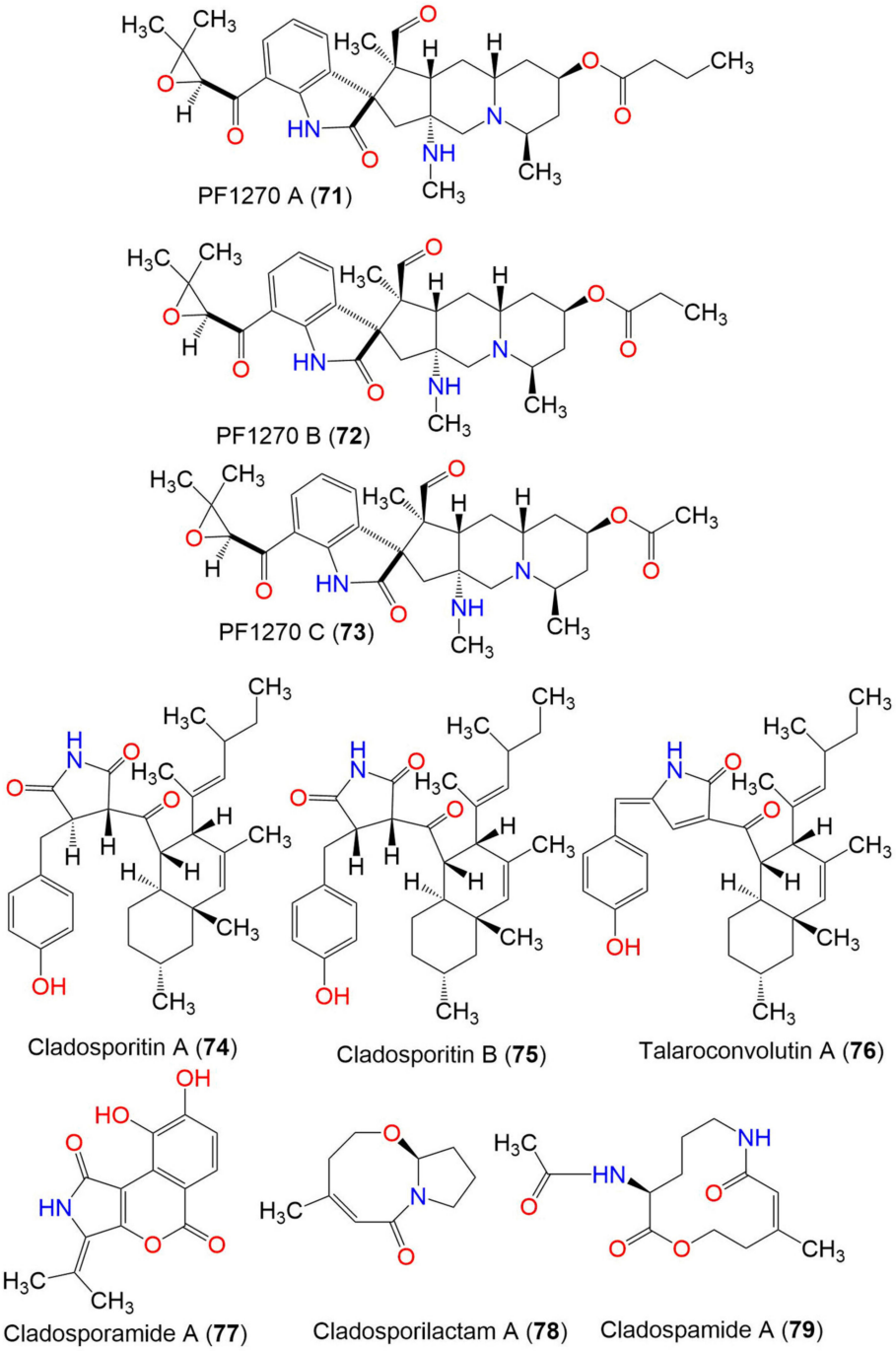

Figure 10. Alkaloids **71**–**79**.

Additionally, **76** exhibited α-glucosidase inhibitory activity (IC_{50} 78.2 μM), compared to acarbose (IC_{50} 275.7 μM) in the glucose oxidase method [67]. Cladosporamide A (**77**) separated from *Cladosporium* sp. TPU1507 derived from marine sponge was assessed for its inhibitory effect towards PTP1B (protein tyrosine phosphatase) and TCPTP (T-cell PTP), using an enzyme-based assay [68]. It had mostly equivalent inhibition towards TCPTP and PTP1B (IC_{50} 48 and 54 μM, respectively), in comparison to oleanolic acid (IC_{50} 0.9 μM) [68]. Cao et al. purified a new 7-oxabicyclic[6.3.0]lactam, **78**, from a gorgonian-

derived *Cladosporium* sp. collected from the South China Sea. It (IC_{50} 0.76–3.11 μM) exhibited significant cytotoxicity towards HeLa, P388, HT-29, and A549 cell lines [69]. On the other hand, it had weak antibacterial activity (MIC > 25.0 μM) in broth dilution assay towards *B. cereus*, *T. halophilus*, *S. epidermidis*, *S. aureus*, *E. coli*, *P. putida*, *N. brasiliensis*, and *V. parahaemolyticus* [69]. *Cladosporium* sp. SCNU-F0001 isolated from a mangrove plant yielded a novel lactam macrolide named cladospamide A (**79**) that was evaluated for cytotoxic effect (conc. 50 μM) versus MDA-MB-435, A549, HCT116, HepG2, and BT549 in the MTT method and for antimicrobial potential (conc. 100 μg/mL) towards *S. aureus*, *B. subtilis*, *E. coli*, *Salmonella* ATCC 14028, and *P. aeruginosa*. Unfortunately, it exhibited no noticeable activity [70].

The new cyano-containing alkaloids, cladosporins A (**80**) and B (**81**) purified from *Cladosporium* sp. SCSIO z015 broth did not have an obvious anti-biofilm activity towards *S. aureus*, *E. coli*, and *B. subtilis* [36] (Figure 11).

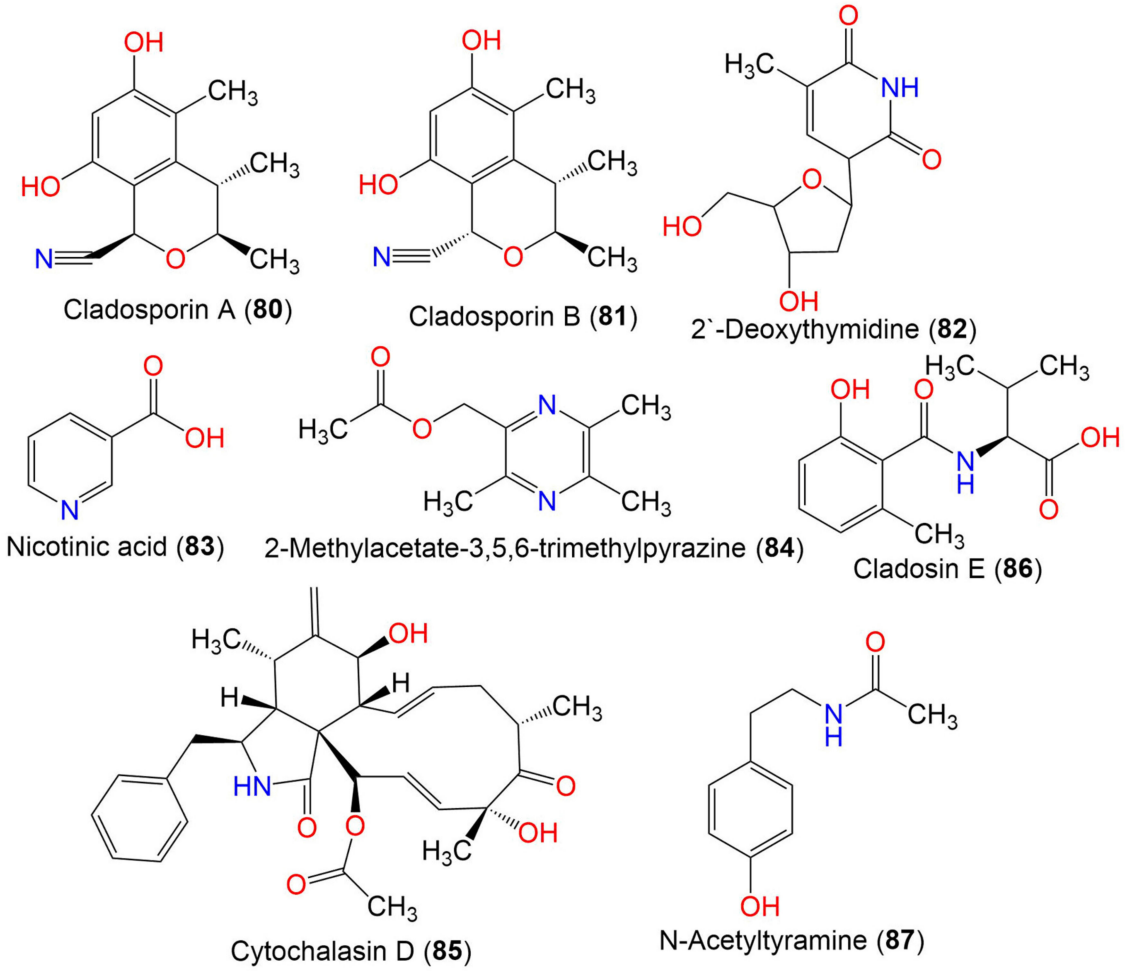

Figure 11. Alkaloids **80**–**87**.

In the DPPH assay, they also had no activity (IC_{50} > 100 μM), compared to ascorbic acid (IC_{50} 4.9 μM). Besides, they showed moderate toxicity towards brine shrine naupalii (LC_{50}s 72.0 and 81.7 μM, respectively), compared with toosendanin (LC_{50} 21.2 μM) in the brine shrimp lethality assay [36]. In 2019, Bai et al. purified **84** and **85** from *Cladosporium* sp. JS1-2 isolated from the mangrove *Ceriops tagal* collected in the South China Sea. Compound **84** moderately prohibited the growth of Helicoverpa armigera Hubner newly hatched larvae (IC_{50} 100 μg/mL), compared to azadirachtin (IC_{50} 25 μg/mL). Further, they showed moderate antibacterial potential versus *S. aureus* with MICs 12.5 and 25.0 μg/mL, respectively, compared with ciprofloxacin (MIC 0.39 μg/mL) [71].

3.4. Macrolides

The term "macrolides" was first used to describe the natural antibiotics that have 12–16-membered macrocyclic lactone ring, functionalized by double bonds, and carrying different aminosaccharide and saccharide components [137]. Among these macrolides are 14-membered lactones (erythromycin and clarithromycin), 15-membered macrolides (azithromycin and spiramycin), and the 16-membered (avermectin B1a) that are clinically used macrolide antibiotics [138]. Members of this group possess a wide range of bioactivities such as antibacterial, anti-inflammatory, antiviral, antimalarial, antimitotic, and anticancer activity. They have been reported from various marine organisms [138,139]. The new 12-membered macrolide, cladospolide D (**91**), together with **88** and **89** were separated from *Cladosporium* sp. FT-0012 was obtained from Pohnpei Island, Federated State of Micronesia, and assessed for antimicrobial activity using paper disks at conc. 10 µg/disk (Figure 12). Compound **91** exhibited activity versus *M. racemosus* KF223, *B. subtilis* KB27, and *P. oryzae* KB110 (IZDs 11.5, 16.0, and 14.0 mm, respectively), while **88** was active (IZD 14.0 mm and IC_{50} 17.0 µg/mL) towards *X. campestris* pv. *oryzae*. Moreover, **91** prohibited *P. oryzae* and *M. racemosus* growth (IC_{50}s 29.0 and 0.15 µg/mL, respectively) [72].

Cladosporium sp. F14 isolated from seawater yielded a nine-membered macrolide, **92** that had weak antibacterial potential towards *M. smegmatis*, *E. coli*, *B. thuringiensis*, *S. aureus*, and *B. subtilis* and weak cytotoxic potential toward A435, HeLa, K562, and A549 in the MTT method [76]. *C. herbarum* isolated from *Callyspongia aerizusa* sponge yielded cladospolide B (**89**) and pandangolides 2–4 (**95**–**97**) that showed no antimicrobial potential versus *S. aureus* ATCC 25923, *B. subtilis* 168, *E. coli* ATCC 25922, and *C. albicans* in the agar plate diffusion assay [74]. Moreover, the EtOAc extract of *Cladosporium* sp. IFB3lp-2 isolated from the mangrove forest of Hainan province of China yielded **88**, **89**, **93**–**96**, **100**, and **116** that had no significant activity against HCT-116, Coxsachievirus A16, A549, MD-MBA-231, HepG2, human enterovirus 71, A375, and SW1116 cell lines (conc. 20 µM) in the MTT assay [73] (Figure 13).

Additionally, *Cladosporium* sp. SCNU-F0001 isolated from a mangrove plant biosynthesized a new macrolide thiocladospolide E (**105**), along with **89** that were evaluated for cytotoxic effect (conc. 50 µM) versus MDA-MB-435, A549, HCT116, HepG2, and BT549 in the MTT method and for antimicrobial potential (conc. 100 µg/mL) towards *S. aureus*, *B. subtilis*, *E. coli*, *Salmonella* ATCC 14028, and *P. aeruginosa*. Unfortunately, none of them exhibited noticeable activity [70]. Cao et al. purified 12-membered macrolides **89** and **117**–**120** from a gorgonian-derived *Cladosporium* sp. collected from the South China Sea. They showed no cytotoxicity towards HeLa, P388, HT-29, and A549 cell lines [69]. Furthermore, they were evaluated for antibacterial activity in broth dilution assay towards *B. cereus*, *T. halophilus*, *S. epidermidis*, *S. aureus*, *E. coli*, *P. putida*, *N. brasiliensis*, and *V. parahaemolyticus*. Compounds **117**–**119** exhibited antibacterial potential against all tested bacteria (MIC values ranging from 3.13 to 25.0 µM), however **89** and **120** had weak activity (MIC > 25.0 µM) [69]. The metabolites **93** and **115** separated from *Cladosporium* sp. F14 at conc. 50 µg/mL had no anti-larval activity towards both *B. neritina* and *B. amphitrite* larvae in the settlement inhibition assays [60]. In 2019, Zhang et al. separated the new polyketides **98** and **99** and a known analog **93** from the rice culture EtOAc extract of *C. cladosporioides* associated with *Bruguiera gymnorrhiza*. Their configuration was established using ECD, modified Mosher's, and X-ray diffraction methods, as well as optical rotations to be 5R, 11R for **98**; 11R for **99**; and 3R, 5*S*, 11*S* for **93**. They had weak AChEI activity (IC_{50} > 50 µM), in comparison to tacrine in the modified Ellman's method [40]. *C. cladosporioides* MA-299 obtained from the mangrove plant *B. gymnorrhiza* yielded 12-membered thio-macrolides **96** and **101**–**104** that were assessed for antimicrobial potential against *E. tarda* QDIO-2 and *E. ictarda* QDIO-9 (aquatic pathogens) and *C. glecosporioides* QDAU-2, *B. sorokiniana* QDAU-5, *P. piricola Nose* QDAU-15, and *F. oxysporum* f. sp. *cucumerinum* QDAU-8 (plant pathogenic fungi) in the microtiter plates assay. All metabolites revealed activity against *C. glecosporioides* (MIC 1 or 2 µg/mL), compared to amphotericin B (MIC 0.5 µg/mL). Moreover, **101** and **104** showed noticeable activity (MIC 1.0 µg/mL) towards with *E. tarda* and *E. ictarda*, respec-

tively, compared to chloramphenicol (MIC 0.5 μg/mL), while **102** and **104** exerted obvious effectiveness (MIC 1.0 μg/mL) versus *F. oxysporum* f. sp. *cucumerinum*, compared to amphotericin B (MIC 0.5 μg/mL). The data revealed that sulfur substituent may influence the macrolides' bioactivities [39]. The newly reported 12-membered macrolides having thioethers **107**–**112** and the related formerly reported **93** and **101** isolated from mangrove-derived *C. oxysporum* HDN13-314 had no cytotoxic activity versus HCT-116, BEL-7402, HL-60, A549, L-02, HeLa, K562, MGC-803, MCF-7, PC-3, SH-SY5Y, and MDA-MB-231 (IC_{50} > 50 μM) [78] (Figure 14).

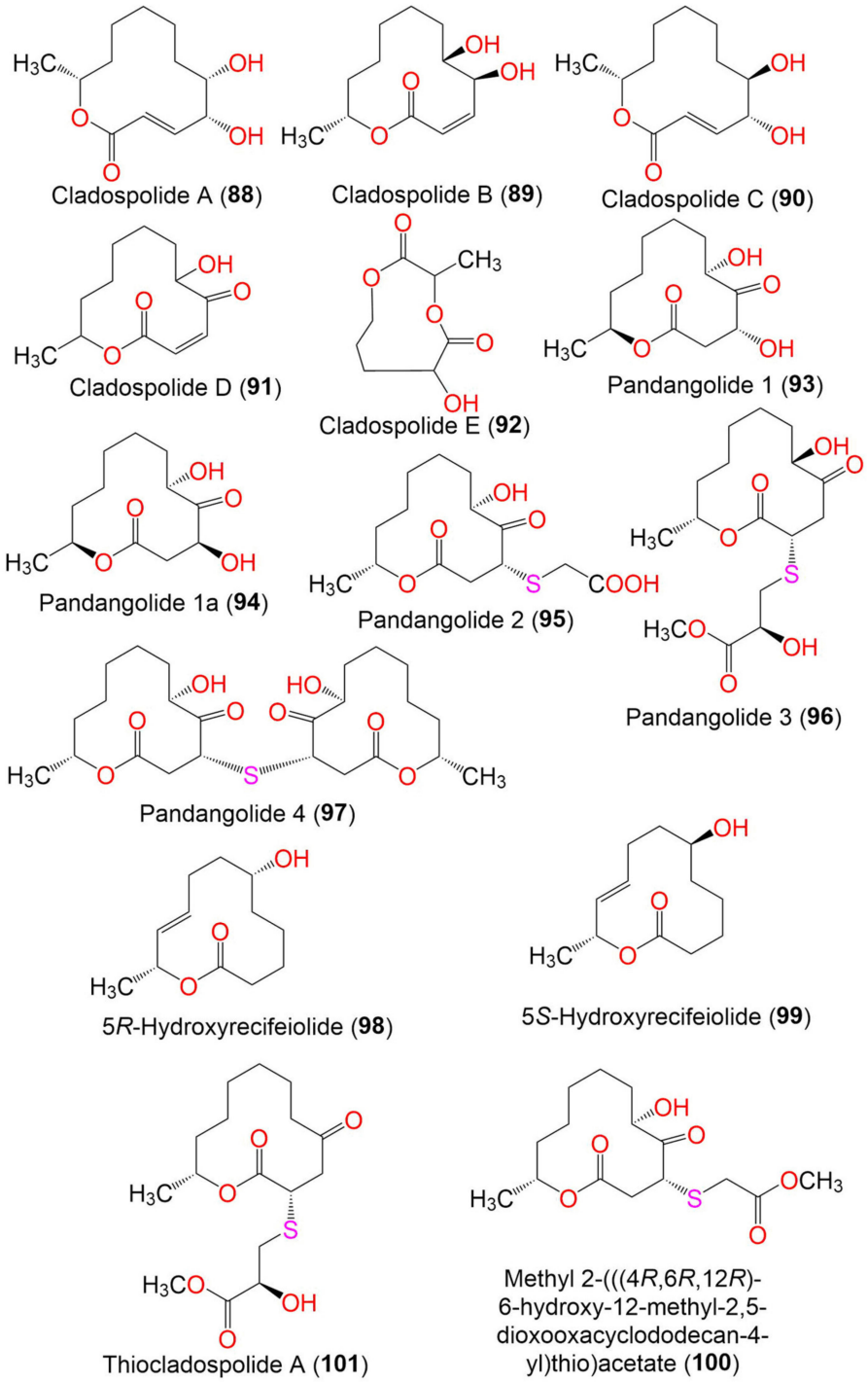

Figure 12. Macrolides **88**–**101**.

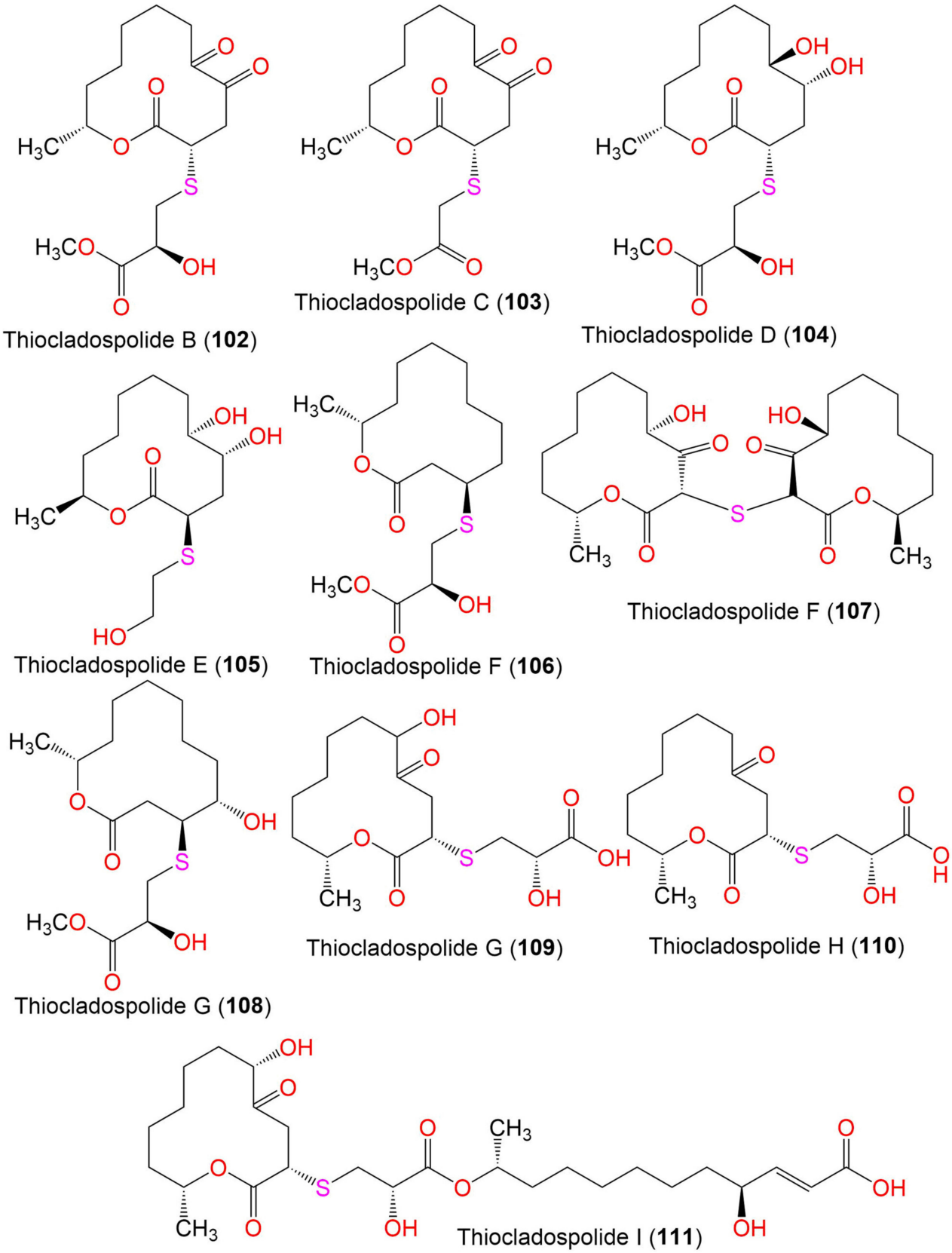

Figure 13. Macrolides **102**–**111**.

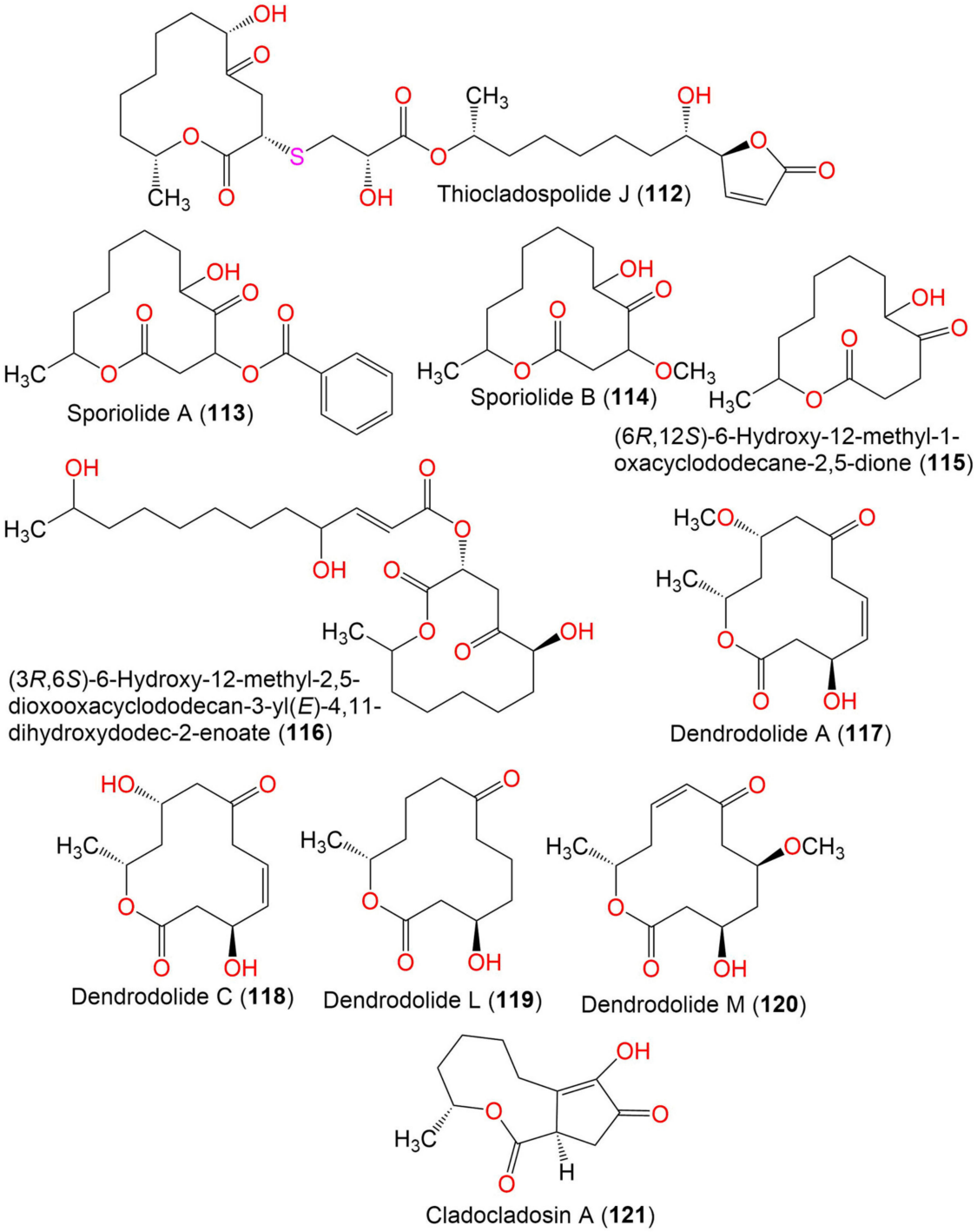

Figure 14. Macrolides **112**–**121**.

Additionally, they exerted antibacterial activities versus the aquatic pathogens *E. ictarda* and *E. tarda* (MICs ranging from 4 to 32 μg/mL), whereas **108** had the best effect (MIC 4 μg/mL) versus *E. tarda* [78]. In 2020, new thiomacrolides thiocladospolides F (**106**) and G (**108**) and cladocladosin A (**121**), a macrolide with bicyclo 5/9-ring, were purified from *C. cladosporioides* MA-299 by Zhang et al. and assessed for antimicrobial effect versus various plant, human, and aquatic pathogenic microbes in the microtiter plates assay. All metabolites revealed activity (MIC ranging from 1.0 to 4.0 μg/mL) towards *V. anguillarum* and *E. tarda* (aquatic pathogenic bacteria) [79].

Moreover, **108** and **121** exerted activity (MICs 4.0 μg/mL) towards *H. maydis* (plant-pathogenic fungus) and *P. aeruginosa* (aquatic-pathogenic bacterium), respectively [79]. The new 12-membered macrolides, **113** and **114**, purified from *Cladosporium* sp. L037 isolated from the Okinawan marine brown alga *Actinotrichia fragilis* exhibited cytotoxic influence (IC_{50} 0.13 and 0.81 μg/mL, respectively) towards L1210 murine lymphoma cells in the MTT assay [80]. Moreover, **113** had antifungal potential against *C. albicans*, *C. neoformans*, *A. niger*, and *N. crassa* (MICs 8.4–16.7 μg/mL), whereas **114** exhibited antibacterial activity only towards *M. luteus* and inactive against the other microorganisms [80].

3.5. Butanolides and Butenolides

Butanolides and butenolides are five-membered γ-lactones which may also be regarded as furan derivatives. They are an important class of structural motifs often encountered in various natural metabolites and synthetic targets [140]. They have an impressive range of bioactivities including antibiotic, antitumor, and anticancer that are intimately connected to their relative and absolute configurations [141].

The newly separated C12-macrolide, cladospolide F (**122**), purified from a soft coral-associated fungus *Cladosporium* sp. TZP-29, together with the formerly isolated derivative **126** showed no cytotoxic effect towards A-549, SMMC-7721, and HeLa cells in the SRB method [41]. Wuringege et al. reported that the butenolide, **126** isolated from *Cladosporium* sp. IFB3lp-2 exhibited no significant activity against HCT-116, Coxsachievirus A16, A549, MD-MBA-231, HepG2, human enterovirus 71, A375, and SW1116 cell lines (Conc. 20 μM) in the MTT assay [73]. Moreover, it showed no cytotoxicity towards various cancer cell lines: HeLa, P388, HT-29, HCT-116, BEL-7402, HL-60, A549, L-02, HeLa, K562, MGC-803, MCF-7, PC-3, SH-SY5Y, MDA-MB-231, and A549 [69,78]. On the other hand, it had antibacterial activity in broth dilution assay towards *B. cereus*, *T. halophilus*, *S. epidermidis*, *S. aureus*, *E. coli*, *P. putida*, *N. brasiliensis*, and *V. parahaemolyticus* (MIC values ranging from 6.25 to 25.0 μM) [46]. Qi et al. stated that **126** displayed no anti-larval activity towards both *B. neritina* and *B. amphitrite* larvae in the settlement inhibition assays [60]. Additionally, it exerted antimicrobial activity versus *E. ictarda* and *Cytospora mandshurica Miura* (MIC 8 μg/mL) [78]. The new metabolites **123**, **124**, and **127** and the known analog **126** separated from *C. cladosporioides* were assessed for AChEI activity using modified Ellman's method (Figure 15). Only **123** exhibited potent AChEI activity with the IC_{50} value of 40.26 μM, in comparison to tacrine, while other metabolites possessed weak activity (IC_{50} > 50 μM) [40].

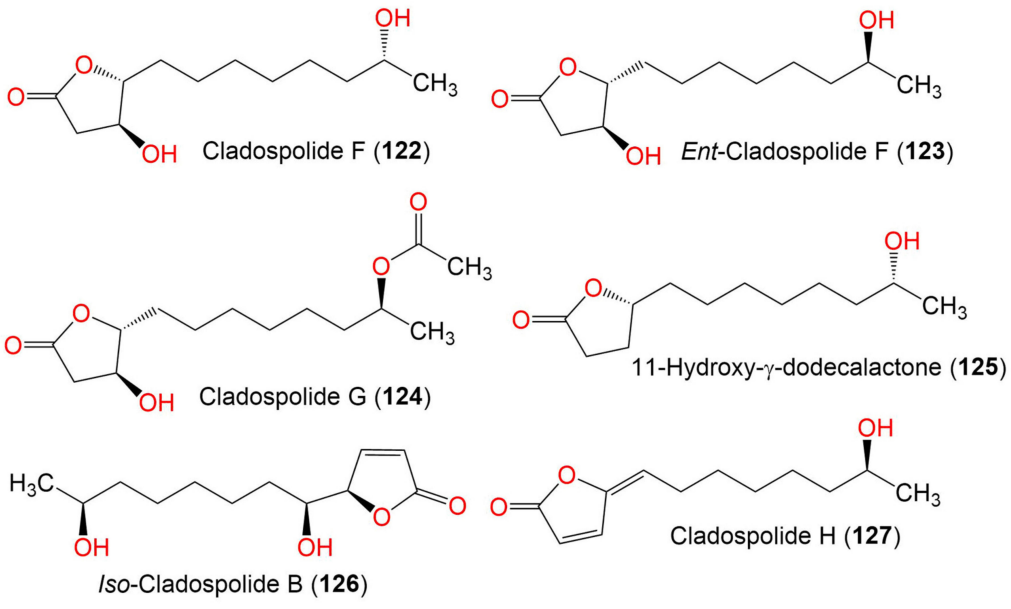

Figure 15. Butenolides and butanolides **122**–**127**.

3.6. Seco-Acids

The seco-acids **128**, **130**, and **141** isolated from *Cladosporium* sp. IFB3lp-2 EtOAc extract had no noticeable cytotoxicity versus HCT-116, Coxsachievirus A16, A549, MDMBA-231, HepG2, human enterovirus 71, A375, and SW1116 cell lines (Conc. 20 μM) in the MTT assay [73]. Compound **131** did not show any anti-larval activity towards both *B. neritina* and *B. amphitrite* larvae [60]. Moreover, **132** did not have cytotoxic activity towards HCT-116, BEL-7402, HL-60, A549, L-02, HeLa, K562, MGC-803, MCF-7, PC-3, SH-SY5Y, and MDA-MB-231 (IC_{50} > 50 μM) [78], while it exhibited weak activity versus the aquatic pathogens *E. ictarda*, *E. tarda*, and *Cytospora glecosporioides* (MICs ranging from 16 to 32 μg/mL) [78]. Cladospolide E (**129**) separated from a soft coral-associated *Cladosporium* sp. TZP-29, together with the formerly isolated derivatives **130** and **131** had no cytotoxic effect towards A-549, SMMC-7721, and HeLa cells in the SRB method. Moreover, **129**–**131** with IC_{50} ranged from 7.1 to 13.1 μM remarkably reduced the accumulation of lipid elicited by oleic acid (OA) in the HepG2 liver cells, in comparison to lovastatin as determined by oil-red O staining and intracellular triglyceride (TG) and total cholesterol (TC) quantification (Figure 16).

Further, they exhibited potent lipid-lowering potential in HepG2 hepatocytes, revealing a promising anti-hyperlipidemic capacity [41]. The new fatty acid esters **133**, **134**, and **138** and new fatty acids **135**–**137**, **139**, and **140** isolated from *C. cladosporioides* OUCMDZ-187 obtained from the mangrove plant *Rhizophora stylosa* collected in Shankou, Guangxi Province of China showed no cytotoxic effects (IC_{50} > 50 μM) towards K562, A549, and HeLa cells in the SRB method [81]. Additionally, they revealed no antimicrobial activities (MIC > 150 μM) towards *S. aureus* CGMCC-1.2465, *E. coli* CGMCC-1.2389, *E. aerogenes* CGMCC-1.0876, *P. aeruginosa* CGMCC-1.1785, *B. subtilis* CGMCC-1.3376, and *C. albicans* CGMCC-2.2086 in the agar dilution method [81].

3.7. Tetralones (Napthalenones)

Tetralones comprise a bicyclic aromatic hydrocarbon and a ketone and are regarded as benzo-fused cyclohexanone derivatives. They played a substantial role as a starting material for the synthesis of a range of synthetic heterocyclic compounds and pharmaceuticals due to their potential reactivity and suitability [142]. Additionally, they are precursors of many natural metabolites and their derivatives. They have been used in the synthesis of therapeutically functional compounds such as antibiotics, acetylcholinesterase inhibitors, antidepressants, and antitumor alkaloids [142,143].

Cladosporone A (**152**), a new dimeric tetralone bridged via C-C linkage, was separated from *Cladosporium* sp. KcFL6 derived from the mangrove plant *Kandelia candel*, together with **142**–**144** (Figure 17). In anti-COX-2 assay, **144** and **152** displayed COX-2 inhibitory activities (IC_{50} 60.2 and 49.1 μM, respectively), in comparison to NS-398 and indomethacin [82]. Moreover, none of these metabolites had antimicrobial activities against *A. baumannii* ATCC-19606, *S. aureus* ATCC-29213, *E. faecalis* ATCC-29212, *A. hydrophila* ATCC-7966, *E. coli* ATCC-25922, *K. pneumonia* ATCC-13883, *Fusarium* sp., *F. oxysporum* f. sp. *cucumeris*, *F. oxysporum* f. sp. *niveum*, *A. niger*, and *R. solani* in the disc diffusion assay [82].

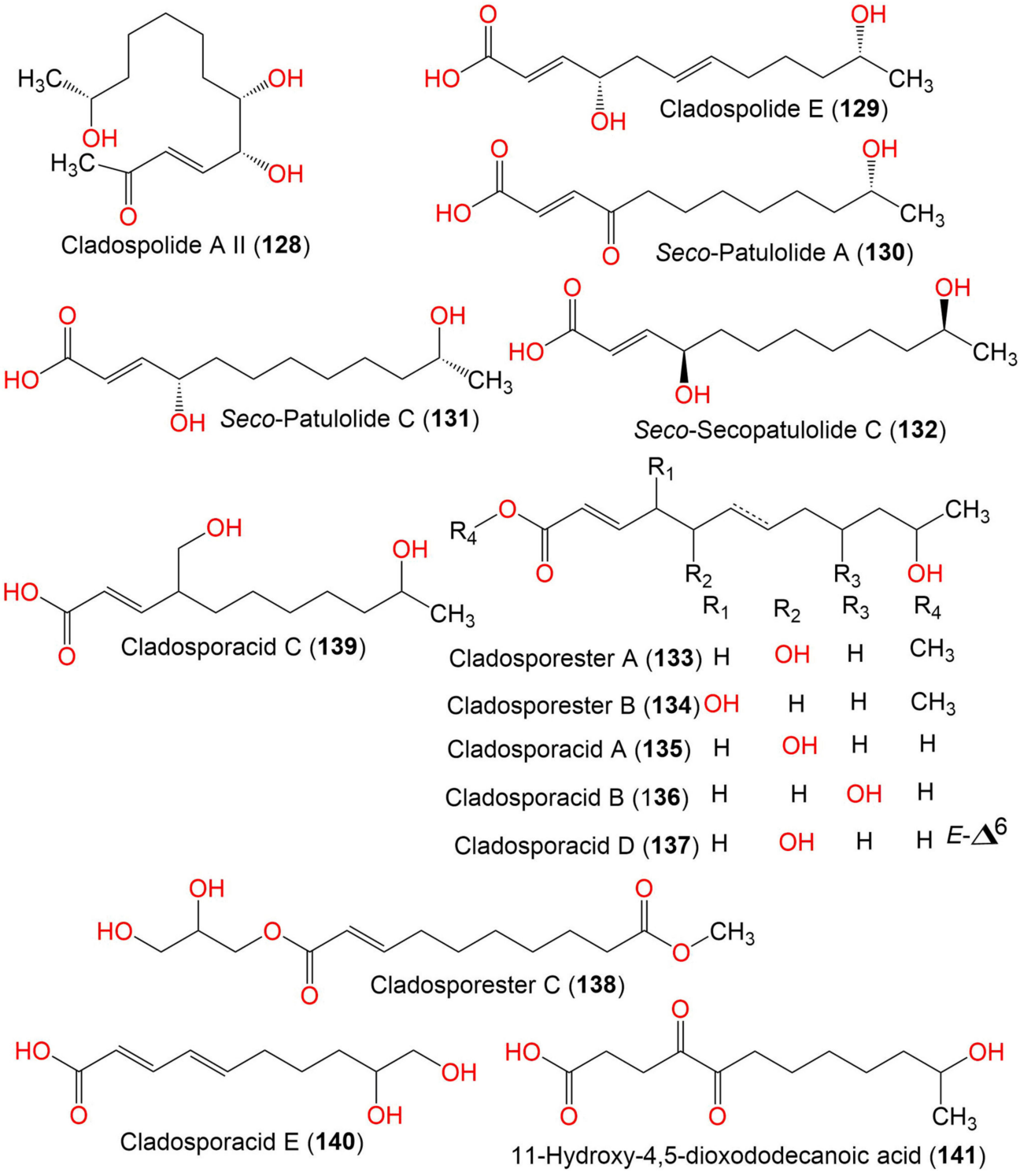

Figure 16. Seco-acids **128**–**141**.

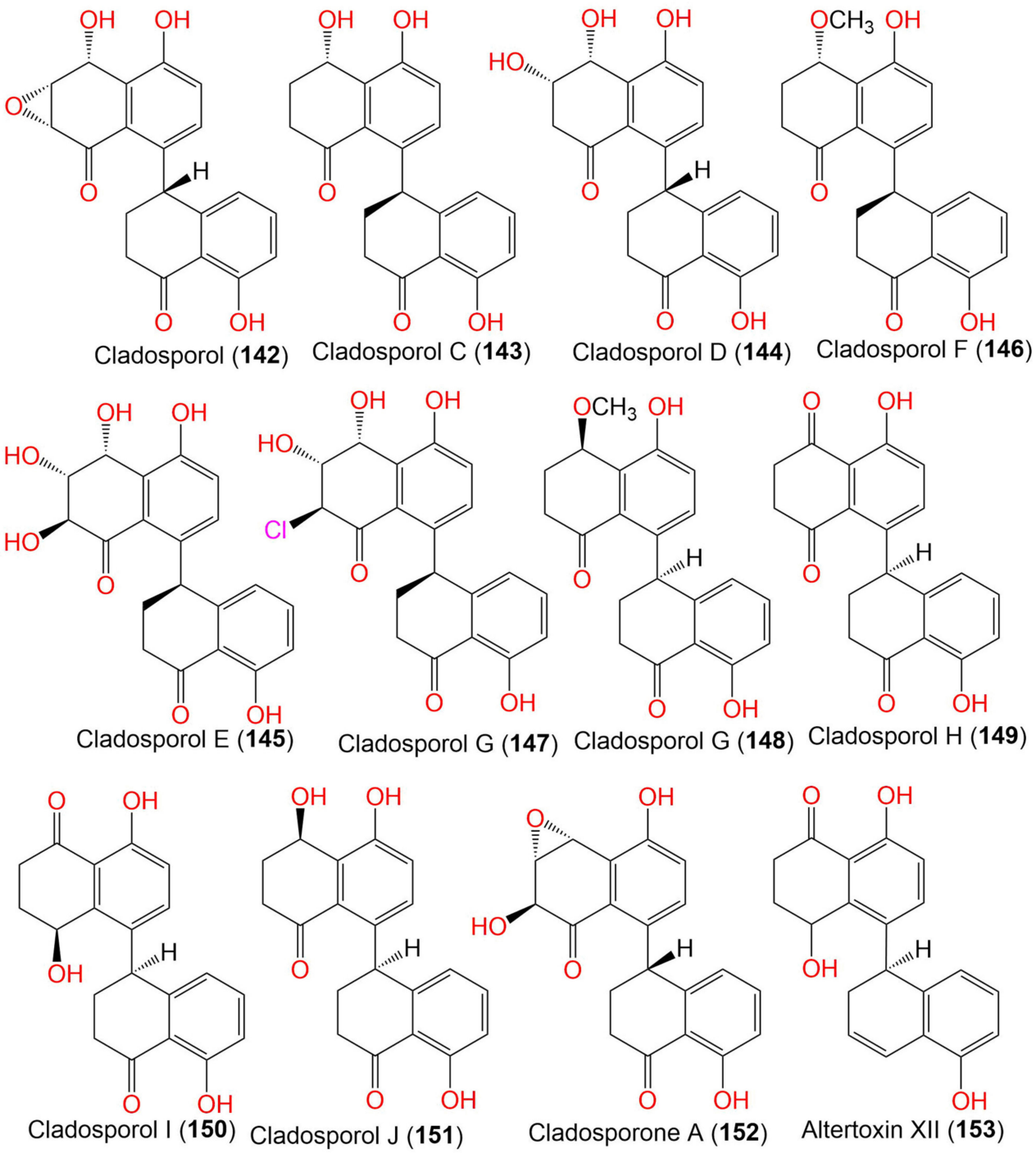

Figure 17. Tetralones (napthalenones) **142**–**153**.

Compounds **143** and **152** had moderate cytotoxic activity towards Huh-7, K562, HL-60, MCF-7, H1975, U937, A549, BGC823, MOLT-4, and HeLa cell lines (IC_{50} of **143** ranging from 11.4 to 72.5 μM and for **152** ranging from 10.1 to 53.7 μM), compared to trichostatin A in the trypan blue-cell viability assay [82]. Zurlo et al. reported that **142** had a remarkable anti-proliferative potential towards SW480, HT-29, and CaCo-2, in particular towards HT-29. It was revealed that HT-29 cells exposure to **142** produced G1/S phase cell cycle arrest, assisted by a vigorous $p21^{waf1/cip1}$ expression, a significant down-regulation of CDK4, CDK2, cyclin E, and cyclin D1, and repression of CDK4 and CDK2 kinase activity [144]. It was demonstrated that its antiproliferative potential towards HT-29 cells was mediated via activation PPARγ, resulting in upregulation of $p21^{waf1/cip1}$ expression and inducing

degradation of β-catenin, as well as impairing TCF/β-catenin pathway as evident by reduced cyclin D1 and c-Myc transcription. Finally, it induced the expression of E-cadherin, therefore antagonizing invasion and metastasis [145]. *C. cladosporioides* HDN14-342 isolated from marine sediments yielded tetralone derivatives **143**, **145**–**147**, **154**, and **155** that were evaluated for cytotoxic activities towards HCT-116, HeLa, and A549 cell lines by SRB method and towards HL-60 and K562 cell lines by MTT method, in comparison to doxorubicin (IC_{50} 0.2–0.8 μM). Compounds **146** and **147** were active towards K562, HeLa, and HCT-116 cell lines (IC_{50} ranging from 3.9 to 23.0 μM), while other metabolites had no activity (IC_{50} > 50.0 μM) [83]. In 2020, He et al. reported that **143** possessed no anti-allergic effect (IC50 > 200 μM) on RBL-2H3 cells, in comparison to loratadine (IC50 35.01 μM) using fluorometric assay [75]. In 2017, Li et al. separated six cladosporol derivatives, cladosporol C (**143**) and cladosporols F-J (**146** and **148**–**151**) from the marine algal-derived *C. cladosporioides* EN-399 and evaluated their cytotoxic activities towards H446, A549, HeLa, L02, Huh7, LM3, SW1990, and MCF-7 using MTT assay. Note that **143**, **148**, and **149** displayed cytotoxic activities towards most of the tested cell lines with IC_{50} ranging from 1.0 to 20.0 μM. Notably, **149** had cytotoxic effect towards LM3, A549, and Huh7 cell lines (IC_{50} 4.1, 5.0, and 1.0 μM, respectively), compared to cisplatin (IC_{50} 1.3 μM for A549 and 9.1 μM for LM3) and fluorouracil (IC_{50} 6.2 μM for Huh7), whereas **143** exhibited cytotoxic activity (IC_{50} 4.0 μM) towards H446 cell line, compared to adriamycin (IC_{50} 4.0 μM). These results revealed that the existence of dihydro-1,4-naphthoquinone nucleus was important for the activity (**149** vs. **146**, **148**, and **143**, **150**, and **151**) and C-4 methoxyl strengthened the activity (**148** vs. **151**) [84].

Moreover, their antimicrobial potential was assessed versus *E. coli*, *A. hydrophila*, *S. aureus*, *E. tarda*, *P. aeruginosa*, *M. luteus*, *V. alginolyticus*, *V. parahemolyticus*, *V. harveyi*, *A. brassicae*, *F. oxysporum*, *G. graminis*, *C. gloeosporioides*, and *P. piricolav* using micro-plate assay. Compounds **143**, **146**, and **148**–**151** showed inhibitory potential towards *M. luteus*, *E. coli*, and *V. harveyi* (MICs 4–128 μg/mL). None of them had activity (MIC > 128 μg/mL) towards other tested microbes [84]. Bai et al. purified **143** and **145** from *Cladosporium* sp. JS1-2 isolated from the mangrove Ceriops tagal collected in the South China Sea [71]. Compound **145** prohibited the growth of Helicoverpa armigera Hubner newly hatched larvae (IC_{50} 150 μg/mL), compared to azadirachtin (IC_{50} 25 μg/mL) [71]. Further, they showed antibacterial potential versus *S. aureus* with MIC 6.25 and 1.56 μg/mL, respectively, compared with ciprofloxacin (MIC 0.39 μg/mL) [71]. Cladosporium sp. KFD33 isolated from blood cockle collected from Haikou Bay produced **150** and **153** that exhibited quorum sensing inhibitory potential towards *Chromobacterium violaceum* CV026 (MICs 30 and 20 μg/well, respectively) in the well diffusion assay [85]. Nevertheless, **156** had no observable cytotoxic activity towards SF-268, NCI-H460, MCF-7, and HepG-2 (conc. 100 μM) in the SRB assay [87]. The new naphthalenone derivative **157**, in addition to **156**, **158**, and **159** isolated *Cladosporium* sp. JJM22 associated with the mangrove plant *C. tagal* had no cytotoxic effect (IC_{50} > 10 μM) versus HeLa cell line in the MTT assay, compared to epirubicin [88] (Figure 18). In the micro-plate assay, only **158** exhibited noticeable antibacterial potential towards *S. aureus*, *B. cereus*, *E. coli*, *V. alginolyticus*, *V. parahemolyticus*, and MR *S. aureus* (conc. 20 μM) [88]. One new tetralone derivative, aladothalen (**160**) and previously reported (3S,4S)-3,4,8-trihydroxy-1-tetralone (**159**) were isolated from a sediment-associated *Cladosporium* sp. HDN17-58 (Figure 17). Note that **160** possessed potent bacteriostatic potential versus *Mycobacterium phlei*, *B. cereus*, and MRCNS (methicillin-resistant coagulase-negative Staphylococci) (MIC values of 25, 50, and 25 μM, respectively), compared to ciprofloxacin [89].

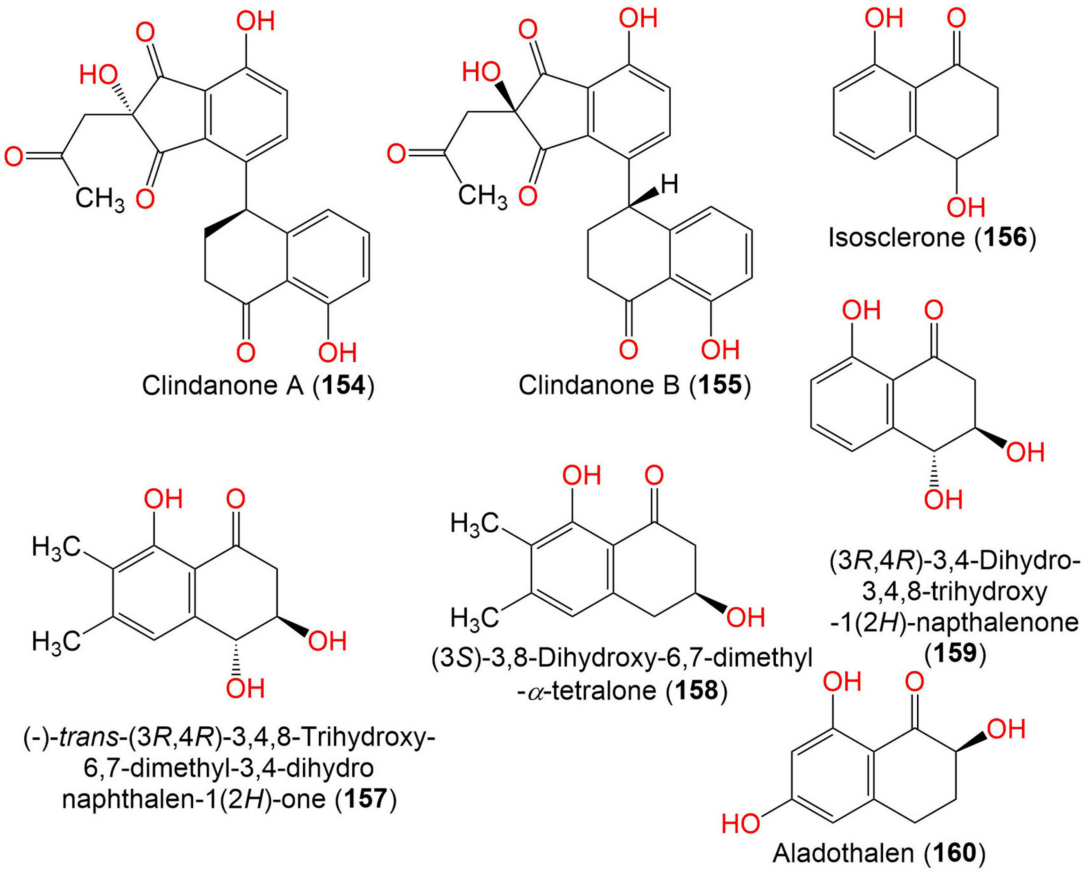

Figure 18. Tetralones (napthalenones) **154**–**160**.

3.8. Perylenequinones

Perylenequinones comprise a class of natural products characterized by an oxidized pentacyclic core. They are dark-colored pigments isolated from diverse sources such as mold species, plants, and aphids [146]. They reported to have anthelmintic, photoactivity, antiviral and antitumor [146].

Four new perylenequinone derivatives, altertoxins VIII–XI (**161**–**164**), were isolated from *Cladosporium* sp. KFD33 (Figure 19). They exhibited quorum sensing inhibitory potential towards *C. violaceum* CV026 with MICs ranging from 20 to 30 µg/well in the well diffusion assay [85]. Structurally, these metabolites related to altertoxins I–III previously were reported from *Alternaria alternata* [147].

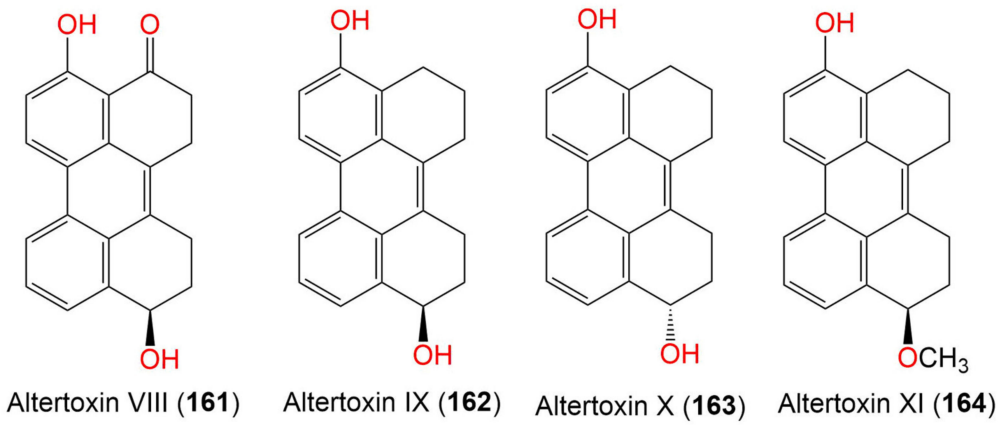

Figure 19. Perylenequinone **161**–**164**.

3.9. Naphthalene Derivatives

Naphthalenes are a class of arenes containing two *ortho*-fused benzene rings that have been reported from plants, liverworts, fungi, and insects [148]. Their derivatives exhibited anti-inflammatory, antimicrobial, antioxidant, anti-protozoal, cytotoxic, and anti-platelet aggregation activities [148].

Cladosporium sp. associated with the mangrove *C. tagal* biosynthesized the naphthalene derivatives **166**–**168** that had anti-inflammatory potential via in-vitro inhibition of induced NO (nitric oxide) production by LPS (lipopolysaccharide) in RAW264.7 cells [91] (Figure 20). The mangrove-associated fungus *Cladosporium* sp. JJM22 yielded new naphthalene-chromane derivatives, cladonaphchroms A (**169**) and B (**170**), and related metabolites **165** and **168** that were assessed for antibacterial effectiveness versus *S. albus* ATCC-8799, *E. coli* ATCC-25922, *B. subtilis* ATCC-6633, *Micrococcus tetragenus* ATCC-13623, and *M. luteus* ATCC-9341, employing microplate assay. Compound **169** possessed significant potential against *S. albus* (MIC 1.25 μg/mL), compared to ciprofloxacin (MIC 0.6 μg/mL). Moreover, **169** and **170** demonstrated broad-spectrum antifungal activities (MICs 25.0–100.0 μg/mL) towards *P. parasitica* var. *nicotianae*, *A. brassicicola*, *B. oryzae*, *C. capsici*, *C. paradoxa* Moreau, and *D. medusaea* Nitschke, compared to pochloraz (MICs 12.5–50.0 μg/mL) [90]. Wu et al. stated that **166** had no cytotoxic effect (IC_{50} > 10 μM) versus HeLa cell line in the MTT assay and no antibacterial activity towards *S. aureus*, *B. cereus*, *E. coli*, *V. alginolyticus*, *V. parahemolyticus*, and MR *S. aureus* (conc. 20 μM) in the microplate assay [88].

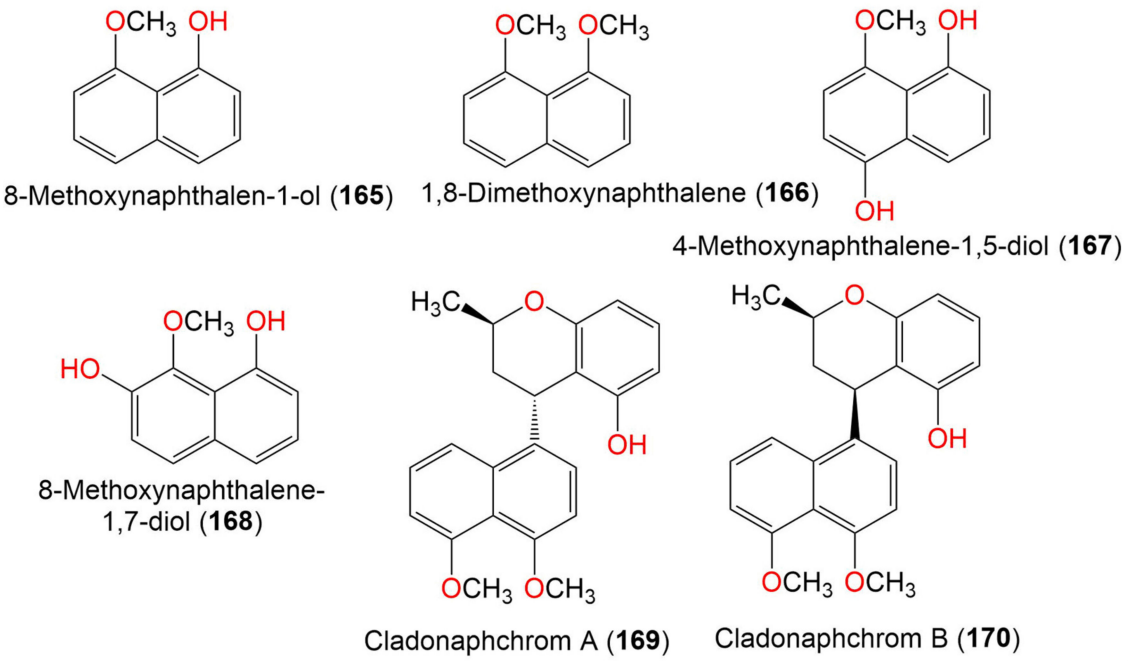

Figure 20. Naphthalene derivatives **165**–**170**.

3.10. Xanthones

Xanthones are secondary metabolites commonly reported from plants, fungi, and lichen [149]. They are heterocyclic metabolites with a xanthene-9-one framework, which is connected to different functional groups: methoxy, hydroxyl, prenyl, and dihydrofuran [150]. These metabolites showed diverse bioactivities: anti-HIV, anti-leishmanial, antitumor, anti-quorum sensing, antimicrobial, anti-inflammatory, antimalarial, advanced glycation end-products inhibitory, antioxidant, antihypertensive, and cytotoxic [150,151].

C. halotolerans GXIMD 02502 associated with the coral *Porites lutea* yielded compounds **171**–**177** that were evaluated for their cytotoxicity versus 22RV1 and C4-2B (prostatic cancer cell lines), as well as RWPE-1 (normal prostate epithelial cell). Among them, **171**–**173**, **175**, and **176** revealed notable cytotoxicity versus C4-2B and 22RV1 cells (inhibitions ranged

from 55.8% to 82.1% at conc. 10 μM), whereas **176** was the potent one (inhibitions 77.7% and 82.1%, respectively). On the other hand, they exhibited nearly no cytotoxic effect versus RWPE-1 cell (inhibition < 27% at conc. 10 μM) [92] (Figure 21).

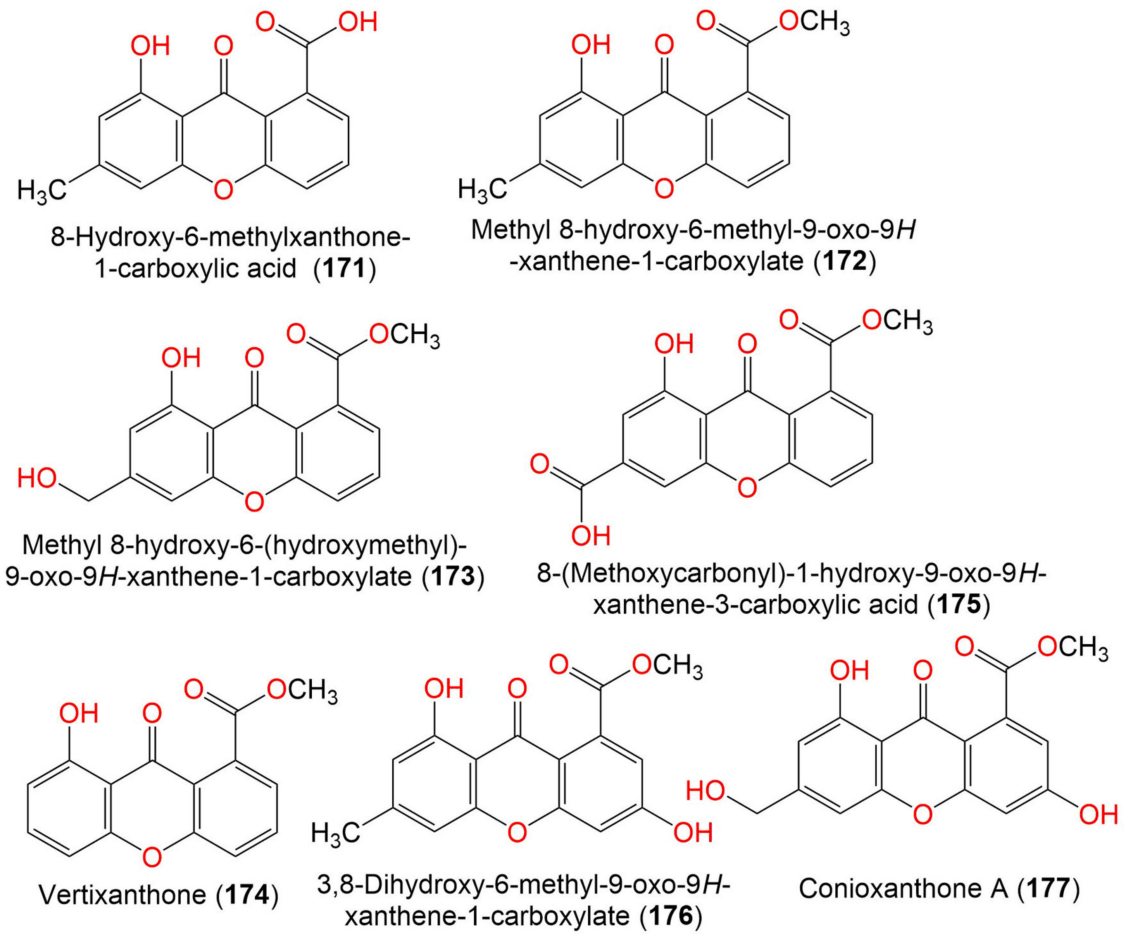

Figure 21. Xanthones **171**–**177**.

3.11. Tropolones

Tropolones are natural metabolites with a cyclohepta-2,4,6-trienone moiety [152]. They are known to be produced by fungi, bacteria, and plants. It was reported to display diverse bioactivities, including antimicrobial, antiviral, anti-HIV, hepatitis, anti-inflammatory, and anticancer [152].

Silber et al. reported the isolation of malettinins A–C (**178**–**180**), along with the new metabolite, malettinin E (181) from *Cladosporium* sp. strain KF501 isolated from the German Wadden Sea (Figure 22). These metabolites have dihydropyran/tropolone structures connected to a furan ring. The configuration of 181 was determined by the single-crystal X-ray diffraction method. Interestingly, this was the first report for tropolones isolation from genus *Cladosporium*. They were evaluated for antimicrobial activity towards *X. campestris*, *B. subtilis*, *S. epidermidis*, *C. albicans*, and *Trichophyton rubrum* using the microplate assay. Note that **178**–**181** exhibited weak antifungal potential towards *Trichophyton rubrum* (IC_{50} 30.7–83.2 μM), whereas **179**–**181** exhibited weak antibacterial effect towards *Xanthomonas campestris* (IC_{50} 28.3–37.9 μM), compared to chloramphenicol (IC_{50} 2.1 μM) [93].

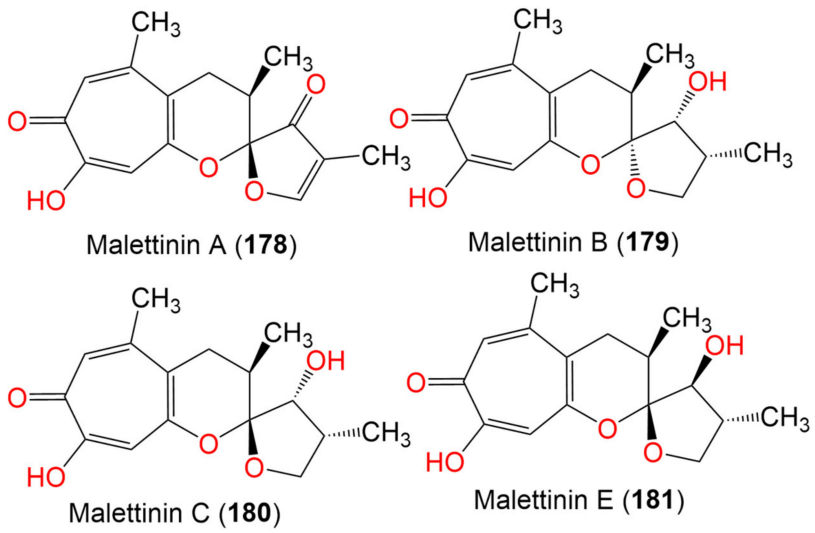

Figure 22. Tropolones **178**–**181**.

3.12. Binaphthopyrones

Bisnaphthopyrones are dimers, belonging to naphthopyrones. They have C13 basic skeleton (C6-C4-C3) that consists of naphthalene and pyrone cores [153].

The new binaphthopyrone, cladosporinone (**182**), and the formerly isolated viriditoxin (**183**) and viriditoxin derivatives (**184** and **185**) were separated the sediment associated *C. cladosporioides* (Figure 23). Note that **183** was firstly reported from *Aspergillus viridinutans* [154]. They were assayed for their cytotoxic potential versus L5178Y cells in the MTT assay. Compound **183** was the most potent one (IC_{50} 0.1 μM), however **182** and **184** had a cytotoxic effect (IC_{50} 0.88 and 0.25 μM, respectively). However, **185** was ineffective [94]. Note that all metabolites had selective potential towards *S. aureus* ATCC-29213, with **183** being the most effective (MIC 0.023 μM) [94].

3.13. Benzopyranes, Benzopyrones, and Pyrones

Wang et al. reported the separation of compounds **188**–**190**, **193**, **200**, **201**, and **203** from *Cladosporium* sp. OUCMDZ-302 isolated from mangrove plant *Excoecaria agallocha*. They possessed no cytotoxic effect towards BEL-7402, A549, HeLa, K562, HL-60, and H1975 cell lines in the MTT and SRB methods. Whilst **201** and **203** showed radical scavenging activity against DPPH (IC_{50} 5.66 and 6.67 μM, respectively). None of these metabolites exhibited antimicrobial activities against *E. coli*, *E. aerogenes*, *P. aeruginosa*, *B. subtilis*, and *C. albicans* [95]. The newly isolated benzopyrone, clapone (**192**), had no α-glycosidase inhibitory effect and no cytotoxic activity towards SGC-7901, K562, Hela, and BEL-7042 cell lines in the MTT assay [67]. Furthermore, **186** and **205** displayed no cytotoxic effect (IC_{50} > 10 μM) versus HeLa cell line in the MTT assay, as well as no antibacterial potential towards *S. aureus*, *B. cereus*, *E. coli*, *V. alginolyticus*, *V. parahemolyticus*, and MR *S. aureus* (conc. 20 μM) in the microplate assay [88]. *C. halotolerans* GXIMD 02502 associated with the coral *Porites lutea* yielded a new benzopyranone derivative, coniochaetone K (**196**) with unusual C-8 carboxyl, along with **194**, **195**, **197**, and **198** that were evaluated for their cytotoxicity versus 22RV1, C4-2B, and RWPE-1 cell lines (Figure 24).

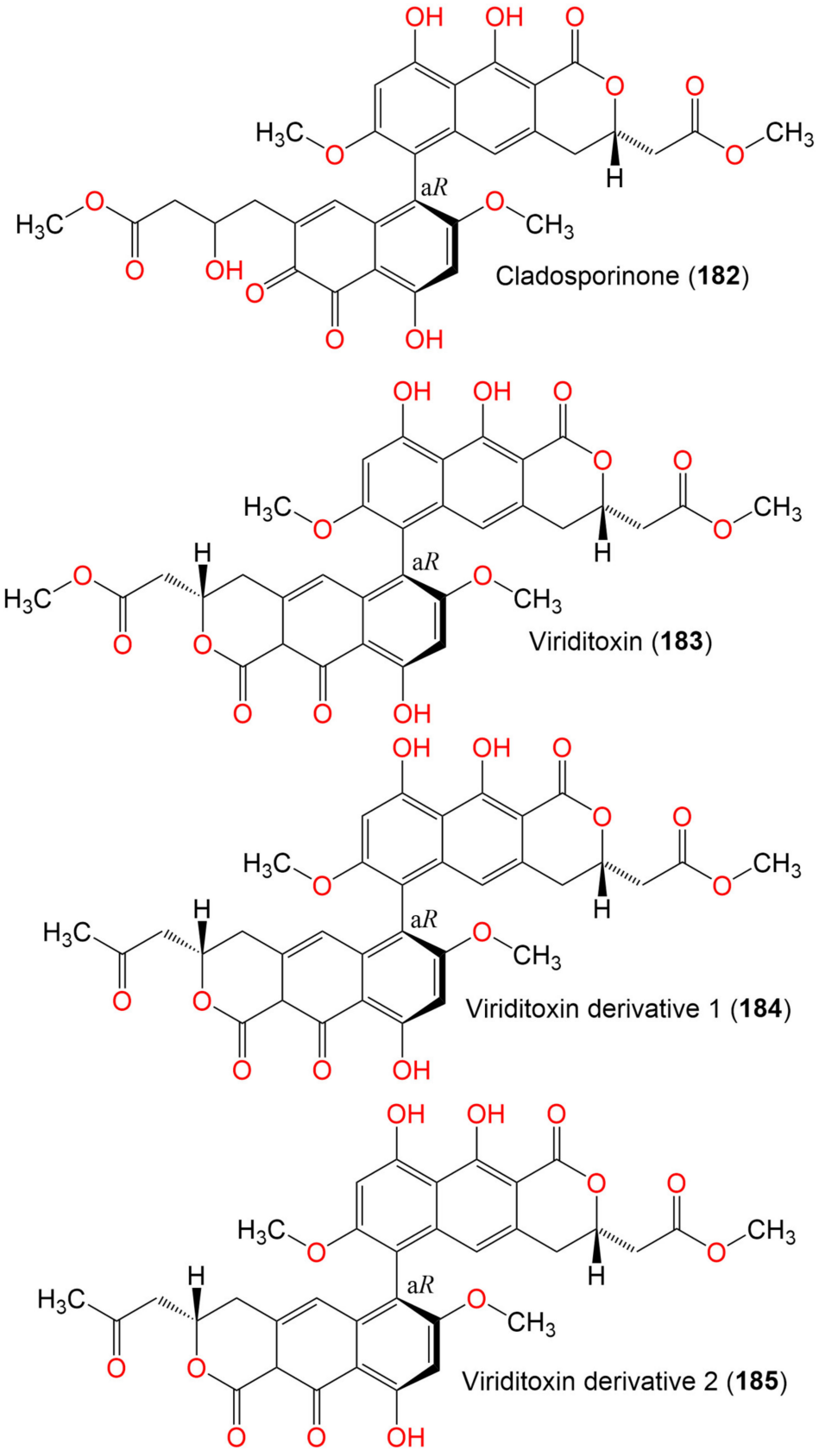

Figure 23. Binaphthopyrones **182**–**185**.

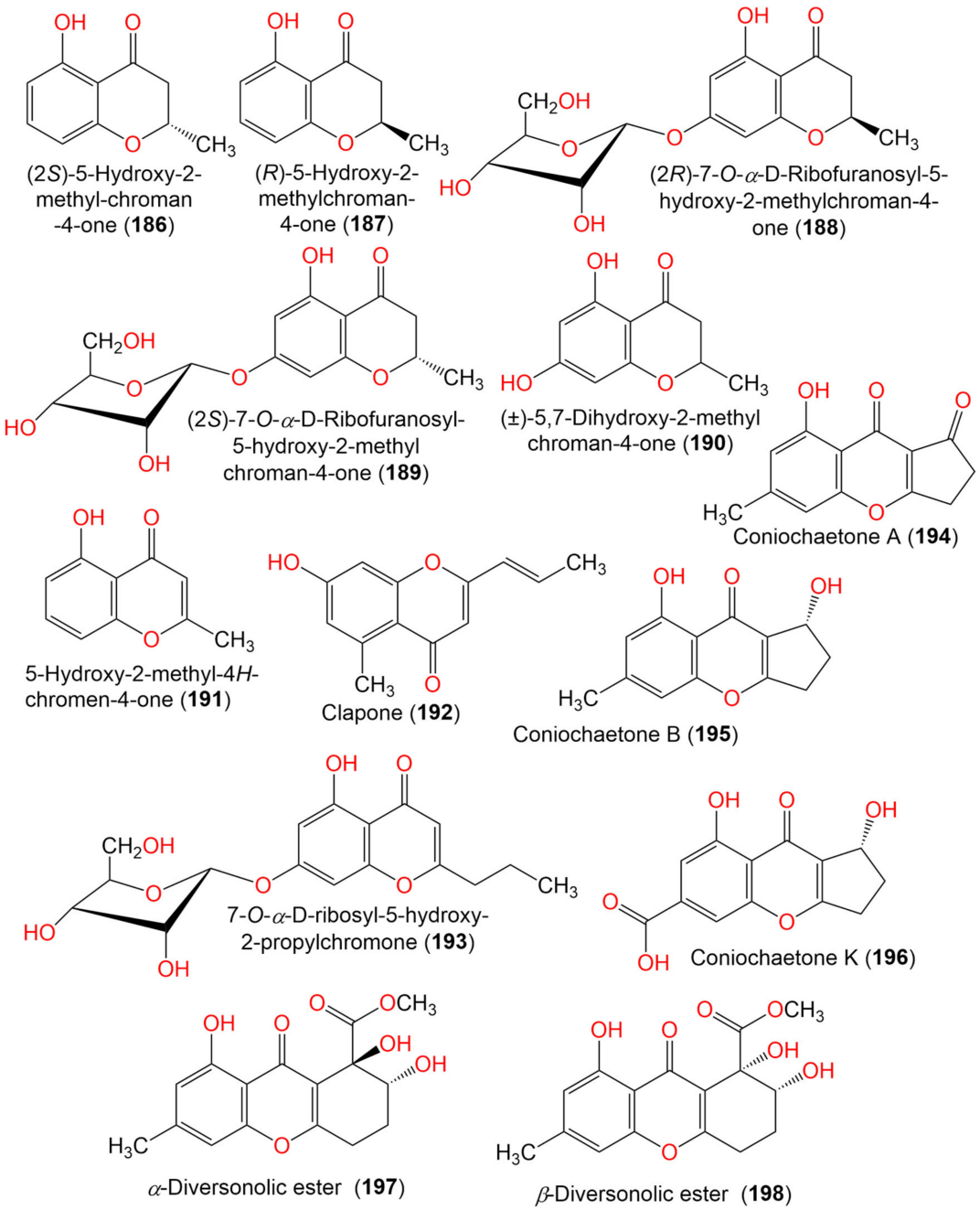

Figure 24. Benzopyrone derivatives **186**–**198**.

Among them, **194** and **196** revealed notable cytotoxicity versus 22RV1 cells (inhibition 67.4% and 64.6%, respectively, at conc. 10 μM). On the other hand, they exhibited nearly no cytotoxic effect versus RWPE-1 and C4-2B cells [92]. Bai et al. reported that **206** prohibited the growth of H. armigera Hubner newly hatched larvae (IC_{50} 100 μg/mL), compared to azadirachtin (IC_{50} 25 μg/mL) [71]. Further, it showed moderate antibacterial potential versus *S. aureus* (MIC 6.25 μg/mL), compared with ciprofloxacin (MIC 0.39 μg/mL) [71]. Cladosporin C (**207**) did not have obvious anti-biofilm activity towards *S. aureus*, *E. coli*, and *B. subtilis* [36]. On the other hand, it showed moderate toxicity towards brine shrine naupalii (LC_{50} 49.9 μM), compared to toosendanin (LC_{50} 21.2 μM) in the brine shrimp lethality assay [36]. Furthermore, **210** possessed no anti-allergic effect (IC_{50} > 200 μM) on RBL-2H3 cells, in comparison to loratadine (IC_{50} 35.01 μM) using fluorometric assay [75]. α-Pyrone derivatives **211**–**213** were separated from *C. herbarum* isolated from the sponge

Aplysina aerophoba (Figure 25). Compounds **211** and **212** had activity towards *Artemia salina* (conc. 100 µg and 50 µg) with mortality rates 85 and 75% and 80 and 65%, respectively, while **213** did not have any activity. Besides, **213** showed growth inhibitory activity towards *Spodoptera littoralis* larvae (7 and 33% at conc. 250 and 100 ppm, respectively) [96]. However, **211–213** did not show any noticeable antimicrobial activity in the agar plate diffusion assay [96].

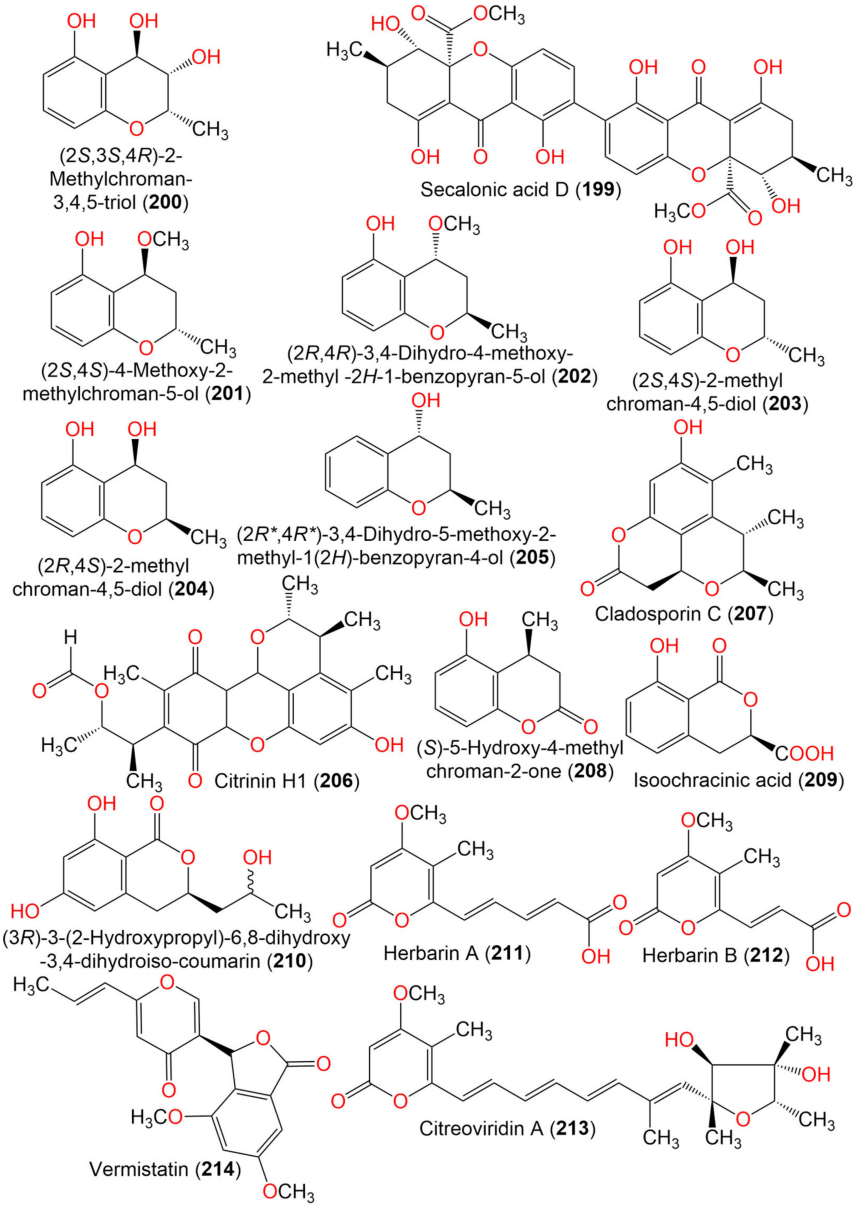

Figure 25. Benzopyrone **199–210** and pyrone (**211–214**) derivatives.

3.14. Lactones, Cyclohexene, and Azaphilone Derivatives

In 2020, He et al. purified **216** from *C. cladosporioides* that possessed no anti-allergic effect (IC_{50} > 200 µM) on RBL-2H3 cells, in comparison to loratadine (IC_{50} 35.01 µM) using fluorometeric assay [75]. The mangrove plant *C. tagal* associated-fungus *Cladosporium sp.* JJM22 produced new cyclohexene derivatives, cladoscyclitols A–D (**218–221**) (Figure 26). Compound **219** (IC_{50} 2.95 µM) revealed potent α-glucosidase inhibitory activity, compared to acarbose (IC_{50} 2.35 µM) in the colorimetric assay [97]. On the other hand, it had no antimicrobial potential towards *S. aureus* ATCC-6538, *E. coli* ATCC-25922, *B. cereu* ATCC-6633, *V. alginolyticus* ATCC-3787, *V. Parahemolyticus* ATCC-17802, or MRSA CMCC-B-63303

in the micro-plate assay [97]. Perangustols A (**223**) and B (**224**), representing new azaphilone epimers, together with bicyclic diol (**225**) were separated from sea sediment-associated *C. perangustum* FS62 fungus. They had no observable cytotoxic activity towards SF-268, NCI-H460, MCF-7, and HepG-2 (Conc. 100 μM) in the SRB assay [87].

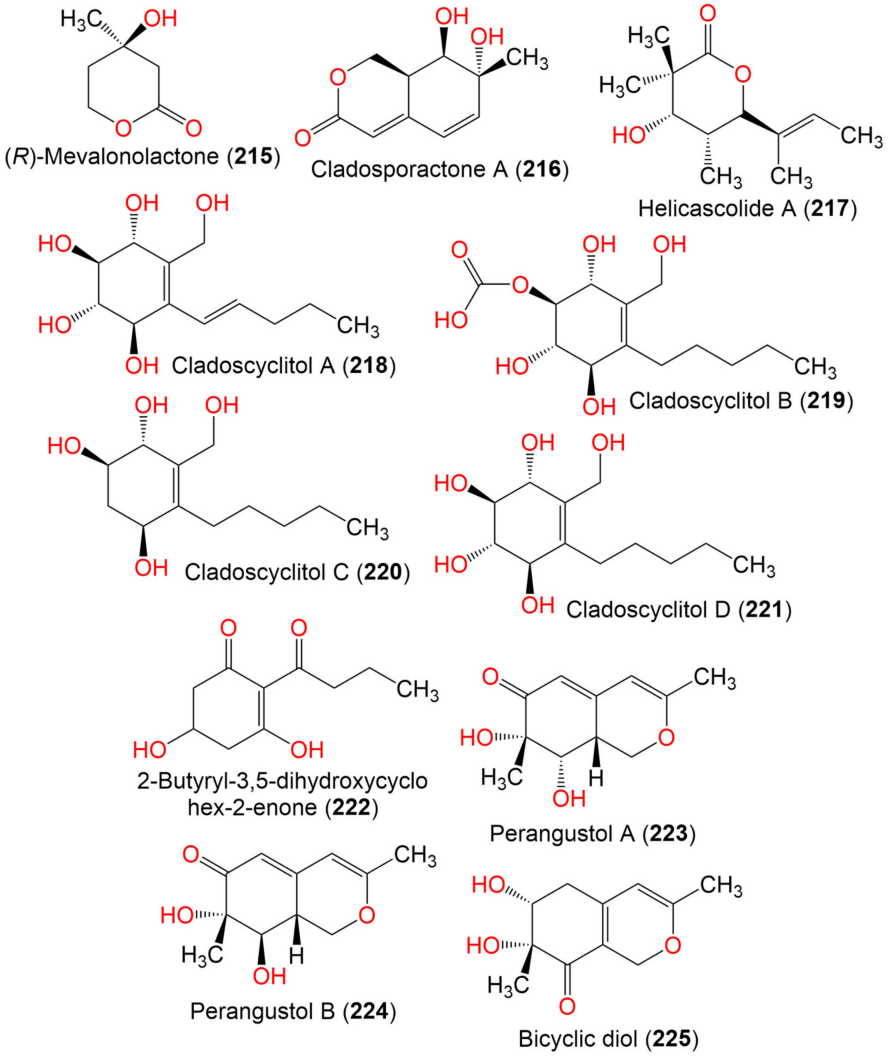

Figure 26. Lactone (**215**–**217**), cyclohexene (**218**–**222**), and azaphilones (**223**–**225**) derivatives.

3.15. Phenolics and Other Aromatic Compounds

In the DPPH assay, **233** and **235** showed DPPH radical scavenging activity (IC_{50}s 0.24 and 2.65 μM, respectively), in comparison to ascorbic acid (IC_{50} 3.29 μM). Further, none of these compounds had antimicrobial potential versus *P. aeruginosa*, *E. aerogenes*, *B. subtilis*, *E. coli*, and *C. albicans* [95]. The metabolites **232**, **238**, and **249** were separated from EtOAc extract of *Cladosporium* sp. F14 isolated from seawater and investigated for their anti-larval activity (conc. 50 μg/mL) towards *B. neritina* and *B. amphitrite* larvae in the settlement inhibition assays [60] (Figure 27). Compound **232** had weak larvae settlement inhibition towards *B. neritina* and *B. Amphitrite*, respectively, whereas **238** and **249** showed weak inhibitory effects towards *B. amphitrite* and *B. neritina* larvae, respectively. In another larval settlement bioassay, **232**, **238**, and **249** inhibited *B. neritina* larval settlement (EC_{50} 11.51, 102.23, and 77.85 μg/mL, respectively) and *B. amphitrite* larval settlement (EC_{50} 84.28, 53.65, and 9.18 μg/mL, respectively). The larval settlement EC_{50} values of **249** towards *B. amphitrite* and **232** towards *B. neritina* were less than the US Navy program established standard requirement (EC_{50} 25.0 μg/mL), revealing the potential of **232** and **249** as antifouling agents [60]. Furthermore, **232** obviously prohibited *L. hongkongensis*

growth (IZD 8 mm and MIC 80 µg/mL), compared to streptomycin (MIC 250 µg/mL) [60]. The ribofuranose phenol derivative, **239** isolated *Cladosporium* sp. JJM22 associated with the mangrove plant *C. tagal* had no cytotoxic effect (IC_{50} > 10 µM) versus HeLa cell line in the MTT assay, compared to epirubicin [88].

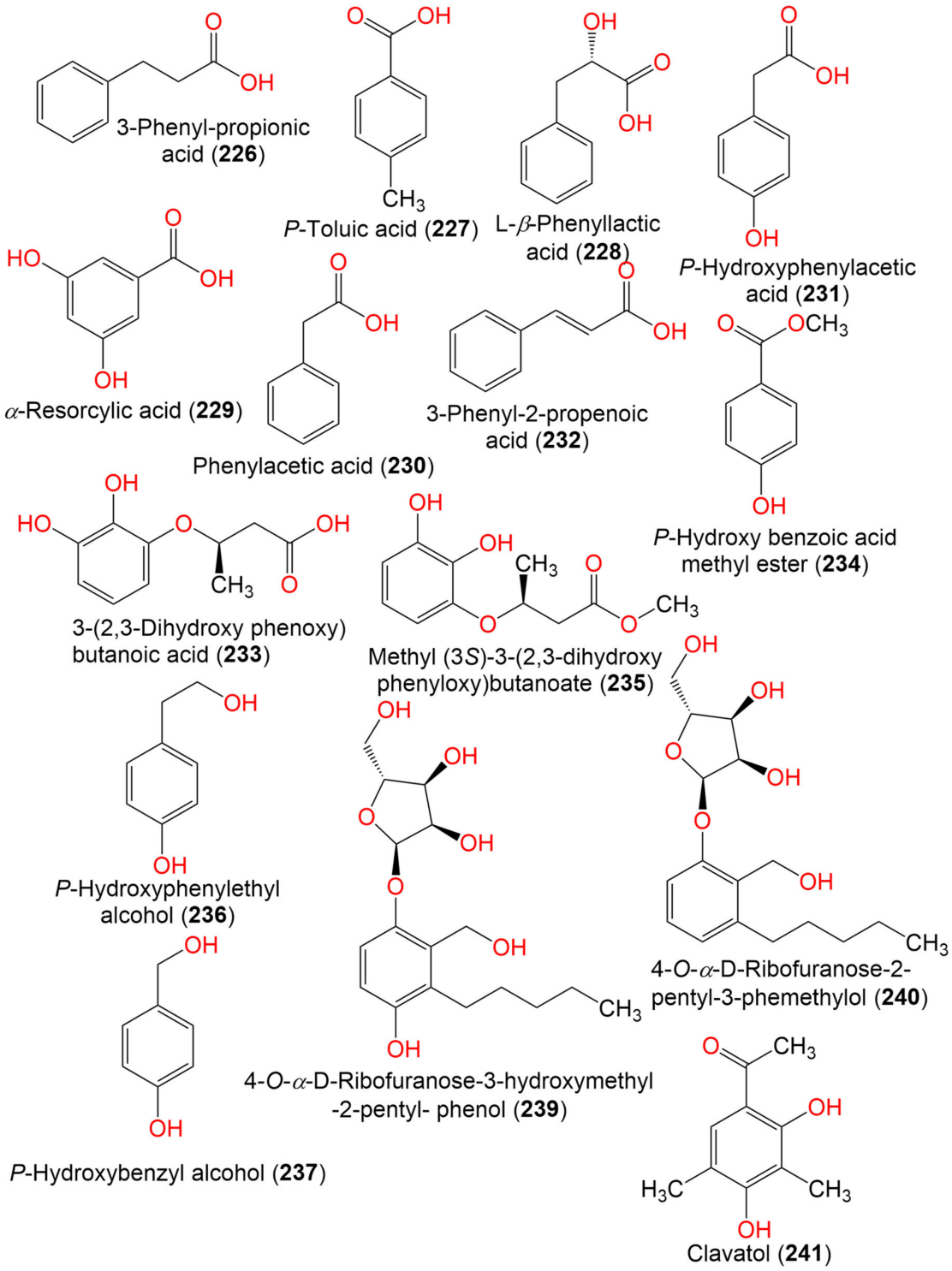

Figure 27. Phenolics **226**–**241**.

Additionally, it exhibited no noticeable antibacterial potential towards *S. aureus*, *B. cereus*, *E. coli*, *V. alginolyticus*, *V. parahemolyticus*, and MR *S. aureus* (conc. 20 µM) in the microplate assay [88]. The new ribofuranose phenol derivative, **240** (IC_{50} 2.05 µM)

revealed potent α-glucosidase inhibitory activity, compared to acarbose (IC_{50} 2.35 μM) in the colorimetric assay [97]. On the other hand, it had no antimicrobial potential towards *S. aureus* ATCC-6538, *E. coli* ATCC-25922, *B. cereus* ATCC-6633, *V. alginolyticus* ATCC-3787, *V. Parahemolyticus* ATCC-17802, and MRSA CMCC-B-63303 in the microplate assay [97]. Phytochemical investigation of the mycelium extract of the marine-derived fungus *Cladosporium* sp. associated with *Chondria crassicualis* red alga resulted in the separation of a phenol derivative, clavatol (**241**) that exhibited antioxidant capacity (ED_{50} 227.0 μM) more than oxybenzone (sunscreen agent, ED_{50} 350 μM) as evident by their UV-A protecting potential [65]. On the other hand, it was inactive towards MDRSA, MRSA, and *S. aureus* [65]. Fan et al. stated that compounds **242** and **243** exhibited no observable cytotoxic activity towards SF-268, NCI-H460, MCF-7, and HepG-2 (Conc. 100 μM) in the SRB assay [87] (Figure 28). Cladosporin D (**247**) did not have obvious anti-biofilm activity towards *S. aureus*, *E. coli*, and *B. subtilis* [36], while it exhibited significant antioxidant activity (IC_{50} 16.4 μM), compared with ascorbic acid (IC_{50} 4.9 μM). Besides, it showed moderate toxicity towards brine shrine naupalii (LC_{50} 81.4 μM), comparing with toosendanin (LC_{50} 21.2 μM) in the brine shrimp lethality assay [13].

Compound **248** separated from *Cladosporium* sp. TPU1507 derived from marine sponge and assessed for inhibitory effect towards PTP1B and TCPTP using enzyme-based assay [68]. It showed an inhibitory effect on TCPTP (IC_{50} 27 μM) that was 2-fold weaker than on PTP1B (IC_{50} 11 μM) [68]. The new phthalide, herbaric acid (**250**), separated from *C. herbarum* isolated from *Callyspongia aerizusa* had no activity towards *A. salina* and HL-60 human leukemia cell line [96]. In addition, the newly separated abscisic acid analog **251** from *Cladosporium* sp. OUCMDZ-1635 possessed no cytotoxic effect towards MCF-7, HeLa, HCT-116, HeLa, HCT-116, K562, and HL-60. Furthermore, it did not show antibacterial activity (conc. 100 μg/mL) against *B. subtilis*, *P. aeruginosa*, *C. perfringens*, *S. aureus*, *E. coli*, and *C. albicans* [56]. The new pentenoic acid derivative, 1,1′-dioxine-2,2′-dipropionic acid (**252**) prohibited the growth of H. armigera Hubner newly hatched larvae (IC_{50} 150 μg/mL), compared to azadirachtin (IC_{50} 25 μg/mL) [71]. Further, it showed moderate antibacterial potential versus *S. aureus* (MIC 25.0 μg/mL), compared with ciprofloxacin (MIC 0.39 μg/mL) [71]. The furan carboxylic acid metabolites, Sumiki's acid (**253**) and acetyl Sumiki's acid (**254**) exerted activity towards *S. aureus* and *B. subtilis* (IZDs 7 mm at conc. 5 μg/disk), whereas they had no activity towards *C. albicans* and *E. coli* [74].

3.16. Sterols and Terpenes

A study conducted by Yu et al. in 2018 led to the separation of a new pregnane; 3α-hydroxy-7-ene-6,20-dione (**268**) and six sterol derivatives: **256**, **258**, **260**, **262**, **263**, and **267** from gorgonian-associated *Cladosporium* sp. WZ-2008-0042 [100]. Note that **268** was reported in the same year by Pang et al. as new metabolites with the name cladosporisteroid B from *Cladosporium* sp. SCSIO41007 associated with *Callyspongia* sp. [61]. These metabolites (IC_{50} values ranging from 0.11 to 0.17 μM) revealed antiviral activity against RSV (respiratory syncytial virus) with therapeutic ratio (TC_{50}/IC_{50}) values ranging from 5.18 to 9.92, in comparison to ribavirin in the neuraminidase inhibition assay. This could be due to their binding to RSV GREs (glucocorticoid response elements) [100]. Moreover, they (conc. 0.1 mg/mL) displayed weak to moderate AChEI potential, in comparison to huperzine A and galanthamine using the modified Ellman's method [100]. Further, **268** had no noticeable antibacterial potential towards *B. cereus*, *M. luteus*, *S. aureus*, *V. anguillarum* *E. coli*, *Shigella dysenteriae*, *B. subtilis*, and *V. Parahemolyticus*, while **263** was moderately active (MIC 3.13 μM) towards *S. dysenteriae* [100]. In 2020, He et al. reported that **256**, **261**, **265**, **266**, and **268** separated from *C. cladosporioides* sea sediment-derived fungus possessed no anti-allergic effect on RBL-2H3 cells, in comparison to loratadine using fluorometeric assay [75] (Figures 29 and 30). In 2018, Pang et al. separated new sterol cladosporisteroid A (**264**) and new pregnanes, cladosporisteroid B (**268**) and cladosporisteroid C (**269**), along with **259**, **265**, and **270** from *Cladosporium* sp. SCSIO41007 isolated from *Callyspongia* sp.

and assessed their antiviral activity towards EV71 and H3N2 using CCK-8 and CPE assays, respectively. Only, **268** (IC_{50} 16.2 μM) had weak activity towards H3N2 compared to oseltamivir (IC_{50} 34.0 nM). Moreover, they revealed no cytotoxic effect towards K562, MCF-7, and SGC-7901 in the CCK-8 assay [61]. Additionally, **268** was purified from *C. sphaerospermum* EtOAc fraction by HPLC with the aid of LCMS and assessed for its influence on adipogenesis and lipid metabolism during maturation of adipocyte (Conc. 1.25, 2.5, 5, and 10 μM) using 3T3-L1 preadipocytes [101]. It substantially prohibited lipid accumulation and differentiation of 3T3-L1-preadipocytes into adipocytes, leading to reducing *Adipsin* (adipocyte marker gene) expression. Further, it significantly upregulated *ATGL* (lipolytic gene, Conc. 5 and 10 μM) and reduced *FASN* and *SREBP1* (lipogenic genes, conc. 1.25, 2.5, 5, and 10 μM) expression. Collectively, 268 facilitated lipid metabolism and disrupted adipogenesis via promoting lipolysis and prohibiting lipogenesis [101].

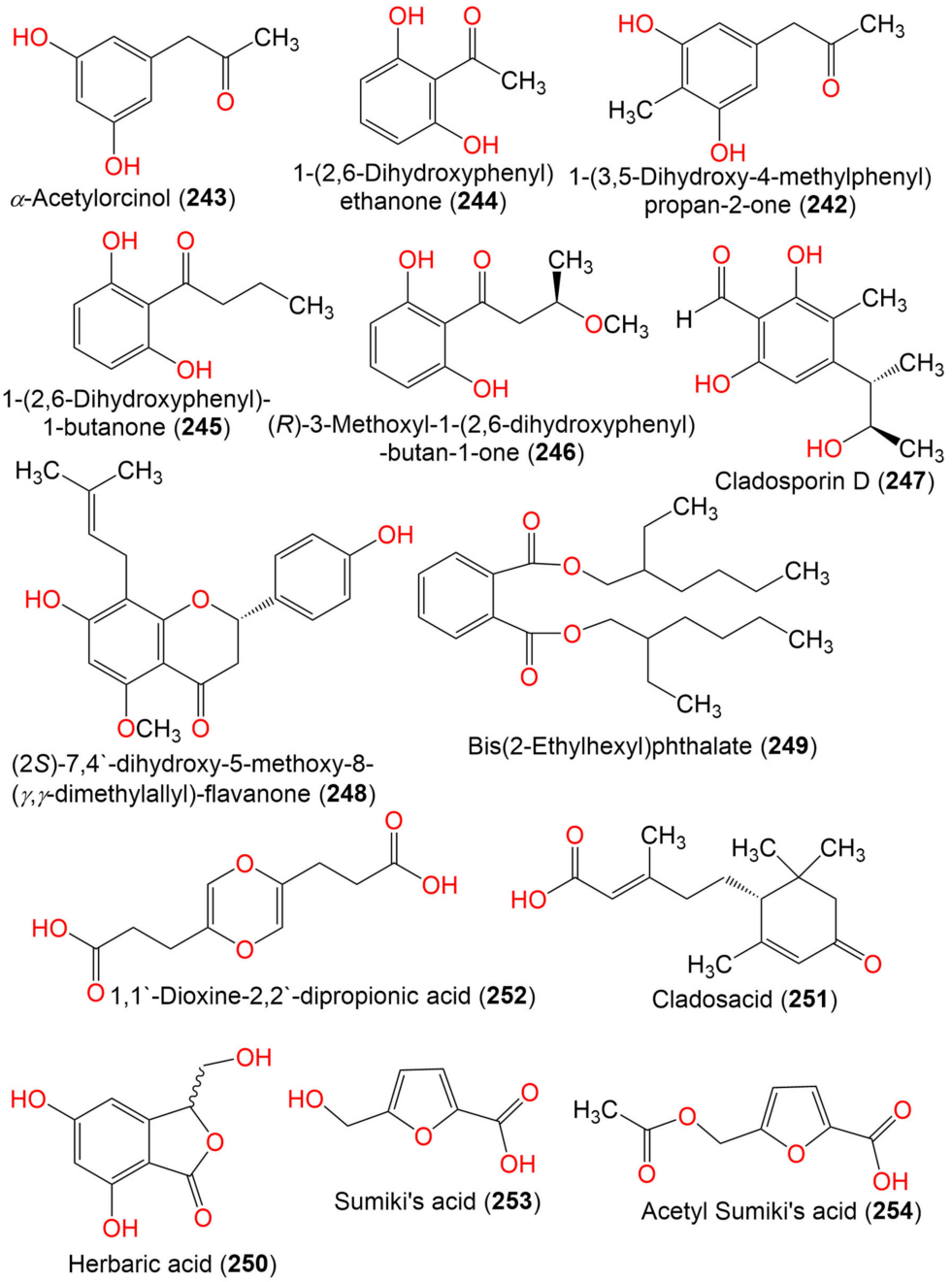

Figure 28. Phenolics **242**–**248** and others **249**–**254**.

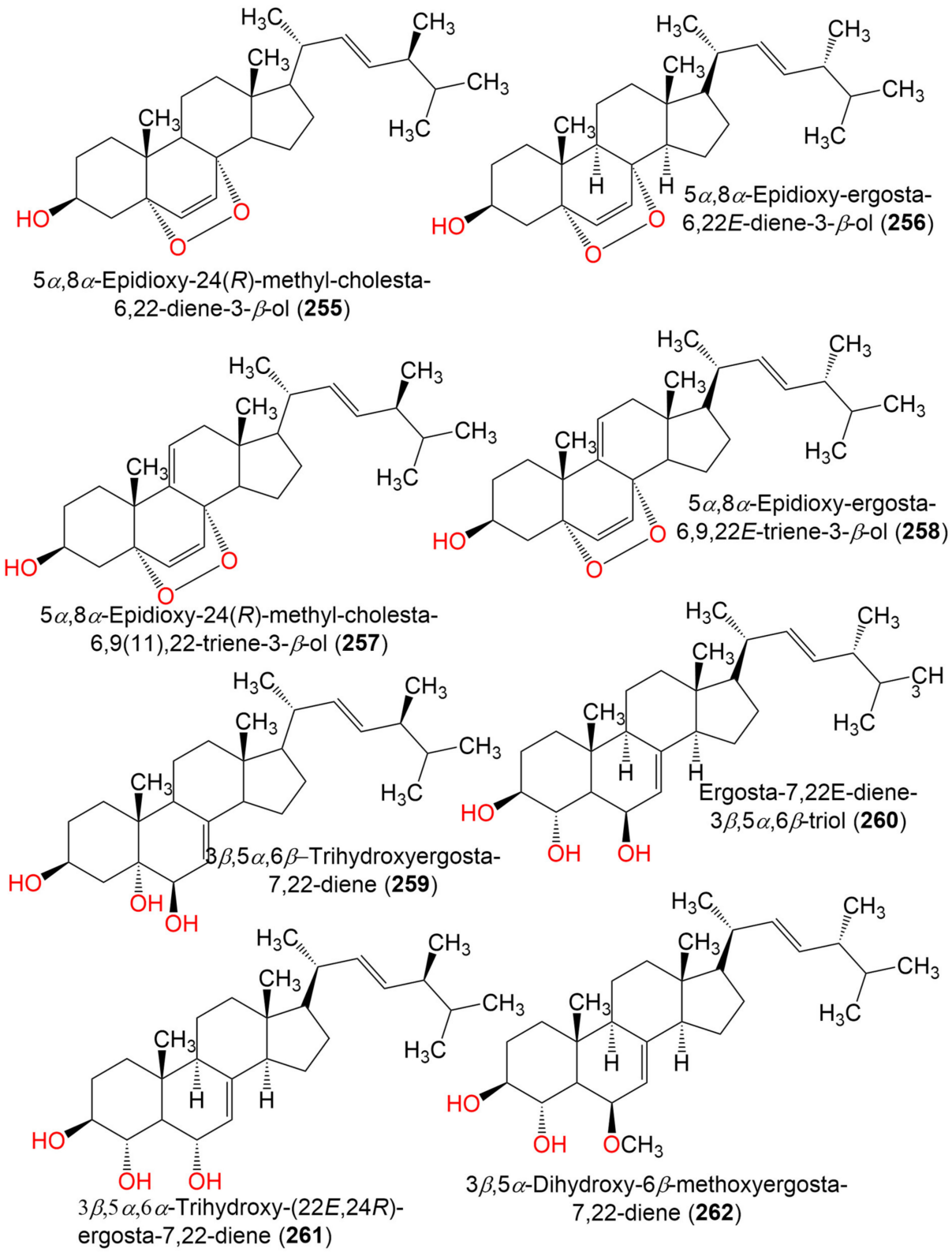

Figure 29. Sterols **255**–**262**.

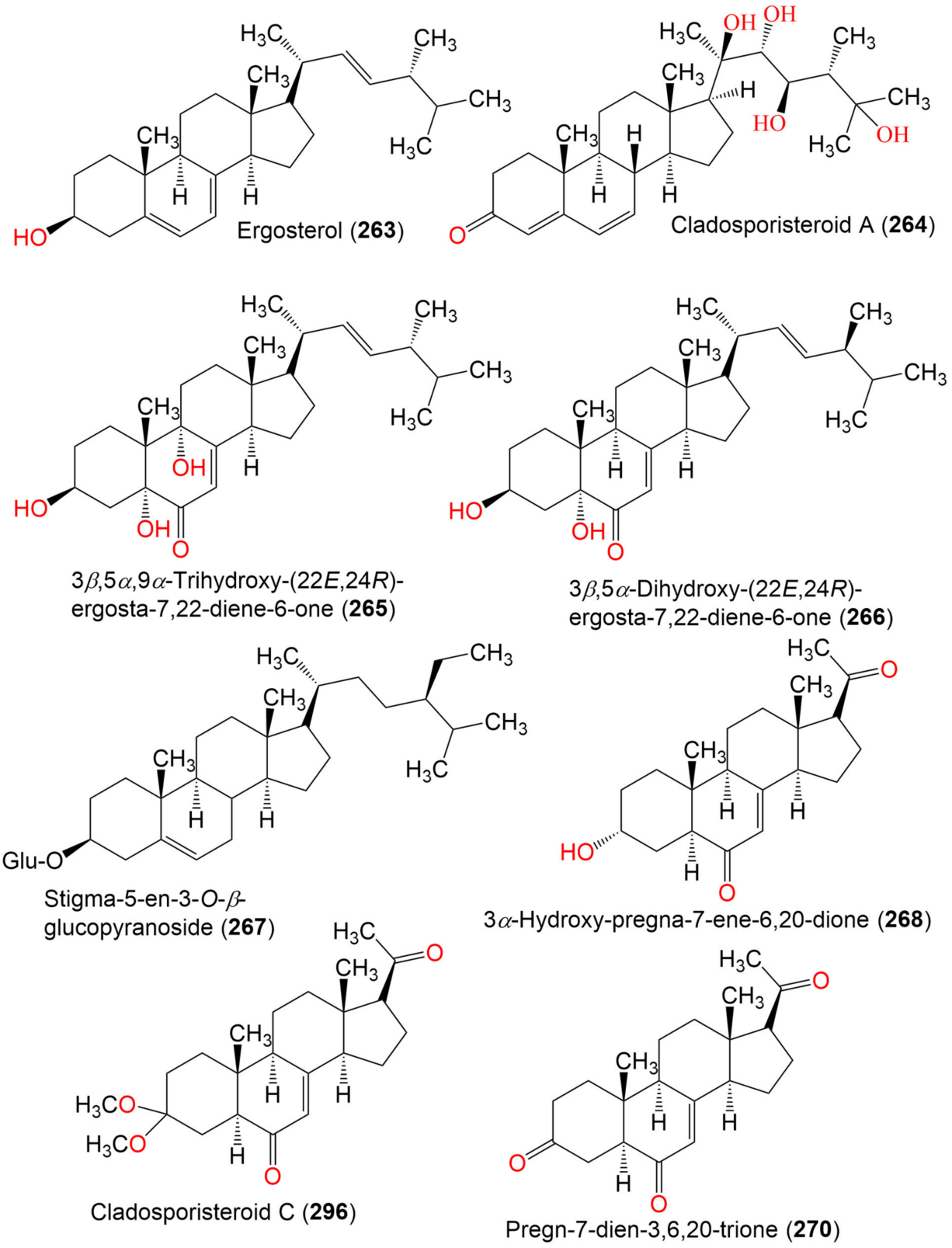

Figure 30. Sterols **263**–**267** and terpenes **268**–**270**.

3.17. Alcohols and Aldehydes

Gallo et al. reported for the first time from fungi the isolation of α,β-unsaturated aldehydes (**271**–**284**) from the culture of *Cladosporium* sp. isolated from intertidal marine sediment [102] (Figure 31). They exerted antimicrobial activity towards *E. coli* ATCC-25922,

B. subtilis ATCC-6633, and *C. albicans* ATCC-18804 in the agar diffusion method. It is noteworthy that this class of metabolites had been reported formerly from red algae (e.g., *Corallina mediterranea* and *Laurencia papillosa*, *L. spectabilis*, and *L. undulata*) [155,156]. The new aliphatic alcohols, (2*S*,3*S*,4*E*)-hepta-4,6-diene-2,3-diol (**285**) and (3*E*,8*E*,6*S*)-Undeca-3,8,10-trien-1,6-diol (**286**) were assessed for cytotoxic potential versus HeLa, BEL-7402, HL-60, A549, K562, and H1975 cell lines. Compound **286** had a cytotoxic effect versus H1975 cell line (IC_{50} 10.0 μM), compared to ADR (IC_{50} 0.38 μM). While both metabolites revealed no antioxidant and antimicrobial capacities [95].

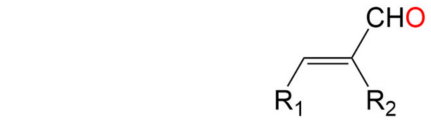

Compound	R1	R2	Compound	R1	R2
(**271**)	$C_{14}H_{29}$	$C_{13}H_{27}$	(**278**)	$C_{16}H_{33}$	$C_{13}H_{27}$
(**272**)	$C_{16}H_{29}$	$C_{13}H_{27}$	(**279**)	$C_{16}H_{29}$	$C_{15}H_{27}$
(**273**)	$C_{14}H_{29}$	$C_{15}H_{27}$	(**280**)	$C_{16}H_{31}$	$C_{15}H_{27}$
(**274**)	$C_{14}H_{25}$	$C_{15}H_{31}$	(**281**)	$C_{16}H_{29}$	$C_{15}H_{29}$
(**275**)	$C_{16}H_{31}$	$C_{13}H_{27}$	(**282**)	$C_{16}H_{31}$	$C_{15}H_{27}$
(**276**)	$C_{14}H_{29}$	$C_{15}H_{29}$	(**283**)	$C_{16}H_{29}$	$C_{15}H_{29}$
(**277**)	$C_{14}H_{29}$	$C_{15}H_{31}$	(**284**)	$C_{16}H_{31}$	$C_{15}H_{29}$

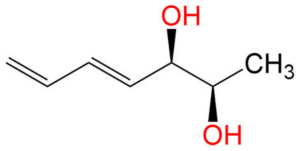

(2*S*,3*S*,4*E*)-Hepta-4,6-diene-2,3-diol (**285**)

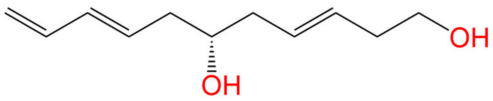

(3*E*,8*E*,6*S*)-Undeca-3,8,10-trien-1,6-diol (**286**)

Figure 31. Aldehydes (**271**–**284**) and alcohols (**285** and **286**).

3.18. Bioactivities of Cladosporium Species Extracts

Ding et al. stated that *Cladosporium* sp. isolate N5 associated with *Porphyra yezoensis* red alga did not produce any pathogenic symptoms in the reinfection assay. Further, its EtOAc extract displayed no lethality to *A. salina* and had a moderate antimicrobial activity which indicated that *Cladosporium* sp. had no toxicity to the aquatic ecosystem and could be applied as a biocontrol agent [59]. In the disc diffusion method, *Cladosporium* sp. EIODSF 008 EtOAc extract exhibited significant antibacterial potential towards *E. coli*, *M. luteus*, and *B. subtilis* (conc. 100 μg/disc) [57]. The EtOAc extract of *Cladosporium* sp. EN-S01 isolated from *Sargassum cinereum* brown algae showed anticancer activity towards MCF-7, HeLa, and DU-145 cell lines (IC_{50} 8.46, 9.87, and 98.03 μg/mL, respectively). The extract had greater cytotoxic activity and anti-proliferative towards MCF-7 and HeLa cell lines than towards DU-145 [157]. Moreover, the EtOAc extract of *C. cladosporioides* KT384175 isolated from the seaweed *Sargassum wightii* possessed remarkable antioxidant potential

that was comparable to ascorbic acid, as well as significant Fe^{3+} reducing power that could be referred to its phenolic contents. Moreover, it revealed anti-angiogenic potential as evidenced by the decrease in the number and length of blood vessel branches on CAM (chick chorioallantoic membrane) in-vivo in the CAM assay. Further, *C. cladosporioides* extract (conc. 1.0 mg/mL) had lower wound healing potential than thalidomide (conc. 1.0 µg/mL) in the in vitro scratch assay using MCF-7 cells [158]. The sea water-derived fungus *Cladosporium* sp. F14 can produce antifouling and antibiotic metabolites in the existence of xylose or glucose. Significantly, it showed higher antibiotic activity towards *M. luteus*, *P. piscida*, *Rhodovulum* sp., *Ruegeria* sp., *V. fluvialis*, and *V. harveyi* in the existence of a sugar carbon source than in its absence in the disc diffusion assay, even though the fungal cells were well-grown under both conditions. Moreover, it possessed antifouling potential as it reduced the attachment of *B. neritina* (bryozoan larvae) in the larval settlement assay [159]. The gold nanoparticles synthesized from *C. cladosporioides* isolated from the seaweed *S. wightii* possessed noticeable antimicrobial potential towards *E. coli* MTCC-118, *B. subtilis* MTCC-441, *S. aureus* MTCC-7443, *P. aeruginosa MTCC-424*, and *A. niger* MTCC-281 with the highest growth inhibition towards *S. aureus* (IZD 12 mm) and least activity against *B. subtilis* (IZD 9.5 mm), compared to ampicillin (IZDs 15 and 12 mm, respectively) in the well diffusion method. Furthermore, they also had significant antioxidant potential comparable to ascorbic acid in the DPPH assay and moderate effectiveness in reducing power assay [160]. Ameen et al. reported that the AgNPs synthesized from *C. halotolerans* biomass isolated from the marine debris collected around Tarout Island showed a significant free radical scavenging effect (%inhibition 78% within 30 min incubation) in the DPPH assay. Moreover, it exhibited cytotoxic potential towards MCF-7 (IC_{50} 34.27 µL/mL), compared to cisplatin (IC_{50} 17.69 µL/mL) in the MTT assay, as well as an antifungal effect against *A. niger* (%inhibition 70 and 45% at conc. 1000 and 500 ppm, respectively) in the broth dilution method [161].

From the comprehensive review of the available literature, it was noticed that *C. phlei* (causal agent of Timothy leaf spot disease) and *C. cucumerinum* (causal agent of scab disease of many Cucurbitaceae plants) were isolated mainly from plant sources [162–165]. These species produced perylenequinone derivatives as major metabolites which are responsible for pigmentation and discolorations of the leaves [162,165]. Additionally, cotylenins, plant growth regulators were isolated from an unidentified *Cladosporium* species [166–170]. However, tetralones, *seco*-acids, macrolides, diketopiperazines, alkaloids, and tetramic acid derivatives were reported mainly from marine-associated *Cladosporium* species.

4. Conclusions

Numerous structurally diverse biometabolites are discovered from marine-derived fungi that represent a rich library for the development of drug lead. Marine-associated *Cladosporium* species are of biotechnological and industrial relevance and could be considered as substantial enzyme producers. Their enzymes are active in harsh conditions such as extremely low temperatures and high salinity. Therefore, they can be utilized in various industrial and biotechnological applications. Besides, these species were found to be a wealthy pool covering a wide array of metabolites with various bioactivities. Over the past 22 years, 286 metabolites have been separated from marine-associated *Cladosporium* species isolated from various marine samples, including mangrove, sediment, sponges, corals, gorgonians, algae, bivalves, hydroids, and others (Figure 32).

More than 75% of these metabolites have been reported from unidentified *Cladosporium* sp. (175 metabolites, 61%) and *C. cladosporioides* (53 metabolites, 18.5%) (Figure 33).

The results revealed that alkaloids, macrolides, tetramic acid and pyrone derivatives, and phenolics are the major metabolites reported from this marine-associated fungal species (Figure 34). They could be privileged and useful candidates for chemists and biologists to design structurally novel and pharmacologically important compounds for various diseases.

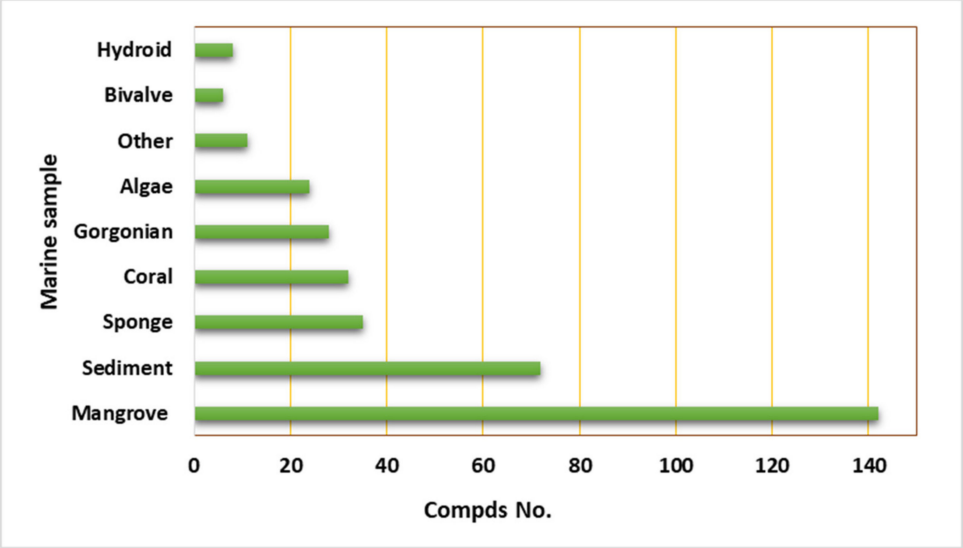

Figure 32. Number of compounds separated from *Cladosporium* species isolated from various marine samples.

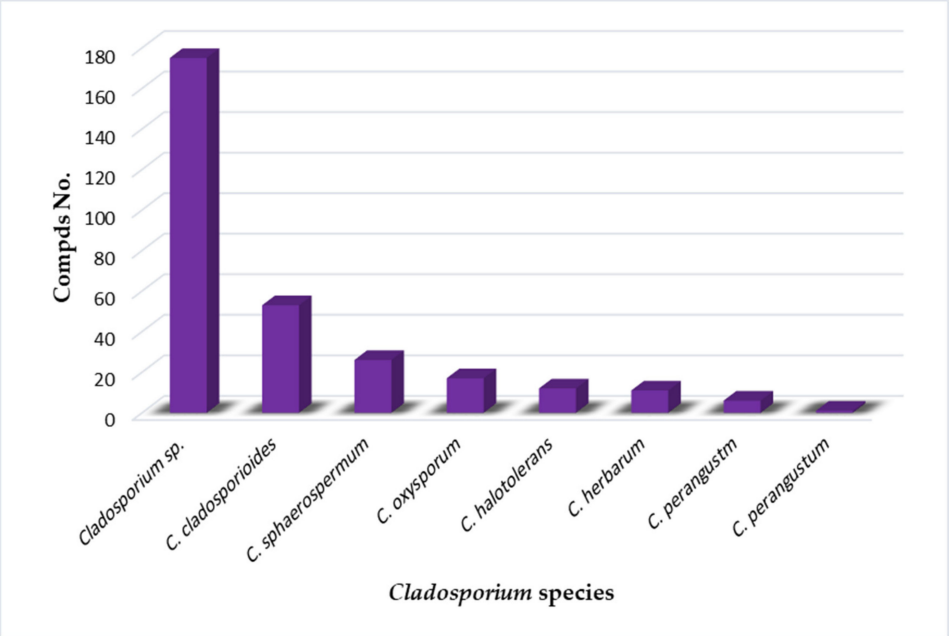

Figure 33. Number of compounds separated from marine-derived *Cladosporium* species.

Although the structural diversity of these metabolites, they were insufficiently evaluated for their bioactivities. Most of them had been assessed for their antimicrobial, cytotoxicity, antiviral, and insecticidal activities (Figure 35).

Figure 36 illustrated the prominent activities of each class of secondary metabolites.

However, there are limited studies that focus on the mechanism of action of these metabolites. Many of the tested metabolites possessed no noticeable efficacy in some of the tested activities. Therefore, estimation of other potential bioactivities and derivatization of these metabolites, as well as the mechanistic and in vivo studies of the active metabolites should clearly be the target of future research.

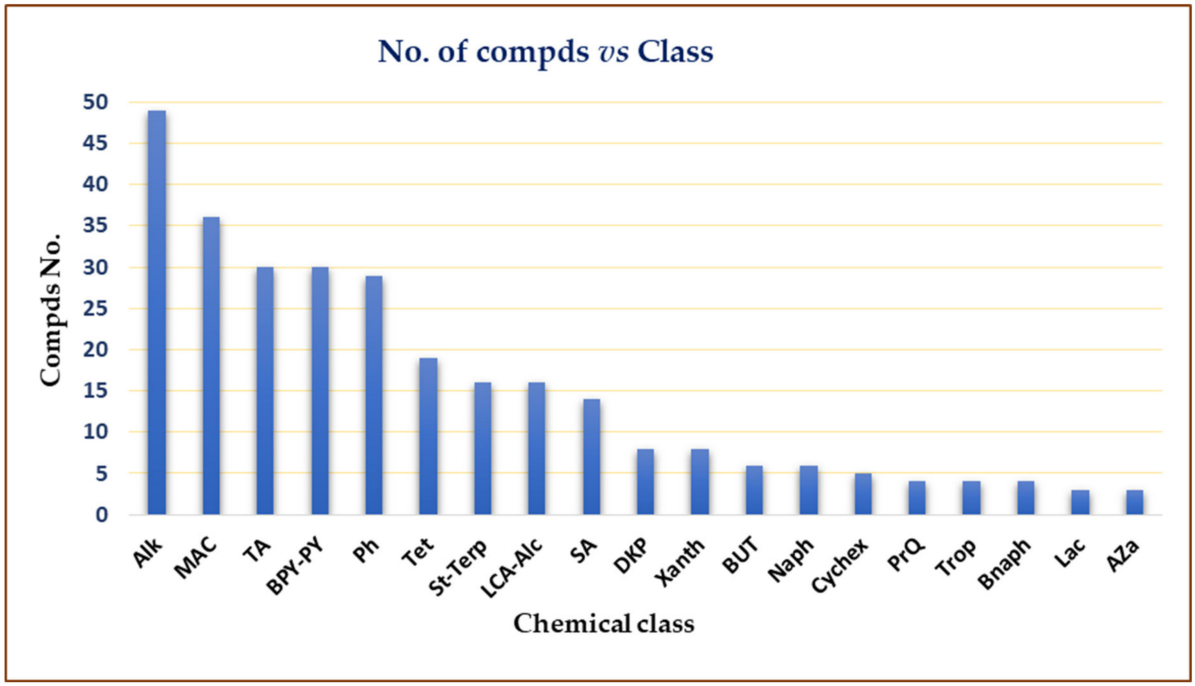

Figure 34. Number of metabolites from each class of natural products.

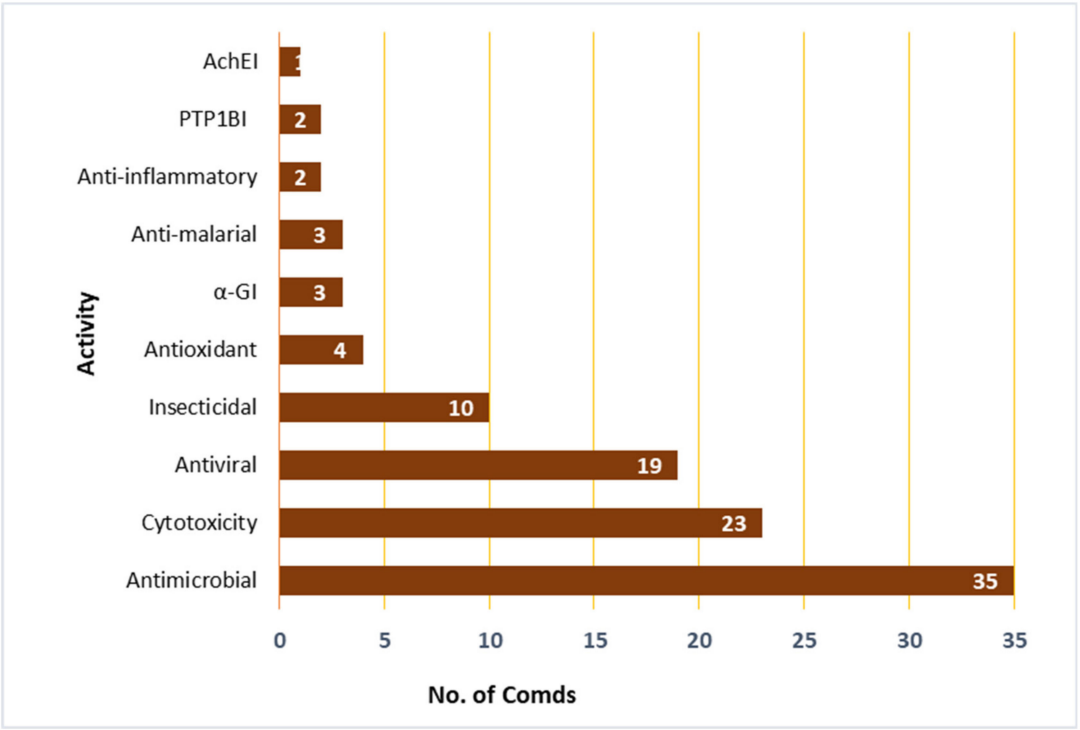

Figure 35. Number of bioactive compounds in each tested activity.

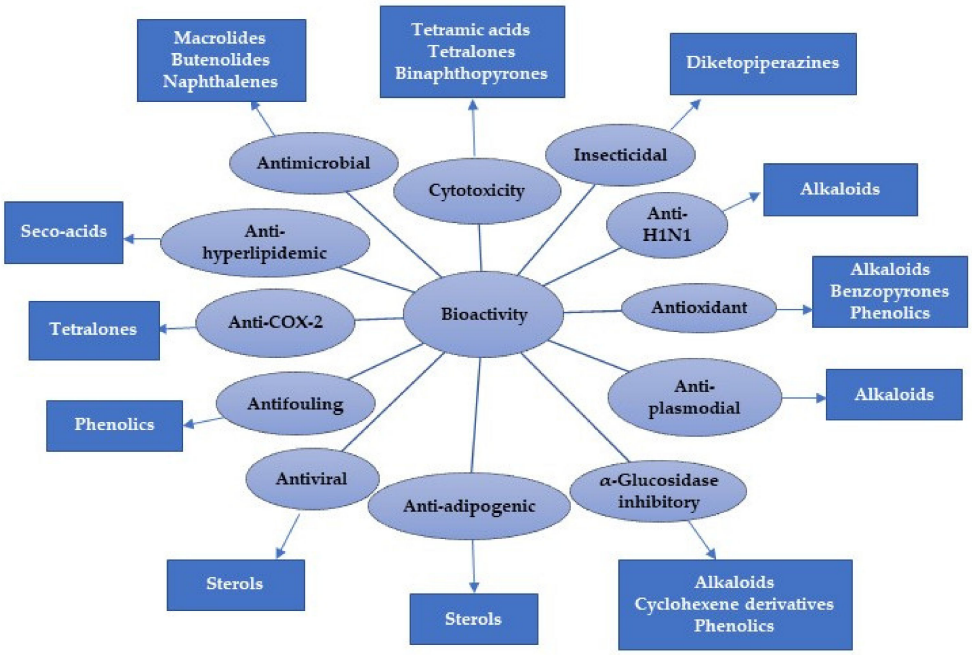

Figure 36. Prominent activities of each class of metabolite from *Cladosporium* species.

5. Strategies for Activating Silencing Gene Clusters

Growing evidence has revealed that the activation of silent gene clusters has the potential to significantly enhance the discovery of new natural metabolites of high-therapeutic leads. Different strategies to awake the silent biosynthetic gene clusters of *Cladosporium* species such as co-cultivation of organisms and elicitors epigenetic, as well as, modifiers can be applied [171–174]. The production of secondary metabolites (SMs) is affected by cultivation media, environment, and conditions [171,175]. Therefore, manipulating the culture conditions can improve the outputs from living organisms. Small changes in the growth media composition can induce not only variation in the amount of SMs, but also the production of a completely different pattern of molecules [171–173]. OSMAC (one strain many compounds) is a form of strain improvement that summarized the ability of single strains to produce different compounds when growing under different conditions e.g., aeration rate, media composition, type of culturing vessel, or a combination of these factors [174–176]. Challenging the fungi with external cues or chemicals has been shown to enhance the SMs production. Antibiotics have been widely reported as elicitors that can activate a broad spectrum of silent BGCs [171–174]. The co-cultivation of strains of the same or different species has been shown to represent a promising strategy for the activation of silent BGCs that enhances the production of SMs and discovery of new bioactive SMs [171,172,177]. Activation of silent biosynthetic gene clusters (BGCs) by quorum sensing class of signaling molecule is another strategy that has been shown to dramatically increase SMs production [171–173]. Engineering strains to circumvent the regulatory systems has the potential to free silent BGCs from their locked-in state and result in a significantly enhancement of SMs production. This can be done through various ways such as ribosome and polymerase engineering, an awakening of the genes encoding transcriptional regulatory proteins, and deletion or deactivation of the suppressor proteins. Another approach is the insertion of inducible artificial promoters to drive the expression of the silent genes [171,172,178]. Modulating epigenetic control also plays a role in the expression of silent gene clusters linked to natural product expression [173,179].

Author Contributions: G.A.M. and S.R.M.I. contributed equally to this work. All authors have read and agreed to the published version of the manuscript.

Funding: The authors extend their appreciation to the Deputyship for Research & Innovation, Ministry of Education in Saudi Arabia for funding this research work through the project number IFPRP: 50-166-1442 and King Abdulaziz University, DSR, Jeddah, Saudi Arabia.

Institutional Review Board Statement: Not applicable.

Informed Consent Statement: Not applicable.

Acknowledgments: The authors extend their appreciation to the Deputyship for Research & Innovation, Ministry of Education in Saudi Arabia for funding this research work through the project number IFPRP: 50-166-1442 and King Abdulaziz University, DSR, Jeddah, Saudi Arabia.

Conflicts of Interest: The authors declare no conflict of interest.

Abbreviations

[^{3}H]PDBu: [^{3}H]Phorbol-12,13-dibutyrate; 22RV1: Human prostatic cancer cell line; 3T3-L1; Mouse adipocyte-like cell line; 786-0: Human renal carcinoma cell line; A2780; Human ovarian cancer cell; A375: Melanoma cell line; A549: Lung adenocarcinoma epithelial cell line; Ab1: Proto-oncogene 1, non-receptor tyrosine kinase; ABPA: Allergic bronchopulmonary aspergillosis; ADR: Adriamycin; ATGL: Adipose triglyceride lipase; ATP: Adenosine triphosphate; Bax/Bcl-2: Apoptosis regulator BAX; Bcap-37: Human breast carcinoma cell line; Bel-7402: Human hepatocellular carcinoma cell line; BGC-823: Human gastric cancer cell line; BT549: Human breast cancer cells line; C4-2B: Human prostatic cancer cell line; C4-2B: Human prostatic cancer cell line; CAM: Chick chorioallantoic membrane assay; CCK8: Cell Counting kit-8; CD25: Cluster of differentiation 25; CD28: Cluster of differentiation 28; CD3: Cluster of differentiation 3; CDK: Cyclin-dependent kinase; CDKI: Cyclin-dependent kinase Inhibitor; CDPSs: Cyclodipeptide synthases; CM: Corrected mortality; COX-2: Cyclooxygenase-2; CPE: Cytopathic effect; DAPI: 4,6-Diamidino-2-phenylindole; DELFIA: Dissociation-enhanced lanthanide fluorescence immunoassay; DKPs: Diketopiperazines; DMSO: Dimethylsulfoxide; DPPH: 1,1-Diphenyl-2-picrylhydrazyl; DU-145: Human prostate cancer cell line; ED_{50}: Effective dose 50; EGFR: Epidermal growth factor receptor; ERK: Extracellular signal-regulated protein kinase; EtOAc: Ethyl acetate; EtOH: Ethanol; EV71: Enterovirus 71; FASN: Fatty acid synthase; FRAP: Ferric reducing antioxidant power; FSW: Filtered seawater; Fyn: Proto-oncogene tyrosine-protein kinase; GREs: Glucocorticoid response elements; GW9662: Selective PPAR antagonist for PPARγ; H1974: Human colorectal cancer cell line; H3N2: Influenza A virus subtype H3N2; H446: Human small cell lung carcinoma; HCC70: Human breast cancer cells line; HCT-116: Human colon cancer cell line; HCT-15: Human colon cancer cell line; HCT-8: Human colorectal cancer cell line; HeLa: Human epithelioid cervix carcinoma cell line; HeLa S3: Human cervix carcinoma cell line; HepG-2: Human liver cancer cell line; HL-60: Human promyelocytic leukemia cell; HT-29: Human colorectal adenocarcinoma cell line; HTRF: Homogeneous time-resolved fluorescence assay; Huh-7: Differentiated hepatocyte-derived cellular carcinoma cell line; IC_{50}: Half-maximal inhibitory concentration; IFNγ: Interferon γ; IL-2: Interleukin-2; IZD: Inhibition zone diameter; JNK: c-Jun NH2-terminal kinase; Jurkat: Human T lymphoblastic leukemia cell lines; K562: Human kidney cancer cell line; L02: Human hepatic cancer cell line; L1210: Mouse lymphocytic leukemia cell line; L5178Y: Murine lymphoma cell line; Lac: Laccase; LBD: Ligand binding domain; LC3-I, II: Microtubule-associated proteins 1A/1B light chain 3B; LC_{50}: Lethal concentration 50; LCK: Lymphocyte-specific protein tyrosine kinase; LiP: Lignin peroxidase; LLC-PK1: Epithelial-like pig kidney cell line; LM3: Human hepatocellular carcinoma cell line; LNCap: Human prostate cancer cell line; LPS: Lipopolysaccharide; MCF-7: Breast cancer cell line; MDA-MB-231: Human breast cancer cell line; MDA-MB-435: Human breast cancer cell line; MDA-MB-468: Human breast cancer cell line; MDCK: Madin–Darby canine kidney; MD-MBA-231: Breast adenocarcinoma cell line; MeOH: Methanol; MGC-803: Human gastric carcinoma cell line; MIC: Minimum inhibitory concentration; MMP: Mitochondrial membrane potential; MnP: Manganese-dependent peroxidase; MOLT-4: T lymphoblast-acute lymphoblastic leukemia; MRCNS: Methicillin-resistant coagulase-negative Staphylococci; mRNA: Messenger ribonucleic acid; MRSA: Methicillin-resistant *Staphylococcus aureus*; MTT: 3-(4,5-Dimethylthiazol-2-yl)-2,5-diphenyltetrazolium bromide; NAC: N-acetylcysteine; NCI-H460: Human lung carcinoma cell line; NF-kB: Nuclear factor Kappa B; NO: Nitric oxide; NRPSs: Non-

ribosomal peptide synthetases; NS-398: N-[2-(cyclohexyloxy)-4-nitrophenyl]methanesulfonamide; OA: Oleic acid; OCI-AML3: Acute myeloid leukemia cell line; OSMAC: One strain many compounds; OVCAR-3: Human ovarian Cancer cell line; P0: PAX6 promoter; P1: PAX6 promoter; P21: N-Myc-cyclin-dependent kinase inhibitor 1A; p21waf1/cip1: Cyclin kinase inhibitor p21; P388: Mouse lymphocytic leukemia cell line; PANC-1: Human Pancreatic cancer cell line; PAX6: Paired box gene 6; PBMC: Peripheral blood mononuclear cell; PC-3: Human prostate carcinoma cell line; PG: Polygalacturonase; $PGF_{2\alpha}$: Prostaglandin $F_{2\alpha}$; PKA: cAMP-dependent protein kinase; PKC: Protein kinase C; PMA: Phorbol 12-myristate 13-acetate; PME: Pectin methylesterase; PPARγ: Peroxisome proliferator-activated receptor γ; PPRE: Peroxisome proliferator-activated receptor response element; PTP: Protein tyrosine phosphatase; Pα: PAX6 promoter; RHO: Rhodopsin; RSV: Respiratory syncytial virus; RWPE-1: Human normal prostate epithelial cell; SAR: Structure–activity relationship; SF-268: Human glioblastoma cell line; SGC-7901: Human gastric cancer cell line; SH-SY5Y: Human neuroblastoma cell line; SK-BR-3: Human Breast cancer cell line; SMMC-7721: Human hepatoma carcinoma cell line; SPR: Surface plasmon resonance; SRB: Sulforhodamine B; SREBP1: Sterol regulatory element binding transcription factor 1; SW1116: Human colon cancer cell line; SW1990: Human pancreatic adenocarcinoma cell line; T47D: Human breast cancer cell line; TC: Total cholesterol; TC_{50}: Half toxic concentration; TCF: T cell factor; TCPTP: T Cell protein tyrosine phosphatase; TG: Total triglyceride; TRF: Time-resolved fluorescence; U937: Human myeloid leukaemia cell line; WERI: Retinoblastoma cell line; WST-1: (4-[3-4-Iodophenyl]-2-(4-nitrophenyl)-2H-5-tetrazolio)-1,3-benzene disulfonate); Y-79: Retinoblastoma cell line.

References

1. Townsed, M.; Davies, K.; Hanley, N.; Hewitt, J.E.; Lundquist, C.J.; Lohrer, A.M. The challenge of implementing the marine ecosystem service concept. *Front. Mar. Sci.* **2018**, *5*, 359. [CrossRef]
2. Boeuf, G. Marine biodiversity characteristics. *C. R. Biol.* **2011**, *334*, 435–440. [CrossRef] [PubMed]
3. Donato, P.D.; Buono, A.; Poli, A.; Finore, I.; Abbamondi, G.R.; Nicolaus, B.; Lama, L. Exploring marine environments for the identification of extremophiles and their enzymes for sustainable and green bioprocesses. *Sustainability* **2019**, *11*, 149. [CrossRef]
4. Bonugli-Santos, R.C.; Dos Santos Vasconcelos, M.R.; Passarini, M.R.; Vieira, G.A.; Lopes, V.C.; Mainardi, P.H.; Dos Santos, J.A.; de Azevedo Duarte, L.; Otero, I.V.; da Silva Yoshida, A.M.; et al. Marine-derived fungi: Diversity of enzymes and biotechnological applications. *Front. Microbiol.* **2015**, *6*, 269. [CrossRef] [PubMed]
5. Varrella, S.; Barone, G.; Tangherlini, M.; Rastelli, E.; Dell'Anno, A.; Corinaldesi, C. Diversity, Ecological Role and Biotechnological Potential of Antarctic Marine Fungi. *J. Fungi* **2021**, *7*, 391. [CrossRef] [PubMed]
6. Lindequist, U. Marine-derived pharmaceuticals-challenges and opportunities. *Biomol. Ther.* **2016**, *24*, 561–571. [CrossRef] [PubMed]
7. Carroll, A.R.; Copp, B.R.; Davis, R.A.; Keyzers, R.A.; Prinsep, M.R. Marine natural products. *Nat. Prod. Rep.* **2014**, *31*, 160–258.
8. Gerwick, W.H.; Moore, B.S. Lessons from the past and charting the future of marine natural products drug discovery and chemical biology. *Chem. Biol.* **2012**, *19*, 85–98. [CrossRef]
9. Retter, A.; Nilsson, R.H.; Bourlat, S.J. Exploring the taxonomic composition of two fungal communities on the Swedish west coast through metabarcoding. *Biodivers. Data J.* **2019**, *7*, e35332. [CrossRef]
10. Fan, B.; Parrot, D.; Blümel, M.; Labes, A.; Tasdemir, D. Influence of OSMAC-based cultivation in metabolome and anticancer activity of fungi associated with the brown alga Fucus Vesiculosus. *Mar. Drugs* **2019**, *17*, 67. [CrossRef]
11. Furbino, L.E.; Pellizzari, F.M.; Neto, P.C.; Rosa, C.A.; Rosa, L.H. Isolation of fungi associated with macroalgae from maritime Antarctica and their production of agarolytic and carrageenolytic activities. *Polar Biol.* **2018**, *41*, 527–535. [CrossRef]
12. Panno, L.; Bruno, M.; Voyron, S.; Anastasi, A.; Gnavi, G.; Miserere, L.; Varese, G.C. Diversity, ecological role and potential biotechnological applications of marine fungi associated to the seagrass *Posidonia Oceanica*. *New Biotechnol.* **2013**, *30*, 685–694. [CrossRef]
13. Jones, E.B.G.; Sakayaroj, J.; Suetrong, S.; Somrithipol, S.; Pang, K.L. Classification of marine *Ascomycota*, *anamorphic* taxa and *Basidiomycota*. *Fungal Divers.* **2009**, *35*, 187.
14. Jones, E.B.G. Are there more marine fungi to be described? *Bot. Mar.* **2011**, *54*, 343–354. [CrossRef]
15. Marinefungi. Available online: https://www.marinefungi.org/ (accessed on 9 November 2021).
16. Hasan, S.; Ansari, M.I.; Ahmad, A.; Mishra, M. Major bioactive metabolites from marine fungi: A Review. *Bioinformation* **2015**, *11*, 176–181. [CrossRef]
17. Jayawardena, R.S.; Hyde, K.D.; Chen, Y.J.; Papp, V.; Palla, B.; Papp, D.; Bhunjun, C.S.; Hurdeal, V.G.; Senwanna, C.; Manawasinghe, I.S.; et al. One stop shop IV: Taxonomic update with molecular phylogeny for important phytopathogenic genera: 76–100 (2020). *Fungal Divers.* **2020**, *103*, 87–218. [CrossRef]
18. Bensch, K.; Braun, U.; Groenewald, J.Z.; Crous, P.W. The genus *Cladosporium*. *Stud. Mycol.* **2012**, *72*, 1–401. [CrossRef]
19. Levetin, E.; Dorsey, K. Contribution of leaf surface fungi to the air spora. *Aerobiologia* **2006**, *22*, 3–12. [CrossRef]

20. Heuchert, B.; Braun, U.; ScHuBert, K. Morphotaxonomic revision of fungi-colous *Cladosporium* species (hyphomycetes). *Schlechtendalia* **2005**, *13*, 1–78.
21. Bensch, K.; Groenewald, J.Z.; Meijer, M.; Dijksterhuis, J.; Jurjević, Ž.; Andersen, B.; Houbraken, J.; Crous, P.W.; Samson, R.A. *Cladosporium* species in indoor environments. *Stud. Mycol.* **2018**, *89*, 177–301.
22. El-Dawy, E.G.A.E.M.; Gherbawy, Y.A.; Hussein, M.A. Morphological, molecular characterization, plant pathogenicity and biocontrol of *Cladosporium* complex groups associated with faba beans. *Sci. Rep.* **2021**, *11*, 14183. [CrossRef] [PubMed]
23. Denning, D.W.; O'Driscoll, B.R.; Hogaboam, C.M.; Bowyer, P.; Niven, R.M. The link between fungi and severe asthma: A summary of the evidence. *Eur. Resp. J.* **2006**, *27*, 615–626. [CrossRef] [PubMed]
24. Van Kan, J.A.; Van den Ackerveken, G.F.J.M.; De Wit, P.J.G.M. Cloning and characterization of cDNA of avirulence gene avr9 of the fungal pathogen *Cladosporium fulvum*, causal agent of tomato leaf mold. *Mol. Plant Microbe Interact.* **1991**, *4*, 52–59. [CrossRef] [PubMed]
25. Batra, N.; Kaur, H.; Mohindra, S.; Singh, S.; Shamanth, A.S.; Rudramurthy, S.M. *Cladosporium sphaerospermum* causing brain abscess, a saprophyte turning pathogen: Case and review of published reports. *J. Mycol. Med.* **2019**, *29*, 180–184. [CrossRef]
26. Sandoval-Denis, M.; Gené, J.; Sutton, D.A.; Wiederhold, N.P.; Cano-Lira, J.F.; Guarro, J. New species of *Cladosporium* associated with human and animal infections. *Persoonia* **2016**, *36*, 281–298. [CrossRef]
27. Simon-Nobbe, B.; Denk, U.; Pöll, V.; Rid, R.; Breitenbach, M. The spectrum of fungal allergy. *Int. Arch. Allergy Immunol.* **2008**, *145*, 58–86. [CrossRef]
28. De Hoog, G.S.; Guarro, J.; Gené, J.; Figueras, M.J. *Atlas of Clinical Fungi*, 2nd ed.; Centraalbureau voor Schimmelcultures (CBS): Utrecht, The Netherlands, 2000.
29. Hamayun, M.; Khan, S.A.; Ahmad, N.; Tang, D.S.; Kang, S.M.; Na, C.I.; Sohn, E.Y.; Hwang, Y.H.; Shin, D.H.; Lee, B.H.; et al. *Cladosporium sphaerospermum* as a new plant growth-promoting endophyte from the roots of *Glycine max* (L.) Merr. *World J. Microbiol. Biotechnol.* **2009**, *25*, 627–632. [CrossRef]
30. Sellart-Altisent, M.; Torres-Rodríguez, J.M.; Gómez de Ana, S.; Alvarado-Ramírez, E. Microbiota fúngica nasal en sujetos alérgicos y sanos [Nasal fungal microbiota in allergic and healthy subjects]. *Rev. Iberoam. Micol.* **2007**, *24*, 125–130. [CrossRef]
31. Sandoval-Denis, M.; Sutton, D.A.; Martin-Vicente, A.; Cano-Lira, J.F.; Wiederhold, N.; Guarro, J.; Gené, J. Cladosporium species recovered from clinical samples in the United States. *J. Clin. Microbiol.* **2015**, *53*, 2990–3000. [CrossRef]
32. Sun, J.Z.; Liu, X.Z.; McKenzie, E.H.C.; Jeewon, R.; Liu, J.K.; Zhang, X.L.; Zhao, Q.; Hyde, K.D. Fungicolous fungi: Terminology, diversity, distribution, evolution and species checklist. *Fungal Divers.* **2019**, *95*, 337–430. [CrossRef]
33. Torres, D.E.; Rojas-Martínez, R.I.; Zavaleta-Mejia, E.; Guevara-Fefer, P.; Márquez-Guzmán, G.J.; Perez-Martinez, C. *Cladosporium cladosporioides* and *Cladosporium pseudocladosporioides* as potential new fungal antagonists of *Puccinia horiana* Henn., the causal agent of *Chrysanthemum* white rust. *PLoS ONE* **2017**, *12*, e0170782. [CrossRef]
34. Jashni, M.K.; van der Burgt, A.; Battaglia, E.; Mehrabi, R.; Collemare, J.; de Wit, P.J. Transcriptome and proteome analyses of proteases in biotroph fungal pathogen *Cladosporium fulvum*. *J. Plant Pathol.* **2020**, *102*, 377–386. [CrossRef]
35. Ge, J.; Yin, Y.; Jiang, X.; Liu, W.; Yao, B.; Luo, H. Gene cloning and characterization of a novel glucose oxidase from *Cladosporium tianshanense* SL19. *J. Agric. Sci. Technol.* **2019**, *12*, 49–57.
36. Amin, M.; Zhang, X.Y.; Xu, X.Y.; Qi, S.H. New citrinin derivatives from the deep-sea-derived fungus *Cladosporium* sp. SCSIO z015. *Nat. Prod. Res.* **2020**, *34*, 1219–1226. [CrossRef]
37. Pan, F.; El-Kashef, D.H.; Kalscheuer, R.; Müller, W.E.G.; Lee, J.; Feldbrügge, M.; Mándi, A.; Kurtán, T.; Liu, Z.; Wu, W.; et al. New hybrid polyketides from the endophytic fungus *Cladosporium sphaerospermum* WBS017. *Eur. J. Med. Chem.* **2020**, *191*, 112159. [CrossRef]
38. Rischer, M.; Lee, S.R.; Eom, H.J.; Park, H.B.; Vollmers, J.; Kaster, A.-K.; Shin, Y.-H.; Oh, D.-C.; Kim, K.H.; Beemelmanns, C. Spirocyclic cladosporicin A and cladosporiumins I and J from a *Hydractinia*-associated *Cladosporium sphaerospermum* SW67. *Org. Chem. Front.* **2019**, *6*, 1084–1093. [CrossRef]
39. Zhang, F.Z.; Li, X.M.; Yang, S.Q.; Meng, L.H.; Wang, B.G. Thiocladospolides A-D, 12-membered macrolides from the mangrove-derived endophytic fungus *Cladosporium cladosporioides* MA-299 and structure revision of pandangolide 3. *J. Nat. Prod.* **2019**, *82*, 1535–1541. [CrossRef]
40. Zhang, F.Z.; Li, X.M.; Li, X.; Yang, S.Q.; Meng, L.H.; Wang, B.G. Polyketides from the mangrove-derived endophytic fungus *Cladosporium cladosporioides*. *Mar. Drugs* **2019**, *17*, 296. [CrossRef]
41. Zhu, M.; Gao, H.; Wu, C.; Zhu, T.; Che, Q.; Gu, Q.; Guo, P.; Li, D. Lipid-lowering polyketides from a soft coral-derived fungus *Cladosporium* sp. TZP29. *Bioorg. Med. Chem. Lett.* **2015**, *25*, 3606–3609. [CrossRef]
42. Wu, G.; Sun, X.; Yu, G.; Wang, W.; Zhu, T.; Gu, Q.; Li, D. Cladosins A-E, hybrid polyketides from a deep-sea-derived fungus, *Cladosporium sphaerospermum*. *J. Nat. Prod.* **2014**, *77*, 270–275. [CrossRef]
43. Birolli, W.G.; Zanin, L.L.; Jimenez, D.E.Q.; Porto, A.L.M. Synthesis of Knoevenagel adducts under microwave irradiation and biocatalytic ene-reduction by the marine-derived fungus *Cladosporium* sp. CBMAI 1237 for the production of 2-cyano-3-phenylpropanamide derivatives. *Mar. Biotechnol.* **2020**, *22*, 317–330. [CrossRef]
44. Birolli, W.G.; de Santos, A.D.; Alvarenga, N.; Garcia, A.C.F.S.; Romão, L.P.C.; Porto, A.L.M. Biodegradation of anthracene and several PAHs by the marine-derived fungus *Cladosporium* sp. CBMAI 1237. *Mar. Pollut. Bull.* **2018**, *129*, 525–533. [CrossRef]
45. Gil-Durán, C.; Ravanal, M.C.; Ubilla, P.; Vaca, I.; Chávez, R. Heterologous expression, purification and characterization of a highly thermolabile endoxylanase from the Antarctic fungus *Cladosporium* sp. *Fungal Biol.* **2018**, *122*, 875–882. [CrossRef]

46. Taskin, M.; Ortucu, S.; Unver, Y.; Tasar, O.C.; Ozdemir, M.; Kaymak, H.C. Invertase production and molasses decolourization by cold-adapted filamentous fungus *Cladosporium herbarum* ER-25 in non-sterile molasses medium. *Process Saf. Environ. Prot.* **2016**, *103*, 136–143. [CrossRef]
47. Trivedi, N.; Reddy, C.; Radulovich, R.; Jha, B. Solid state fermentation (SSF)-derived cellulase for saccharification of the green seaweed *Ulva* for bioethanol production. *Algal Res.* **2015**, *9*, 48–54. [CrossRef]
48. Del-Cid, A.; Ubilla, P.; Ravanal, M.C.; Medina, E.; Vaca, I.; Levicán, G.; Eyzaguirre, J.; Chávez, R. Cold-active xylanase produced by fungi associated with Antarctic marine sponges. *Appl. Biochem. Biotechnol.* **2014**, *172*, 524–532. [CrossRef]
49. Bastos, S.C.; Pimenta, C.J.; Dias, D.R.; Chalfoun, S.M.; Ange'lico, C.L.; Tavares, L.S. Pectinases from a new strain of *Cladosporium cladosporioides* (Fres.) De Vries isolated from coffee bean. *World J. Agric. Sci.* **2013**, *9*, 167–172.
50. Bonugli-Santos, R.C.; Durrant, L.R.; da Silva, M.; Sette, L.D. Production of laccase, manganese peroxidase and lignin peroxidase by Brazilian marine-derived fungi. *Enzyme Microb. Technol.* **2010**, *46*, 32–37. [CrossRef]
51. Duarte, A.W.F.; Dayo-Owoyemi, I.; Nobre, F.S.; Pagnocca, F.C.; Chaud, L.C.S.; Pessoa, A.; Felipe, M.G.; Sette, L.D. Taxonomic assessment and enzymes production by yeasts isolated from marine and terrestrial Antarctic samples. *Extremophiles* **2013**, *17*, 1023–1035. [CrossRef]
52. Ball, A.; Truskewycz, A. Polyaromatic hydrocarbon exposure: An ecological impact ambiguity. *Environ. Sci. Pollut. Res.* **2013**, *20*, 4311–4326. [CrossRef]
53. Lee, S.R.; Lee, D.; Eom, H.J.; Rischer, M.; Ko, Y.-J.; Kang, K.S.; Kim, C.S.; Beemelmanns, C.; Kim, K.H. Hybrid polyketides from a *Hydractinia*-associated *Cladosporium sphaerospermum* SW67 and their putative biosynthetic origin. *Mar. Drugs* **2019**, *17*, 606. [CrossRef] [PubMed]
54. Yu, G.H.; Wu, G.W.; Zhu, T.J.; Gu, Q.Q.; Li, D.H. Cladosins F and G, two new hybrid polyketides from the deep-sea-derived *Cladosporium sphaerospermum* 2005-01-E3. *J. Asian Nat. Prod. Res.* **2015**, *17*, 120–124. [CrossRef] [PubMed]
55. Zhang, Z.; He, X.; Wu, G.; Liu, C.; Lu, C.; Gu, Q.; Che, Q.; Zhu, T.; Zhang, G.; Li, D. Aniline-tetramic acids from the deep-sea-derived fungus *Cladosporium sphaerospermum* L3P3 cultured with the HDAC inhibitor SAHA. *J. Nat. Prod.* **2018**, *81*, 1651–1657. [CrossRef] [PubMed]
56. Zhu, G.; Kong, F.; Wang, Y.; Fu, P.; Zhum, W. Cladodionen, a cytotoxic hybrid polyketide from the marine-derived *Cladosporium* sp. OUCMDZ-1635. *Mar. Drugs* **2018**, *16*, 71. [CrossRef]
57. Liang, X.; Huang, Z.H.; Ma, X.; Qi, S.H. Unstable tetramic acid derivatives from the deep-sea-derived fungus *Cladosporium sphaerospermum* EIODSF 008. *Mar. Drugs* **2018**, *16*, 448. [CrossRef]
58. Huang, Z.-H.; Nong, X.-H.; Liang, X.; Qi, S.-H. New tetramic acid derivatives from the deep-sea-derived fungus *Cladosporium* sp. SCSIO z0025. *Tetrahedron* **2018**, *74*, 2620–2626. [CrossRef]
59. Ding, L.; Qin, S.; Li, F.; Chi, X.; Laatsch, H. Isolation, antimicrobial activity, and metabolites of fungus *Cladosporium* sp. associated with red alga *Porphyra yezoensis*. *Curr. Microbiol.* **2008**, *56*, 229–235. [CrossRef]
60. Qi, S.-H.; Xu, Y.; Xiong, H.-R.; Qian, P.-Y.; Zhang, S. Antifouling and antibacterial compounds from a marine fungus *Cladosporium* sp. F14. *World J. Microbiol. Biotechnol.* **2009**, *25*, 399–406. [CrossRef]
61. Pang, X.; Lin, X.; Wang, J.; Liang, R.; Tian, Y.; Salendra, L.; Luo, X.; Zhou, X.; Yang, B.; Tu, Z.; et al. Three new highly oxygenated sterols and one new dihydroisocoumarin from the marine sponge-derived fungus *Cladosporium* sp. SCSIO41007. *Steroids* **2018**, *129*, 41–46. [CrossRef]
62. Gu, B.; Zhang, Y.; Ding, L.; He, S.; Wu, B.; Dong, J.; Zhu, P.; Chen, J.; Zhang, J.; Yan, X. Preparative separation of sulfur-containing diketopiperazines from marine fungus *Cladosporium* sp. using high-speed counter-current chromatography in stepwise elution mode. *Mar. Drugs* **2015**, *13*, 354–365. [CrossRef]
63. Manríquez, V.; Galdámeza, A.; Veliz, B.; Rovirosa, J.; Díaz-Marrero, A.R.; Cueto, M.; Darias, J.; Martínez, C.; San-Martín, A. N-methyl-1H-indole-2-carboxamide from the marine fungus *Cladosporium cladosporioides*. *J. Chil. Chem. Soc.* **2009**, *54*, 314–316. [CrossRef]
64. Peng, J.; Lin, T.; Wang, W.; Xin, Z.; Zhu, T.; Gu, Q.; Li, D. Antiviral alkaloids produced by the mangrove-derived fungus *Cladosporium sp.* PJX-41. *J. Nat. Prod.* **2013**, *76*, 1133–1140. [CrossRef]
65. Yang, G.; Nenkep, V.N.; Siwe, X.N.; Leutou, A.S.; Feng, Z.H.; Zhang, D.; Choi, H.D.; Kang, J.S.; Son, B.W. An acetophenone derivative, clavatol, and a benzodiazepine alkaloid, circumdatin A, from the marine-derived fungus *Cladosporium*. *Nat. Prod. Sci.* **2009**, *15*, 130–133.
66. Kyeremeh, K.; Owusu, K.B.-A.; Ofosuhene, M.; Ohashi, M.; Agyapong, J.; Camas, A.S.; Camas, M. Anti-proliferative and antiplasmodia activity of quinolactacin A2, citrinadin A and butrecitrinadin co-isolated from a Ghanaian mangrove endophytic fungus *Cladosporium oxysporum* strain BRS2A-AR2F. *J. Chem. Appl.* **2017**, *3*, 12.
67. Wang, P.; Cui, Y.; Cai, C.; Chen, H.; Dai, Y.; Chen, P.; Kong, F.; Yuan, J.; Song, X.; Mei, W.; et al. Two new succinimide derivatives cladosporitins A and B from the mangrove-derived fungus *Cladosporium* sp. HNWSW-1. *Mar. Drugs* **2019**, *17*, 4. [CrossRef]
68. Rotinsulu, H.; Yamazaki, H.; Sugai, S.; Iwakura, N.; Wewengkang, D.S.; Sumilat, D.A.; Namikoshi, M. Cladosporamide A, a new protein tyrosine phosphatase 1B inhibitor, produced by an Indonesian marine sponge-derived *Cladosporium* sp. *J. Nat. Med.* **2018**, *72*, 779–783. [CrossRef]
69. Cao, F.; Yang, Q.; Shao, C.L.; Kong, C.J.; Zheng, J.J.; Liu, Y.F.; Wang, C.Y. Bioactive 7-oxabicyclic[6.3.0]lactam and 12-membered macrolides from a gorgonian-derived *Cladosporium* sp. fungus. *Mar. Drugs* **2015**, *13*, 4171–4178. [CrossRef]

70. Huang, C.; Chen, T.; Yan, Z.; Guo, H.; Hou, X.; Jiang, L.; Long, Y. Thiocladospolide E and cladospamide A, novel 12-membered macrolide and macrolide lactam from mangrove endophytic fungus *Cladosporium* sp. SCNU-F0001. *Fitoterapia* **2019**, *137*, 104246. [CrossRef]
71. Bai, M.; Zheng, C.J.; Tang, D.Q.; Zhang, F.; Wang, H.Y.; Chen, G.Y. Two new secondary metabolites from a mangrove-derived fungus *Cladosporium* sp. JS1-2. *J. Antibiot.* **2019**, *72*, 779–782. [CrossRef]
72. Zhang, H.; Tomoda, H.; Tabata, N.; Miura, H.; Namikoshi, M.; Yamaguchi, Y.; Masuma, R.; Omura, S. Cladospolide D, a new 12-membered macrolide antibiotic produced by *Cladosporium* sp. FT-0012. *J. Antibiot.* **2001**, *54*, 635–641. [CrossRef]
73. Wuringege Guo, Z.K.; Wei, W.; Jiao, R.H.; Yan, T.; Zang, L.Y.; Jiang, R.; Tan, R.X.; Ge, H.M. Polyketides from the plant endophytic fungus *Cladosporium* sp. IFB3lp-2. *J. Asian Nat. Prod. Res.* **2013**, *15*, 928–933. [CrossRef]
74. Jadulco, R.; Proksch, P.; Wray, V.; Sudarsono Berg, A.; Gräfe, U. New macrolides and furan carboxylic acid derivative from the sponge-derived fungus *Cladosporium herbarum*. *J. Nat. Prod.* **2001**, *64*, 527–530. [CrossRef]
75. He, Z.H.; Zhang, G.; Yan, Q.X.; Zou, Z.B.; Xiao, H.X.; Xie, C.L.; Tang, X.X.; Luo, L.Z.; Yang, X.W. Cladosporactone A, a unique polyketide with 7-methylisochromen-3-one skeleton from the deep-sea-derived fungus *Cladosporium cladosporioides*. *Chem. Biodivers.* **2020**, *17*, e2000158. [CrossRef]
76. Gao, C.H.; Nong, X.H.; Qi, S.H.; Luo, X.M.; Zhang, S.; Xiong, H.R. A new nine-membdered lactone from a marine fungus *Cladosporium* sp. F14. *Chin. Chem. Lett.* **2010**, *21*, 1355–1357. [CrossRef]
77. Gesner, S.; Cohen, N.; Ilan, M.; Yarden, O.; Carmeli, S. Pandangolide 1a, a metabolite of the sponge-associated fungus *Cladosporium* sp., and the absolute stereochemistry of pandangolide 1 and iso-cladospolide B. *J. Nat. Prod.* **2005**, *68*, 1350–1353. [CrossRef]
78. Wang, W.; Feng, H.; Sun, C.; Che, Q.; Zhang, G.; Zhu, T.; Li, D. Thiocladospolides F-J, antibacterial sulfur containing 12-membered macrolides from the mangrove endophytic fungus *Cladosporium oxysporum* HDN13-314. *Phytochemistry* **2020**, *178*, 112462. [CrossRef]
79. Zhang, F.Z.; Li, X.M.; Meng, L.H.; Wang, B.G. Cladocladosin A, an unusual macrolide with bicyclo 5/9 ring system, and two thiomacrolides from the marine mangrove-derived endophytic fungus, *Cladosporium cladosporioides* MA-299. *Bioorg. Chem.* **2020**, *101*, 103950. [CrossRef]
80. Shigemori, H.; Kasai, Y.; Komatsu, K.; Tsuda, M.; Mikami, Y.; Kobayashi, J. Sporiolides A and B, new cytotoxic twelve-membered macrolides from a marine-derived fungus *Cladosporium* pecies. *Mar. Drugs* **2004**, *2*, 164–169. [CrossRef]
81. Peng, X.; Wang, Y.; Zhu, G.; Zhu, W. Fatty acid derivatives from the halotolerant fungus *Cladosporium cladosporioides*. *Magn. Reson. Chem.* **2018**, *56*, 18–24. [CrossRef]
82. Ai, W.; Lin, X.; Wang, Z.; Lu, X.; Mangaladoss, F.; Yang, X.; Zhou, X.; Tu, Z.; Liu, Y. Cladosporone A, a new dimeric tetralone from fungus *Cladosporium* sp. KcFL6′ derived of mangrove plant Kandelia candel. *J. Antibiot.* **2015**, *68*, 213–215. [CrossRef]
83. Zhang, Z.; He, X.; Liu, C.; Che, Q.; Zhu, T.; Gu, Q.; Li, D. Clindanones A and B and cladosporols F and G, polyketides from the deep-sea derived fungus *Cladosporium cladosporioides* HDN14-342. *RSC Adv.* **2016**, *6*, 76498–76504. [CrossRef]
84. Li, H.L.; Li, X.M.; Mándi, A.; Antus, S.; Li, X.; Zhang, P.; Liu, Y.; Kurtán, T.; Wang, B.G. Characterization of cladosporols from the marine algal-derived endophytic fungus *Cladosporium cladosporioides* en-399 and configurational revision of the previously reported cladosporol derivatives. *J. Org. Chem.* **2017**, *82*, 9946–9954. [CrossRef] [PubMed]
85. Zhang, F.; Zhou, L.; Kong, F.; Ma, Q.; Xie, Q.; Li, J.; Dai, H.; Guo, L.; Zhao, Y. Altertoxins with quorum sensing inhibitory activities from the marine-derived fungus *Cladosporium* sp. KFD33. *Mar. Drugs* **2020**, *18*, 67. [CrossRef] [PubMed]
86. Zhen, F.; Zhang-hua, S.; Yu-chan, C.; Hao-hua, L.; Wei-min, Z. Cladosperanol A, a new dimeric tetralone from marine-derived fungus *cladosporium perangustum*. *Nat. Prod. Res. Dev.* **2016**, *28*, 486–489.
87. Fan, Z.; Sun, Z.H.; Liu, H.X.; Chen, Y.C.; Li, H.H.; Zhang, W.M. Perangustols A and B, a pair of new azaphilone epimers from a marine sediment-derived fungus *Cladosporium perangustm* FS62. *J. Asian Nat. Prod. Res.* **2016**, *18*, 1024–1029. [CrossRef]
88. Wu, J.T.; Zheng, C.J.; Zhang, B.; Zhou, X.M.; Zhou, Q.; Chen, G.Y.; Zeng, Z.E.; Xie, J.L.; Han, C.R.; Lyu, J.X. Two new secondary metabolites from a mangrove-derived fungus *Cladosporium* sp. JJM22. *Nat. Prod. Res.* **2019**, *33*, 34–40. [CrossRef]
89. Fan, C.; Zhou, G.; Wang, W.; Zhang, G.; Zhu, T.; Che, Q.; Li, D. Tetralone derivatives from a deep-sea derived fungus *Cladosporium* sp. HDN17-58. *Nat. Prod. Commun.* **2021**, *16*, 1934578X211008322. [CrossRef]
90. Ma, R.-Z.; Zheng, C.-J.; Zhang, B.; Yang, J.-Y.; Zhou, X.-M.; Song, X.-M. Two New naphthalene-chroman coupled derivatives from the mangrove-derived fungus *Cladosporium* sp. JJM22. *Phytochem. Lett.* **2021**, *43*, 114–116. [CrossRef]
91. Li, Z.; Yang, J.Y.; Caj, J.; Ouyang, Z.J.; Zhou, C.H.; Chen, G.Y.; Zhou, X.M. Study on secondary metabolites *of endophytic fungus Cladosporium sp. JJM22* hosted in *Ceriops tagal*. *Zhongguo Zhong Yao Za Zhi* **2021**, *46*, 2079–2083.
92. Wang, C.N.; Lu, H.M.; Gao, C.H.; Guo, L.; Zhan, Z.Y.; Wang, J.J.; Liu, Y.H.; Xiang, S.T.; Wang, J.; Luo, X.W. Cytotoxic benzopyranone and xanthone derivatives from a coral symbiotic fungus *Cladosporium halotolerans* GXIMD 02502. *Nat. Prod. Res.* **2020**, 1–8. [CrossRef]
93. Silber, J.; Ohlendorf, B.; Labes, A.; Wenzel-Storjohann, A.; Näther, C.; Imhoff, J.F. Malettinin E, an antibacterial and antifungal tropolone produced by a marine *Cladosporium* strain. *Front. Mar. Sci.* **2014**, *1*, 35. [CrossRef]
94. Liu, Y.; Kurtán, T.; Yun Wang, C.; Han Lin, W.; Orfali, R.; Müller, W.E.; Daletos, G.; Proksch, P. Cladosporinone, a new viriditoxin derivative from the hypersaline lake derived fungus *Cladosporium cladosporioides*. *J. Antibiot.* **2016**, *69*, 702–706. [CrossRef]
95. Wang, L.; Han, X.; Zhu, G.; Wang, Y.; Chairoungdua, A.; Piyachaturawat, P.; Zhum, W. Polyketides from the endophytic fungus *Cladosporium* sp. isolated from the mangrove plant *Excoecaria agallocha*. *Front. Chem.* **2018**, *6*, 344. [CrossRef]

96. Jadulco, R.; Brauers, G.; Edrada, R.A.; Ebel, R.; Wray, V.; Sudarsono, S.; Proksch, P. New metabolites from sponge-derived fungi *Curvularia lunata* and *Cladosporium herbarum*. *J. Nat. Prod.* **2002**, *65*, 730–733. [CrossRef]
97. Zhang, B.; Wu, J.T.; Zheng, C.J.; Zhou, X.M.; Yu, Z.X.; Li, W.S.; Chen, G.Y.; Zhu, G.Y. Bioactive cyclohexene derivatives from a mangrove-derived fungus *Cladosporium* sp. JJM22. *Fitoterapia* **2021**, *149*, 104823. [CrossRef]
98. San-Martin, A.; Painemal, K.; Diaz, Y.; Martinez, C.; Rovirosa, J. Metabolites from the marine fungus *Cladosporium cladosporioides*. *J. Argent. Chem. Soc.* **2005**, *93*, 247–251.
99. Kuznetsova, T.A.; Afiyatullov, S.A.; Denisenko, V.A.; Pivkin, M.V.; Elyakov, G.B. Sterols from a marine isolate of the fungus *Cladosporium sphaerospermum* Penz. *Biochem. Syst. Ecol.* **1998**, *26*, 365–366. [CrossRef]
100. Yu, M.L.; Guan, F.F.; Cao, F.; Jia, Y.L.; Wang, C.Y. A new antiviral pregnane from a gorgonian-derived *Cladosporium* sp. fungus. *Nat. Prod. Res.* **2018**, *32*, 1260–1266. [CrossRef]
101. Lee, S.R.; Kang, H.; Yoo, M.J.; Yu, J.S.; Lee, S.; Yi, S.A.; Beemelmanns, C.; Lee, J.; Kim, K.H. Anti-adipogenic pregnane steroid from a *Hydractinia*-associated fungus, *Cladosporium sphaerospermum* SW67. *Nat. Prod. Sci.* **2020**, *26*, 230–235.
102. Gallo, M.L.; Seldes, A.M.; Cabrera, G.M. Antibiotic long-chain and α,β-unsaturated aldehydes from the culture of the marine fungus *Cladosporium* sp. *Biochem. Syst. Ecol.* **2004**, *32*, 545–551. [CrossRef]
103. AlMatar, M.; Makky, E.A. *Cladosporium cladosporioides* from the perspectives of medical and biotechnological approaches. *3 Biotech* **2016**, *6*, 4. [CrossRef]
104. Armisén, R.; Galatas, F.; Hispanagar, A.S. Agar. In *Handbook of Hydrocolloids*; Phillips, G.O., Williams, P.A., Eds.; Woodhead Publishing: Cambridge, UK, 2000; pp. 21–40.
105. Wang, J.; Jiang, X.; Mou, H.; Guan, H. Anti-oxidation of agar oligosaccharides produced by agarase from a marine bacterium. *J. Appl. Phycol.* **2004**, *16*, 333–340. [CrossRef]
106. Necas, J.; Bartosikova, L. Carrageenan: A review. *Vet. Med.* **2013**, *58*, 187–205. [CrossRef]
107. Ibrahim, S.R.M.; Mohamed, S.G.A.; Altyar, A.E.; Mohamed, G.A. Natural products of the fungal genus *Humicola*: Diversity, biological activity, and industrial importance. *Curr. Microbiol.* **2021**, *78*, 2488–2509. [CrossRef]
108. Ibrahim, S.R.M.; Mohamed, S.G.A.; Sindi, I.A.; Mohamed, G.A. Biologically active secondary metabolites and biotechnological applications of species of the family Chaetomiaceae (Sordariales): An updated review from 2016 to 2021. *Mycol. Prog.* **2021**, *20*, 595–639. [CrossRef]
109. Ibrahim, S.R.M.; Mohamed, S.G.A.; Altyar, A.E.; Mohamed, G.A. Genus *Thielavia*: Phytochemicals, industrial importance and biological relevance. *Nat. Prod. Res.* **2021**, 1–16. [CrossRef]
110. Collins, T.; Gerday, C.; Feller, G. Xylanases, xylanase families and extremophilic xylanases. *FEMS Microb. Rev.* **2005**, *29*, 3–23. [CrossRef] [PubMed]
111. D'Souza, D.T.; Tiwari, R.; Sah, A.K.; Raghukumara, C. Enhanced production of laccase by a marine fungus during treatment of colored effluents and synthetic dyes. *Enzym. Microb. Technol.* **2006**, *38*, 504–511. [CrossRef]
112. Kuwahara, M.; Glenn, J.K.; Morgan, M.A.; Gold, M.H. Separation and characterization of two extracellular H_2O_2 dependent oxidases from ligninolytic cultures of *Phanerochaete chrysosporium*. *FEBS Lett.* **1984**, *169*, 247–250. [CrossRef]
113. Raghukumar, C.; Muraleedharan, U.; Gaud, V.R.; Mishra, R. Simultaneous detoxification and decolorization of molasses spent wash by the immobilized white-rot fungus Flavodon flavusisolated from a marine habitat. *Enzym. Microb. Technol.* **2004**, *35*, 197–202. [CrossRef]
114. Da Silva, M.; Passarini, M.R.Z.; Bonugli, R.C.; Sette, L.D. Cnidarian-derived filamentous fungi from Brazil: Isolation, characterisation and RBBR decolourisation screening. *Environ. Technol.* **2008**, *29*, 1331–1339. [CrossRef]
115. Panno, L.; Voyron, S.; Anastasi, A.; Mussat Sarto, R.; Varese, G.C. Biodiversity of marine fungi associated with the seagrass *Posidonia oceanica*: An ecological and biotechnological perspective. *Biol. Mar. Mediterr.* **2011**, *18*, 85–88.
116. Taskin, M.; Esim, N.; Genisel, M.; Ortucu, S.; Hasenekoglu, I.; Canli, O.; Erdal, S. Enhancement of invertase production by *Aspergillus niger* OZ-3 using low-intensity static magnetic fields. *Prep. Biochem. Biotechnol.* **2013**, *43*, 177–188. [CrossRef]
117. Veana, F.; Martínez-Hernández, J.L.; Aguilar, N.; Rodríguez-Herrera, R.; Michelena, G. Utilization of molasses and sugar cane bagasse for production of fungal invertase in solid state fermentation using *Aspergillus niger* GH1. *Braz. J. Microbiol.* **2014**, *5*, 373–377. [CrossRef]
118. Yadav, S.; Chandra, R. Biodegradation of organic compounds of molasses melanoidin (MM) from biomethanated distillery spent wash (BMDS) during the decolourisation by a potential bacterial consortium. *Biodegradation* **2012**, *23*, 609–620. [CrossRef]
119. Gavrilescua, M.; Chisti, Y. Biotechnology-a sustainable alternative for chemical industry. *Biotechnol. Adv.* **2005**, *23*, 471–499. [CrossRef]
120. Winkler, C.K.; Faber, K.; Hall, M. Biocatalytic reduction of activated C=C-bonds and beyond: Emerging trends. *Curr. Opin. Chem. Biol.* **2018**, *43*, 97–105. [CrossRef]
121. Garzon-Posse, F.; Becerra-Figueroa, L.; Hernandez-Arias, J.; Gamba-Sanchez, D. Whole cells as biocatalysts in organic transformations. *Molecules* **2018**, *23*, 1265. [CrossRef]
122. Khare, R.; Pandey, J.; Smriti, R.R. The importance and applications of Knoevenagel reaction (brief review). *Orient. J. Chem.* **2019**, *35*, 423–429. [CrossRef]
123. Rocha, L.C.; Ferreira, H.V.; Luiz, R.F.; Sette, L.D.; Porto, A.L. Stereoselective bioreduction of 1-(4-methoxyphenyl) ethanone by whole cells of marine-derived fungi. *Mar. Biotechnol.* **2012**, *14*, 358–362. [CrossRef]

124. Rocha, L.C.; Seleghim, M.H.R.; Comasseto, J.V.; Sette, L.D.; Porto, A.L.M. Stereoselective bioreduction of alpha-azido ketones by whole cells of marine-derived fungi. *Mar. Biotechnol.* **2015**, *17*, 736–742. [CrossRef] [PubMed]
125. Athanasellis, G.; Igglessi-Markopoulou, O.; Markopoulos, J. Tetramic and tetronic acids as scaffolds in bioinorganic and bioorganic chemistry. *Bioinorg. Chem. Appl.* **2010**, *2010*, 315056. [CrossRef] [PubMed]
126. Royles, B.J.L. Naturally occurring tetramic acids: Structure, isolation, and synthesis. *Chem. Rev.* **1995**, *95*, 1981–2001. [CrossRef]
127. Mo, X.; Li, Q.; Ju, J. Naturally occurring tetramic acid products: Isolation, structure elucidation and biological activity. *RSC Adv.* **2014**, *4*, 50566–50593. [CrossRef]
128. Jiang, M.; Chen, S.; Li, J.; Liu, L. The Biological and Chemical Diversity of Tetramic Acid Compounds from Marine-Derived Microorganisms. *Mar. Drugs* **2020**, *18*, 114. [CrossRef]
129. Gomes, N.G.M.; Pereira, R.B.; Andrade, P.B.; Valentao, P. Double the chemistry, double the fun: Structural diversity and biological activity of marine-derived diketopiperazine dimers. *Mar. Drugs* **2019**, *17*, 551. [CrossRef]
130. Huang, R.M.; Yi, X.X.; Zhou, Y.Y.; Su, X.D.; Peng, Y.; Gao, C.H. An update on 2,5-diketopiperazines from marine organisms. *Mar. Drugs* **2014**, *12*, 6213–6235. [CrossRef]
131. Borgman, P.; Lopez, R.D.; Lane, A.L. The expanding spectrum of diketopiperazine natural product biosynthetic pathways containing cyclodipeptide synthases. *Org. Biomol. Chem.* **2019**, *17*, 2305–2314. [CrossRef]
132. Song, Z.; Hou, Y.; Yang, Q.; Li, X.; Wu, S. Structures and Biological Activities of Diketopiperazines from Marine Organisms: A Review. *Mar. Drugs* **2021**, *19*, 403. [CrossRef]
133. Urban, S.; Hickford, S.J.H.; Blunt, J.W.; Munro, M.H.G.; Yue, Y.F.; Chang, Q.H.; Zhu, H.J.; Cao, F. Bioactive marine alkaloids. *Curr. Org. Chem.* **2000**, *4*, 765–807. [CrossRef]
134. Meng, Z.H.; Sun, T.T.; Zhao, G.Z.; Yue, Y.-F.; Chang, Q.-H.; Zhu, H.-J.; Cao, F. Marine-derived fungi as a source of bioactive indole alkaloids with diversified structures. *Mar. Life Sci. Technol.* **2021**, *3*, 44–61. [CrossRef]
135. Islam, M.T.; Mubarak, M.S. Pyrrolidine alkaloids and their promises in pharmacotherapy. *Adv. Tradit. Med.* **2020**, *20*, 13–22. [CrossRef]
136. Netz, N.; Opatz, T. Marine indole alkaloids. *Mar. Drugs* **2015**, *13*, 4814–4914. [CrossRef]
137. Woodward, R.B. Struktur und biogenese der makrolide. *Angew. Chem.* **1957**, *69*, 50–58. [CrossRef]
138. Janas, A.; Przybylski, P. 14- and 15-membered lactone macrolides and their analogues and hybrids: Structure, molecular mechanism of action and biological activity. *Eur. J. Med. Chem.* **2019**, *182*, 111662. [CrossRef]
139. Zhang, H.; Zou, J.; Yan, X.; Chen, J.; Cao, X.; Wu, J.; Liu, Y.; Wang, T. Marine-Derived Macrolides 1990–2020: An Overview of Chemical and Biological Diversity. *Mar. Drugs* **2021**, *19*, 180. [CrossRef]
140. Ray Choudhury, A.; Mukherjee, S. Deconjugated butenolide: A versatile building block for asymmetric catalysis. *Chem. Soc. Rev.* **2020**, *49*, 6755–6788. [CrossRef]
141. Kumar, A.; Singh, V.; Ghosh, S. *Butenolide: A Novel Synthesis and Biological Activities*, 1st ed.; LAP Lambert Academic Publishing: Saarbrücken, Germany, 2012.
142. Gibson, M.Z.; Nguyen, M.A.; Zingales, S.K. Design, synthesis, and evaluation of (2-(pyridinyl)methylene)-1-tetralone chalcones for anticancer and antimicrobial activity. *Med. Chem.* **2018**, *14*, 333–343. [CrossRef]
143. Gauni, B.; Mehariya, K.; Shah, A.; Duggirala, S.M. Tetralone scaffolds and their potential therapeutic applications. *Lett. Drug Des. Disc.* **2021**, *18*, 222–238. [CrossRef]
144. Zurlo, D.; Leone, C.; Assante, G.; Salzano, S.; Renzone, G.; Scaloni, A.; Foresta, C.; Colantuoni, V.; Lupo, A. Cladosporol a stimulates G1-phase arrest of the cell cycle by up-regulation of $p21^{waf1/cip1}$ expression in human colon carcinoma HT-29 cells. *Mol. Carcinog.* **2013**, *52*, 1–17. [CrossRef]
145. Zurlo, D.; Assante, G.; Moricca, S.; Colantuoni, V.; Lupo, A. Cladosporol A, a new peroxisome proliferator-activated receptor γ (PPARγ) ligand, inhibits colorectal cancer cells proliferation through β-catenin/TCF pathway inactivation. *Biochim. Biophys. Acta* **2014**, *1840*, 2361–2372. [CrossRef]
146. Mulrooey, C.A.; O'Brien, E.M.; Morgan, B.J.; Kozlowski, M.C. Perylenequinones: Isolation, synthesis, and biological activity. *Eur. J. Org. Chem.* **2012**, *2012*, 3887–3904. [CrossRef]
147. Stack, M.E.; Prival, M.J. Mutagenicity of the Alternaria metabolites altertoxins I., II, and III. *Appl. Environ. Microbiol.* **1986**, *52*, 718–722. [CrossRef]
148. Ibrahim, S.R.M.; Mohamed, G.A. Naturally occurring naphthalenes: Chemistry, biosynthesis, structural elucidation, and biological activities. *Phytochem. Rev.* **2016**, *15*, 279–295. [CrossRef]
149. Vieira, L.; Kijjoa, A. Naturally-occurring xanthones: Recent developments. *Curr. Med. Chem.* **2005**, *12*, 2413–2446. [CrossRef]
150. Ibrahim, S.R.M.; Abdallah, H.M.; El-Halawany, A.M.; Radwan, M.F.; Shehata, I.A.; Al-Harshany, E.M.; Zayed, M.F.; Mohamed, G.A. Garcixanthones B and C, new xanthones from the pericarps of *Garcinia mangostana* and their cytotoxic activity. *Phytochem. Lett.* **2018**, *25*, 12–16. [CrossRef]
151. Mohamed, G.A.; Al-Abd, A.M.; El-Halawany, A.M.; Abdallah, H.M.; Ibrahim, S.R.M. New xanthones and cytotoxic constituents from *Garcinia mangostana* fruit hulls against human hepatocellular, breast, and colorectal cancer cell lines. *J. Ethnopharmacol.* **2017**, *198*, 302–312. [CrossRef]
152. Guo, H.; Roman, D.; Beemelmanns, C. Tropolone natural products. *Nat. Prod. Rep.* **2019**, *36*, 1137–1155. [CrossRef]
153. Choque, E.; El Rayess, Y.; Raynal, J.; Mathieu, F. Fungal naphtho-γ-pyrones—Secondary metabolites of industrial interest. *Appl. Microbiol. Biotechnol.* **2015**, *99*, 1081–1096. [CrossRef] [PubMed]

154. Suzuki, K.; Nozawa, K.; Nakajima, S.; Kawai, K. Structure revision of mycotoxin, viriditoxin, and its derivatives. *Chem. Pharm. Bull.* **1990**, *38*, 3180–3181. [CrossRef]
155. De Rosa, S.; De Giulio, A.; Iodice, C.; Alcaraz, M.J.; Paya, M. Long-chain aldehydes from the red alga, *Corallina Mediterr*. *Phytochemistry* **1995**, *40*, 995–996. [CrossRef]
156. Suzuki, M.; Kurosawa, E.; Kurata, K. (*E*)-2-Tridecyl-2-heptadecenal, an unusual metabolite from the red alga *Laurencia* sp. *Bull. Chem. Soc. Jpn.* **1987**, *60*, 3793–3794. [CrossRef]
157. Wulandari, A.P.; Examinati, R.R.I.N.; Madihah; Huspa, D.H.P.; Andayaningsih, P.; Andayaningsih, P. Cytotoxicity of metabolites produced by endophytic fungus *Cladosporium* sp. isolated from marine macroalgae on in-vitro MCF-7, HeLa, and DU-145 cell lines. *Int. J. Pharm. Pharm. Sci.* **2018**, *10*, 72–76. [CrossRef]
158. Hulikere, M.M.; Joshi, C.G.; Ananda, D.; Poyya, J.; Nivya, T. Antiangiogenic, wound healing and antioxidant activity of *Cladosporium cladosporioides* (Endophytic Fungus) isolated from seaweed (*Sargassum wightii*). *Mycology* **2016**, *7*, 203–211. [CrossRef]
159. Xiong, H.; Qi, S.; Xu, Y.; Miao, L.; Qian, P.Y. Antibiotic and antifouling compound production by the marine-derived fungus *Cladosporium* sp. F14. *J. Hydro-Environ. Res.* **2009**, *2*, 264–270. [CrossRef]
160. Hulikere, M.M.; Joshi, C.G.; Danagoudar, A.; Poyya, J.; Kudva, A.K.; Dhananjaya, B.L. Biogenic synthesis of gold nanoparticles by marine endophytic fungus *Cladosporium cladosporioides* isolated from seaweed and evaluation of their antioxidant and antimicrobial properties. *Process Biochem.* **2017**, *63*, 137–144.
161. Ameen, F.; Al-Homaidan, A.A.; Al-Sabr, A.; Almansob, A.; AlNAdhari, S. Anti-oxidant, anti-fungal and cytotoxic effects of silver nanoparticles synthesized using marine fungus *Cladosporium halotolerans*. *Appl. Nanosci.* **2021**. [CrossRef]
162. Arnone, A.; Assante, G.; Modugno, V.D.; Merlini, L.; Nasini, G. Perylenequinones from cucumber seedlings infected with *Cladosporium cucumerinum*. *Phytochemisry* **1988**, *27*, 1675–1678. [CrossRef]
163. Arnone, A.; Camarda, L.; Nasini, G.; Merlini, L. Secondary mould metabolites. Part 13. Fungal perylenequinones: Phleichrome, isophleichrome, and their endoperoxides. *J. Chem. Soc. Perkin Trans. 1* **1985**, 1387–1392. [CrossRef]
164. Arone, A.; Assante, G.; Merlini, L.; Nasini, G. Structure and stereochemistry of cladochrome D and E, novel perylenequinone pigment from *Cladosporium cladosporioides*. *Gazetta Chem. Ital.* **1989**, *119*, 557–559.
165. Mino, Y.; Idonuma, T.; Sakai, R. Effect of Phleichrome Produced by the Timothy Leaf Spot Fungus, Cladosporium phlei on the Invertases from the Host Leaves. *Ann. Phytopathol. Soc. Jpn.* **1979**, *45*, 463–467. [CrossRef]
166. Sassa, T.; Negoro, T.; Ueki, H. Production and Characterization of a new fungal metabolite, cotylenol. *Agric. Biol. Chem.* **1972**, *36*, 2281–2285. [CrossRef]
167. Sassa, T.; Ooi, T.; Nukina, M.; Ikeda, M.; Kato, N. Structural confirmation of cotylenin A, a novel fusicoccane-diterpene glycoside with potent plant growth-regulating activity from *Cladosporium* fungus sp. 501-7W. *Biosci. Biotechnol. Biochem.* **1998**, *62*, 1815–1818. [CrossRef]
168. Sassa, T.; Togashi, M.; Kitaguchi, T. The structures of cotylenins A., B., C., D and E. *Agric. Biol. Chem.* **1975**, *39*, 1735–1744. [CrossRef]
169. Sassa, T. Cotylenins, ^{13}C NMR of cotylenins. *Agric. Biol. Chem.* **1979**, *43*, 385–387.
170. Sassa, T. Cotylenins, leaf growth substances produced by a fungus. Part, I. Isolation and characterization of cotylenins A and B. *Agric. Biol. Chem.* **1971**, *35*, 1415–1418.
171. Baral, B.; Akhgari, A.; Metsä-Ketelä, M. Activation of microbial secondary metabolic pathways: Avenues and challenges. *Synth. Syst. Biotechnol.* **2018**, *3*, 163–178. [CrossRef]
172. Reich, M.; Labes, A. How to boost marine fungal research: A first step towards a multidisciplinary approach by combining molecular fungal ecology and natural products chemistry. *Mar. Genom.* **2017**, *36*, 57–75. [CrossRef]
173. Scharf, D.H.; Brakhage, A.A. Engineering fungal secondary metabolism: A roadmap to novel compounds. *J. Biotechnol.* **2013**, *163*, 179–183. [CrossRef]
174. Reen, F.J.; Romano, S.; Dobson, A.D.W.; O'Gara, F. The sound of silence: Activating silent biosynthetic gene clusters in marine microorganisms. *Mar. Drugs* **2015**, *13*, 4754–4783. [CrossRef]
175. Bode, H.B.; Bethe, B.; Höfs, R.; Zeeck, A. Big effects from small changes: Possible ways to explore nature's chemical diversity. *ChemBioChem* **2002**, *3*, 619–627. [CrossRef]
176. Scherlach, K.; Hertweck, C. Triggering cryptic natural product biosynthesis in microorganisms. *Org. Biomol. Chem.* **2009**, *7*, 1753–1760. [CrossRef] [PubMed]
177. Oh, D.C.; Kauffman, C.A.; Jensen, P.R.; Fenical, W. Induced production of emericellamides A and B from the marine-derived fungus Emericella sp. in competing co-culture. *J. Nat. Prod.* **2007**, *70*, 515–520. [CrossRef] [PubMed]
178. Yeh, H.H.; Ahuja, M.; Chiang, Y.M.; Oakley, C.E.; Moore, S.; Yoon, O.; Hajovsky, H.; Bok, J.W.; Keller, N.P.; Wang, C.C.; et al. Resistance Gene-Guided Genome Mining: Serial Promoter Exchanges in Aspergillus nidulans Reveal the Biosynthetic Pathway for Fellutamide B, a Proteasome Inhibitor. *ACS Chem. Biol.* **2016**, *11*, 2275–2284. [CrossRef]
179. Williams, R.B.; Henrikson, J.C.; Hoover, A.R.; Lee, A.E.; Cichewicz, R.H. Epigenetic remodeling of the fungal secondary metabolome. *Org. Biomol. Chem.* **2008**, *6*, 1895–1897. [CrossRef]